

**Influence of dietary restriction on
body composition, lipid droplet size and gene expression
in *Caenorhabditis elegans***

Dissertation

zur Erlangung des Doktorgrades

der Mathematisch-Naturwissenschaftlichen Fakultät

der Christian-Albrechts-Universität zu Kiel

vorgelegt von

Daniela Palgunow

Kiel

Mai 2012

Referent: Prof. Dr. Thomas Roeder

Koreferent: Prof. Dr. Frank Döring

Datum der mündlichen Prüfung: 06.08.2012

Zum Druck genehmigt: 06.08.2012

Der Dekan

Table of contents

Table of contents.....	I
List of Figures.....	IV
List of Tables.....	V
Abbreviations.....	VI
Zusammenfassung.....	1
Summary.....	3
1 Introduction	5
1.1 Dietary restriction	5
1.2 Dietary restriction mediated longevity	5
1.3 Dietary restriction in <i>Caenorhabditis elegans</i>	6
1.4 Lipid metabolism in <i>C. elegans</i>	7
1.5 Lipid droplets as fat storage organelles.....	8
1.6 Lipid droplet enlargement in <i>C. elegans</i>	9
2 Materials and Methods.....	11
2.1 Strains and Maintenance	11
2.2 Dietary restriction on agar plates.....	11
2.3 Preparation of worm homogenates and biochemical measurements.....	11
2.4 Determination of the body proportion	12
2.5 Motility and pharyngeal pumping rate	12
2.6 Lifespan experiments	13
2.7 <i>Age pigment</i> measurements	13
2.8 Oil Red O staining.....	14
2.9 BODIPY TM 493/503 staining.....	14
2.10 Determination of number and size of lipid droplets	15
2.11 Imaging of lipid droplets by coherent anti-Stokes Raman scattering microscopy.....	15
2.12 Whole genome gene expression analysis.....	16
2.13 Statistical analysis.....	17
3 Results	18
3.1 Establishment of a modified dietary restriction protocol based on different bacterial concentrations on agar plates	18
3.2 Influence of dietary restriction on body size	19

3.3	Influence of dietary restriction on locomotion and feeding rates	22
3.4	Influence of dietary restriction on lifespan and <i>age pigment</i> accumulation	23
3.5	Influence of dietary restriction on the fat-to-fat-free mass ratio	26
3.6	Influence of dietary restriction on lipid droplet size.....	27
3.7	Influence of dietary restriction on lipid droplet size and distribution during development	30
3.7.1	Influence of dietary restriction on the relative number of large-sized lipid droplets in dependence on the developmental stage	32
3.7.2	Influence of dietary restriction on the mean LD volume and on the volume-% of large-sized LDs (>50 μm^3).....	34
3.8	Analysis of gene expression profiles in dietary restricted <i>C. elegans</i>	36
3.8.1	Influence of dietary restriction on the expression of genes involved in fatty acid metabolism and other metabolic pathways	43
3.8.2	Influence of dietary restriction on life span extension, immune response, detoxification and transcriptional regulation	44
3.8.3	Comparison between dietary restriction and fasting responses	44
4	Discussion.....	47
4.1	Development of a solid medium based dietary restriction protocol	47
4.2	Regulation of energy metabolism genes under fasting and dietary restriction conditions.....	48
4.3	Dietary restriction and the influence on body size of wild-type nematodes	49
4.4	Dietary restriction-dependent expansion of lipid droplets and the regulation of genes involved in lipid metabolism	50
4.5	Dietary restriction and development-dependent changes in the distribution of enlarged lipid droplets in intestine and hypodermis	53
4.6	Lipid droplet expansion and down-regulation of lipase encoding genes	54
4.7	Dietary restriction-dependent regulation of genes involved in determination of lifespan, detoxification and innate immunity.....	55
4.8	Conclusion and perspectives	57
	References	60
	Supplementary.....	74
	Danksagung.....	80
	Lebenslauf	81
	Erklärung	82

List of figures

Figure 1. Scheme of the established solid medium based dietary restriction method in <i>C. elegans</i>	18
Figure 2. Influence of dietary restriction on body proportion.....	20
Figure 3. Influence of dietary restriction on body volume of larvae and adult worms.....	22
Figure 4. Influence of dietary restriction on motility and pumping rate.....	23
Figure 5. Influence of dietary restriction on lifespan and accumulation of age pigment	25
Figure 6. Influence of dietary restriction on body composition	26
Figure 7. Fat staining of dietary restricted adult <i>C. elegans</i>	27
Figure 8. Imaging of lipid droplets in dietary restricted adult <i>C. elegans</i> by coherent anti-Stokes Raman scattering microscopy and BODIPY 493/503-based staining.....	28
Figure 9. Imaging of lipid droplets in dietary restricted L2 larvae by confocal laser scanning microscopy.....	30
Figure 10. Imaging of lipid droplets in dietary restricted L4 larvae by confocal laser scanning microscopy.....	31
Figure 11. Imaging of lipid droplets in dietary restricted adult worms by confocal laser scanning microscopy.....	31
Figure 12. Size classification of BODIPY 493/503-stained lipid droplets in pharynx and tail region of dietary restricted larvae and adult <i>C. elegans</i>	33
Figure 13. Mean lipid droplet volume and volume-% of large-sized lipid droplets of dietary restricted larvae and adult <i>C. elegans</i>	35
Figure 14. Illustration of shared genes regulated under stringent and moderate DR in wild-type L4 larvae and adults	37
Figure 15. Regulation of genes involved in glucose and lipid metabolism under fasting and two different dietary restriction conditions.....	46
Figure 16. Summary of DR-induced effects on <i>C. elegans</i> phenotypes.....	57

List of tables

Table 1. Genes involved in lipid droplet expansion in <i>C. elegans</i> mutants	9
Table 2. Body proportion of <i>C. elegans</i> cultivated at different dietary restriction conditions	21
Table 3. Mean and maximum lifespan of dietary restricted <i>C. elegans</i>	24
Table 4. Surface to volume ratio of lipid droplets under <i>ad libitum</i> (AL) and dietary restriction (DR) condition	34
Table 5. Volume of the maximum-sized lipid droplets under <i>ad libitum</i> (AL) and dietary restriction (DR) condition	36
Table 6. Summary of dietary restriction (DR) response genes in <i>C. elegans</i>	39
Table S1. Complete list of dietary restriction (DR) response genes	74
Table S2. Dietary restriction (DR) induced alteration of expression of genes implicated in lipid metabolism and storage in <i>C. elegans</i>	77

Abbreviations

<i>acbp</i>	<i>Acyl-CoA binding protein</i>
ACS	Acyl-CoA synthetase
AL	<i>Ad libitum</i>
ATGL	Adipose triacylglycerol lipase
AU	Arbitrary unit
BCA	Bicinchoninic acid
<i>C. elegans</i>	<i>Caenorhabditis elegans</i>
CARS	Coherent anti-Stokes Raman scattering
cfu	Colony forming unit
<i>clcc</i>	<i>C-type lectin</i>
CLS	Confocal laser scanning
COPAS	Complex object parametric analyzer and sorter
<i>cpt</i>	<i>Carnitine palmitoyl transferase</i>
CR	Caloric restriction
CYP	Cytochrome P450
d	Day
<i>daf</i>	<i>Dauer formation</i>
DAG	Diacylglycerol
DGAT	Diacylglycerol acyltransferase
<i>dhs</i>	<i>Dehydrogenase</i>
DNA	Deoxyribonucleic acid
DR	Dietary restriction
<i>E. coli</i>	<i>Escherichia coli</i>
e.g.	For example
FA	Fatty acid
<i>far</i>	<i>Fatty acid/retinol binding protein</i>
<i>fat</i>	<i>Fatty acid desaturase</i>
FIL	Fasting induced lipase
FoxO	Forkhead transcription factor
GC	Gas chromatography
h	Hour
<i>hsp</i>	<i>Heat shock protein</i>

i.e.	That is
IIS	Insulin/IGF-1 signaling
<i>ilys</i>	<i>Invertebrate-type lysozyme</i>
<i>klf</i>	<i>Krüppel-like transcription factor</i>
l	Length
L2	Second larval stage
L4	Fourth larval stage
<i>lbp</i>	<i>Lipid binding protein</i>
LD	Lipid droplet
min	Minute
ml	Millilitre
mRNA	Messenger Ribonucleic acid
<i>mtl</i>	<i>Metallothionein</i>
MUFA	Monounsaturated fatty acid
n.s	Not significant
NAD ⁺	Nicotinamide adenine dinucleotide
NaN ₃	Sodium azide
NGM	Nematode Growth Medium
NHR	Nuclear hormone receptor
NR	Nahrungsrestriktion
OD	Optical density
p	Perimeter
PC	Phosphatidylcholine
<i>pept</i>	<i>Peptide transporter</i>
PFA	Paraformaldehyde
<i>pmt</i>	<i>Phosphoethanolamine N-methyltransferase</i>
r	Radius
RNAi	RNA interference
S	Surface
s	Second
<i>S. cerevisiae</i>	<i>Saccharomyces cerevisiae</i>
<i>sams</i>	<i>S-adenosyl-methionine synthetase</i>
<i>scl</i>	<i>Defense-related</i>
SD	Standard derivation

SEM	Standard error of the mean
<i>spp</i>	<i>Saposin-like protein</i>
SREBP	Sterol-regulatory-element-binding protein
TAG	Triacylglycerol (triglyceride)
TLC	Thin layer chromatography
TOF	Time of flight
TOR	Target of rapamycin
UGT	UDP-glucuronosyltransferase
vs	Versus

Zusammenfassung

Nahrungsrestriktion (NR) ist der einzige umweltbedingte Eingriff, der nachweislich die Lebensdauer zahlreicher Arten, von Wirbellosen bis hin zu Säugetieren, verlängern kann. Während der Einfluss von NR auf die Verlängerung der Lebensdauer bereits intensiv in dem Fadenwurm *Caenorhabditis elegans* untersucht wurde, ist wenig über die Auswirkungen von NR auf den Fettstoffwechsel in diesem Modellorganismus bekannt. Das Ziel dieser Arbeit war daher, den Einfluss von NR während der Larvenentwicklung bis zum Erreichen des adulten Stadiums auf die Körperzusammensetzung, den Fett-Phänotypen sowie auf Veränderungen in der Genexpression im Wildtyp *C. elegans* zu untersuchen.

Für diese Untersuchungen wurde ein standardisiertes NR-Protokoll entwickelt, das auf einer Verdünnungsreihe der bakteriellen Nahrungsquelle auf Festmedium und auf der Verwendung einer konstanten Anzahl von Würmern beruht. Um die Methode zu validieren, wurde die Wirkung auf bereits gut untersuchte NR-Parameter, wie die Lebensdauer und die pharyngeale Pumprate untersucht. Moderate als auch drastische NR führten zu einer erhöhten Lebensdauer. Es wurde zudem gezeigt, dass die Verminderung der Nahrungsmenge nicht durch eine eventuell erhöhte Pumprate kompensiert wird. Des Weiteren wurde der Einfluss von NR auf die Bildung des Alterungspigments Lipofuscin untersucht. Spektrofluorometrische und fluoreszenzmikroskopische Analysen ergaben, dass NR im Vergleich zur *ad libitum* Bedingung zu einer verminderten Ansammlung des Alterungspigments in adulten Würmern führte.

Um den Einfluss von NR auf die Körperzusammensetzung zu untersuchen, wurde der Triglycerid- sowie der Proteingehalt bestimmt, und das Verhältnis der Fettmasse zur fettfreien Masse berechnet. Sowohl moderate als auch drastische NR führten zu einer Zunahme der Fett- zur fettfreien Masse in Larven und in adulten Würmern. Die fixative Färbung der fettspeichernden Organellen, den *lipid droplets* (Öltröpfchen), mit Ölrot und BODIPY 493/503 zeigte, dass NR zu einer deutlichen Vergrößerung der Fettspeicher in intestinalen und hypodermalen Zellen führte. Nicht-invasive CARS (coherent anti-Stokes Raman scattering)-Mikroskopie, welche die Sichtbarmachung von Lipiden ohne Anfärbung erlaubt, bestätigte eine durch NR induzierte Vergrößerung der Fettspeicher. In den Larvenstadien L2 und L4 waren vergrößerte *lipid droplets* in beiden Zelltypen in großer Anzahl nachweisbar. Im

Unterschied dazu wurden im adulten Stadium vergrößerte Fettspeicher hauptsächlich in der Hypodermis nachgewiesen. Die quantitative Analyse von BODIPY 493/503 gefärbten *lipid droplets* ergab, dass der Volumenanteil der großen *lipid droplets* (größer als $50 \mu\text{m}^3$) am Volumen aller *lipid droplets* in restriktiv ernährten L2 und L4 Larven um das fünf- bis sechsfache höher war als in *ad libitum* ernährten Tieren.

Um mögliche Kandidatengene zu identifizieren, die an der Entstehung der beschriebenen Fett-Phänotypen beteiligt sein könnten, wurden die Genexpressionsprofile von restriktiv und *ad libitum* ernährten L4 Larven, beziehungsweise adulten Würmern verglichen. Dabei wurden zahlreiche regulierte Gene identifiziert, die funktionell der Lipogenese und der Lipolyse zugeordnet werden. Des Weiteren führte NR zu einer veränderten Expression von Genen, denen eine Funktion in der Bestimmung der Lebensdauer, im Immunsystem und bei der Entgiftung zugeschrieben wird.

Zusammenfassend konnte in dieser Arbeit gezeigt werden, dass NR während der Larvenentwicklung bis zum adulten Stadium eine Erhöhung der Fett-zur fettfreien Masse und eine Vergrößerung der Fettspeicher in Wildtyp-Nematoden bewirkt. Die Ergebnisse dieser Arbeit unterstützen die Annahme, dass die beschriebenen NR-induzierten Fett-Phänotypen eine effektive Anpassung an restriktive Nahrungsbedingungen in *C. elegans* darstellen, um Fettreserven zu konservieren, und das Überleben und die Fortpflanzung zu sichern.

Summary

Dietary restriction (DR) is an environmental intervention that extends lifespan in many species ranging from invertebrates to mammals. While DR-dependent lifespan extension has been intensively studied in the nematode *Caenorhabditis elegans*, the influence of DR on its lipid metabolism is poorly understood. In this study, the influence of DR from hatching until reaching adulthood on *C. elegans* wild-type body composition, lipid droplet phenotype and genome wide gene expression was investigated. For this purpose, a standardized DR protocol was developed based on serial dilution of living bacteria as food source on peptone-free agar plates. To each plate a defined number of nematodes was applied.

To validate the DR regime, lifespan, body proportions and pharyngeal pumping rates were determined, which are crucial parameters of DR. As expected, moderate and stringent DR prolonged lifespan and caused a reduction of the body size in adult nematodes. Further, DR did not lead to substantial changes in pumping rates. In addition, the influence of DR on the accumulation of *age-pigment* lipofuscin was determined by spectrofluorometric and fluorescence microscopic analysis. Measurements in one-day-old adult nematodes revealed that DR led to a significant decreased accumulation of this age-related marker.

To determine the body composition of dietary restricted worms, triglyceride (TAG) and protein content was measured. Unexpectedly, moderate and stringent DR increased the TAG/protein ratio of L4 larvae and adult worms, which expresses the fat-to-fat-free mass. Fixative fat staining via Oil Red O and BODIPY 493/503 as well as non-invasive coherent anti-Stokes Raman scattering (CARS) microscopy revealed that DR-induced changes in body composition were accompanied by a marked expansion of lipid droplets in the intestine and hypodermis. In L2 and L4 larvae, large-sized lipid droplets were abundant in intestinal and hypodermal cells, whereas enlarged lipid droplets of adult worms were mainly observed in the hypodermis. Quantitative analysis of BODIPY 493/503 stained lipid droplets revealed that relative to the total volume, the percentage (volume-%) of lipid droplets larger than $50 \mu\text{m}^3$ was increased by a factor of about five to six in dietary restricted L2 and L4 larvae relative to *ad libitum* condition.

Microarray-based expression profiling identified several DR-regulated genes of lipolysis and lipogenesis, which may contribute to the observed fat phenotypes. In

addition, DR also altered the expression of several genes, which have been implicated in determination of lifespan, immunity and detoxification.

In conclusion, during development, DR increases the fat-to-fat-free mass ratio, enlarges lipid droplets and alters the expression of genes functioning in lipid metabolism in wild-type *C. elegans*. The observed DR-induced fat phenotypes might be an effective adaptation in the nematode to conserve fat stores necessary for reproduction and to provide a survival advantage during nutrient-limiting conditions.

1 Introduction

1.1 Dietary restriction

Dietary restriction (DR) also referred to as caloric restriction (CR) is defined as a significant reduction of energy and macronutrient intake in the absence of malnutrition [1, 2]. DR is a fundamental nutritional intervention to reduce body weight and to decrease the risk of diabetes type 2, atherosclerosis, neurodegenerative disorders and cancer [1, 3-8]. DR has been shown to increase lifespan and healthspan in many species, ranging from invertebrates to mammals [9-15]. However, the underlying and evolutionary conserved mechanisms of these beneficial and remarkable effects of DR are partially unravelled [1, 16]. In recent years, there has been an increase in the study of DR in short-lived model organisms such as *Saccharomyces cerevisiae*, *Drosophila melanogaster* and the nematode *Caenorhabditis elegans* to uncover key regulatory factors of the DR response system.

1.2 Dietary restriction mediated longevity

Several genetic pathways that mediate DR induced longevity in *S. cerevisiae*, *Drosophila* and *C. elegans* have been identified. These include the NAD⁺-dependent protein deacetylase SIR2 [17, 18], the target of rapamycin (TOR) [19-21], the AMP-activated protein kinase AMPK [22] and the Insulin/IGF-1 signaling (IIS) cascade [23, 24]. Activation of the insulin/IGF receptor tyrosine kinases triggers a kinase cascade, which leads to inhibition of the FoxO transcription factors [24]. In *Drosophila*, insulin-like signaling converges with DR and seems to be a downstream target of DR [25]. In *C. elegans*, loss of function mutations in the Insulin/IGF-1 receptor *daf-2* or in genes acting downstream, such as *age-1*, extend lifespan [26, 27]. This effect is mediated by the transcription factor *daf-16*, a homologue of the mammalian Forkhead transcription factor FoxO [26]. However, in *C. elegans*, insulin/IGF-1 signaling and DR seem to be independent pathways in mediating lifespan extension [9, 22, 28, 29]. In addition, several DR-specific transcription factors including the Forkhead transcription factor *pha-4* [30], the Nrf2 transcription factor *skn-1* and the heat-shock transcription factor *hsf-1* were recognized as important regulators enhancing longevity in *C. elegans*. SKN-1 mediates resistance to oxidative and xenobiotic stress

[31]. HSF-1 is required for *C. elegans* immunity [32]. Thus, DR activates several pathways, which may act in parallel. Several studies in *C. elegans* indicate that the extent of lifespan extension and the involvement of pathways triggered by DR to mediate longevity are dependent on the applied DR regime [33, 34].

1.3 Dietary restriction in *Caenorhabditis elegans*

Many DR studies in *C. elegans* have been examining the effects and molecular mechanisms of DR on lifespan extension. In other studies, it has been demonstrated that DR extends the reproductive period and decreases the brood size [33, 35-38], enhances oxidative and thermal stress resistance [28, 39-41] and reduces the body size of adult nematodes [42]. Starvation decreases pharyngeal pumping rates, whereas DR leads to similar pumping rates when compared with *ad libitum* feeding condition [16, 43]. Only few studies have investigated the influence of DR on *C. elegans* fat phenotype. DR in liquid medium and dietary deprivation result in a pale, lipid depleted phenotype due to the mobilization of intestinal fat stores [44-46].

To date, a number of protocols exist to subject *C. elegans* to DR. Under laboratory conditions, *C. elegans* is usually fed with *Escherichia coli* (*E. coli*) OP50 that have been cultivated on Nematode Growth Medium (NGM) agar plates. One common strategy to generate DR is the limitation of *E. coli* growth on solid medium by UV, heat or antibiotic treatments. The reduction of bactopectone in the NGM agar plates is another strategy to control growth of *E. coli* [11, 35, 42]. Dietary deprivation, the cultivation of *C. elegans* on plates in absence of bacteria is usually performed in adult animals [39, 40, 47]. In liquid media, DR is induced by dilution of *E. coli* in S-Basal medium [28, 30, 37, 46], the use of undefined axenic medium [10] and chemically defined liquid medium (CeMM) [38]. The use of feeding defective mutants, such as *eat-2*, is a further approach to study DR in *C. elegans* [9]. However, none of these DR methods have been yet established as the standard protocol. Rather, the applicability of a DR-method may depend on the biological issue.

1.4 Lipid metabolism in *C. elegans*

Although *C. elegans* is distant from mammals, a majority of about 400 genes identified being involved in lipid storage in *C. elegans* have human homologs [48]. Thus, during the last years, the nematode has become an important model to study the regulation of energy metabolism and lipid storage in the context of the whole organism. Many mammalian metabolic pathways, such as fatty acid (FA) synthesis, elongation and desaturation, mitochondrial and peroxisomal β -oxidation of fatty acids are also found in the nematode. A number of genes involved in pathways that regulate lipid homeostasis in mammals are assumed to control lipid storage as well in *C. elegans*. These pathways include serotonin, insulin, transforming growth factor- β (TGF- β) and TOR kinase signaling [48-52]. In addition, many mammalian transcription factors involved in fat accumulation are also present in the nematode. For example, the *C. elegans* transcription factors SBP-1 and NHR-49 are homologues to the human sterol-regulatory-element-binding protein (SREBP) and peroxisome proliferator-activated receptor- α (PPAR α), respectively [45, 48, 53, 54]. SREBPs are crucial regulators of cholesterol and FA homeostasis [55]. The Forkhead FoxO transcription factor *daf-16* is involved in the regulation of genes predicted to participate in fatty acid metabolism in *C. elegans* under the control of the *daf-2*/insulin-like pathway [56-58]. Loss of the insulin receptor DAF-2 increases fat accumulation through activation of DAF-16 [59].

Besides those similarities *C. elegans* fat metabolism differs from mammals in many aspects. Since *C. elegans* lacks specialized adipose tissues fat is primarily stored in intestinal and hypodermal cells [60]. Unlike mammals, *C. elegans* is cholesterol auxotroph and requires supplementation from the diet. Moreover, the nematode is able to *de novo* synthesize all its mono- and polyunsaturated fatty acids (FAs) as it possesses the full set of required desaturases ($\Delta 3$, $\Delta 5$, $\Delta 6$, $\Delta 12$ and three $\Delta 9$ desaturases) and elongases. Thus, in contrast to mammals, *C. elegans* is not dependent on external supply of essential FAs such as linoleic acid and linolenic acid.

FAs are components of mono-, di- and triglycerols, phospholipids, cholesterol ester and sphingolipids that have multiple functions in the organism. Triglycerides (TAGs), which are composed of three fatty acids esterified to glycerol, are the major long-term

energy storage form in animals [61]. FAs are the main component of cellular membranes and have crucial roles in selective permeability, membrane fluidity and signaling pathways [61, 62]. The balance between saturated and monounsaturated FAs (MUFAs) is an important factor for the membrane fluidity, and the appropriate ratio is maintained by the activity of $\Delta 9$ desaturases [63].

1.5 Lipid droplets as fat storage organelles

Recently, Zhang *et al.* (2010) provided evidence that lipid droplets (LDs) are ubiquitous fat storage organelles in *C. elegans* that are morphologically and functionally distinct from intestinal lysosomes and lysosome-related organelles [64]. LDs are conserved eukaryotic organelles for storage of neutral lipids, including TAGs and cholesterol esters [65, 66]. The neutral LD core is surrounded by a phospholipid monolayer and associated proteins [67]. A large number of proteins that bind to the LD surface have been identified in mammals, *Drosophila* and *C. elegans*. These include lipid synthesis enzymes (e. g. acyl-CoA synthetase, acyl-CoA:diacylglycerol transferase [68, 69]), lipases (e.g. adipose triacylglycerol lipase (ATGL) [64, 70, 71]), structural proteins (e. g. perilipin and CIDE proteins [72, 73]), and membrane-trafficking proteins (Rab proteins [69, 74-76]). The number and size of LDs can dynamically change in response to varying environmental and physiological conditions via both, metabolic pathways and coat proteins.[77]. For instance, excess of free FAs promotes TAG synthesis and storage to protect cells from lipotoxicity subsequently leading to an increased LD volume [78]. Under nutrient limiting conditions, lipids can be rapidly released from LDs by the activity of lipases [79-81]. However, the regulating mechanisms that control LD number and size are not well understood.

In *C. elegans*, the number and size of LDs increases throughout life history [82]. Intestinal fat tends to accumulate in larger-sized droplets relative to smaller-sized droplets in hypodermal cells [82]. In response to adverse environmental conditions (e.g. food limitation, high population density and high temperatures), larval animals can enter an alternate life history trade known as the dauer state [83-85]. Dauer larvae are metabolically arrested and stress-resistant long-lived juvenile forms [86, 87]. Defects in the IIS pathway, for example mutations in *daf-2* and *age-1*, result in dauer formation even under nondauer inducing conditions. Dauer formation is

characterized by an accumulation of fat stores resulting in a greater number and size of LDs (Table 1) [49, 82].

1.6 Lipid droplet enlargement in *C. elegans*

Several studies in *C. elegans* have identified metabolic pathways that seem to be essential for the regulation of LD size in *C. elegans* (Table 1). Genetic defects in genes encoding enzymes of the MAOC-1/DHS-28/DAF-22 peroxisomal β -oxidation pathway cause selective LD expansion in *C. elegans* intestinal cells [64, 88]. Enlargement of LDs in *dhs-28* and *daf-22* mutant animals was accompanied by an increase of lipolysis-resistant TAGs levels. Further, loss of acyl-CoA synthetase-3 (ACS-3) involved in mitochondrial β -oxidation led to the formation of large intestinal LDs due to an elevated FA uptake and increased *de novo* lipid synthesis [71]. LD expansion has been also reported for *C. elegans* mutants deficient for the KLF-3/Krüppel-like transcription factor [89].

Table 1. Genes involved in lipid droplet expansion in *C. elegans* mutants

Gene	Description	Metabolic process	fat content	Quantification ^b	Reference
<i>daf-2^a</i>	Insulin/IGF receptor	insulin/IGF-1 signaling	increased	CARS	[82]
<i>maoc-1</i>	Hydratase	Peroxisomal β -oxidation	increased	FS, TLC, GC	[64]
<i>dhs-28</i>	Dehydrogenase	Peroxisomal β -oxidation	increased	FS, TLC, GC	[64, 88]
<i>daf-22</i>	Thiolase	Peroxisomal β -oxidation	increased	FS, TLC, GC	[64, 88]
<i>acs-3</i>	Acyl-CoA synthetase	Mitochondrial β -oxidation	increased	FS	[71]
<i>lbp-5</i>	Lipid binding protein	Lipid binding	increased	FS, EA	[90]
<i>acbp-1</i>	acyl-CoA binding protein	Lipid binding	decreased	CARS, EA	[91]
<i>sams-1</i>	S-adenosyl-methionine synthetase	Phospholipid synthesis	increased	FS, TLC	[92, 93]
<i>pmt-1</i>	Phosphoethanolamine N-methyltransferase	Phospholipid synthesis	increased	FS, TLC	[92, 93]
<i>klf-3</i>	Krüppel-like transcription factor	Transcription factor	increased	FS, GC	[89]
<i>pept-1</i>	Peptide transporter	Amino acid transporter	increased	FS,GC	[94]

^a*daf-2*(e1370) L2 larval stage

^bFat content in mutant animals was quantified by fat staining (FS), coherent anti-Stokes Raman scattering (CARS) microscopy, enzymatic triglyceride assay (EA), thin layer chromatography (TLC), gas chromatography (GC).

KLF-3 regulates the transcription of genes encoding enzymes of mitochondrial and peroxisomal β -oxidation as well as FA desaturation (*acs-2*/acyl-CoA synthetase, F08A8.1/acy-CoA oxidase and *fat-7*/ $\Delta 9$ desaturase). Loss of functional LBP-5/lipid-binding protein and ACBP-1/acyl-CoA-binding protein, which are involved in the intracellular transport of FAs and fatty acyl-CoA, respectively, have been also reported to cause enlarged LDs [90, 91]. Moreover, impaired phosphatidylcholine synthesis caused enlarged LDs in intestinal cells of *sams-1* and *pmt-1* mutant animals [92, 93]. Mutation in the peptide transporter *pept-1* gene caused an drastic enlargement of LDs due to an enhanced influx of free FAs into intestinal cells [94]. Whether environmental or nutritional factors can lead to LD expansion in wild-type animals has not been investigated yet.

Little is known about the effects of DR on lipid metabolism and lipid storage in *C. elegans*. In this study, we have investigated the impact of DR during development from hatching until reaching adulthood on the body proportion, body composition and fat distribution in *C. elegans*. For this purpose, we have optimized a modified solid medium based DR protocol [41], in which bactopectone is excluded from the agar plates and the addition of antibiotics is not required. Wild-type worms cultivated under this DR regime exhibited a reduced body size in adulthood, an extended lifespan and decreased accumulation of *age pigment*. Surprisingly, DR increased the fat-to-fat-free mass ratio and led to an enlargement of LDs in larval and adult wild-type animals. To gain an insight into underlying mechanisms of these DR induced phenotypes, whole genome gene expression analysis was performed. Among the DR regulated genes, we found an enrichment of genes being involved in lipid metabolism. These genes might contribute to the DR induced fat phenotypes. In addition, DR significantly altered the expression of genes involved in lifespan extension, immune defense and detoxification.

2 Materials and Methods

2.1 Strains and Maintenance

Wild-type *C. elegans* Bristol N2 and mutant strain *daf-2(e1370)* were used. Nematodes were cultivated at 20 °C on Nematode Growth Medium (NGM) agar plates seeded with *E. coli* OP50 as food source [95]. Strains were obtained from the *Caenorhabditis* Genetics Center (Minnesota, USA).

2.2 Dietary restriction on agar plates

To induce DR on agar plates, bactopectone (BD, Heidelberg, Germany) was omitted from the standard NGM recipe [41, 95]. The *E. coli* OP50 suspension was cultivated in DYT medium at 37 °C until reaching an optical density (OD_{600nm}/ml) of 1.5. A serial dilution of *E. coli* OP50 suspended in M9 buffer was prepared ranging from OD₆₀₀=6.0 to OD₆₀₀=0.3. For DR conditions, 250 µl of the respective *E. coli* suspension was seeded onto the DR plates. For *ad libitum* (AL) condition, standard NGM agar seeded with *E. coli* OP50, OD₆₀₀=1.5 was used. Plates were incubated at 37 °C for 16 h. For all experiments, nematodes were synchronized by hypochlorite treatment of gravid adults. To standardize food availability, 500 eggs per plate were sorted via a cytometry-based *complex object parametric analyzer and sorter* (COPAS Biosort, Union Biometra, Geel, Belgium) and cultivated at 20 °C until reaching the L2, L4 or adult stage. Animals were transferred onto fresh plates in the L4 stage to prevent starvation.

2.3 Preparation of worm homogenates and biochemical measurements

Wild-type nematodes were cultivated under AL and two different DR conditions (DR0.7, DR1.5) until reaching L4 and adult stage, respectively. For each replicate, 2000 to 2500 L4 larvae and 800 to 1000 adult worms were collected via the COPAS Biosort system. Animals were homogenized in 100 µl buffer (150 mM NaCl; 1 mM EDTA; 50 mM Tris-HCl, pH7.5; 0.5 % CHAPS) using the Precellys 24 homogenizer (Peqlab, Erlangen, Germany) and ceramic beads (1.4 mm diameter). Cell debris was removed by centrifugation at 21,000 *g* for 20 min. Homogenates were used in 96-well format for colorimetric determination of the TAG and protein content as well as for

quantification of autofluorescent *age pigment*. The TAG content was determined using an enzymatic assay (Analyticon diagnostics, Lichtenfels, Germany) and a TAG standard (Biovision, Hannover, Germany) according to the manufacturer's directions. The protein content was measured using the Pierce[®] BCA protein assay kit (Thermo Fisher Scientific, Bonn, Germany) and bovine serum albumin (BSA) as protein standard.

2.4 Determination of the body proportion

Wild-type worms cultivated under AL and different DR conditions (DR0.3 to DR6.0) were harvested in L2, L4 and adult stage and anesthetized in 2 % NaN₃. Bright-field microscopy images were obtained using a Zeiss Axio Observer.D1 inverted microscope equipped with an AxioCam MRm camera (Zeiss, Jena, Germany). Magnification of animals was 50-fold (5x/0.12 objective). Length (μm), width (μm), perimeter (μm) and area (μm^2) of single worms was obtained using the AxioVision software (Release 4.8, Zeiss, Jena, Germany). The body volume (nl) was calculated using an adapted cylinder volume formula, which includes the worm's area and perimeter [96, 97]. In addition, time of flight (TOF; arbitrary unit, AU) and extinction (AU) of single nematodes were measured via a COPAS Biosort. TOF and extinction values are approximate values for the axial length and volume of the worms, respectively [98]. Using flow cytometry, 500 to 2,000 animals were analyzed for each condition in three independent experiments.

2.5 Motility and pharyngeal pumping rate

For analysis of animal motility and pharyngeal pumping rate, 10 animals per agar plate were cultivated under AL and two different DR conditions (DR0.7, DR1.5), respectively. Single nematodes were analyzed at the first day of adulthood using a Zeiss SteREO Discovery V8 binocular microscope (Zeiss, Jena, Germany). For analysis of animal motility, single worms were recorded for 20 seconds at 8.0-fold magnification using a Zeiss AxioCam ICc 1 and Zeiss AxioVision software (Release 4.8). A worm tracking software (WormTracker 2.0.25, Thomas Bornhaupt, Neustadt adW., Germany) was used to calculate the body bending frequency (Hz), whole animal motility (mm s^{-1}) and head motility (mm s^{-1}) [99]. For measurements of the pharyngeal pumping rate, the pharynx was filmed for 40-60 seconds at 63-fold

magnification using a Canon camera (Legria HF20). The pharyngeal pumping rate (pumps/min) was counted on slowed films. 20 randomly chosen animals were recorded for each condition in three independent experiments.

2.6 Lifespan experiments

Wild-type strain N2 and *daf-2(e1370)* mutant were used for lifespan analysis. All experiments were performed at 20 °C. Synchronized animals were cultivated under AL and two different DR conditions (DR0.7, DR1.5). *daf-2* mutants were exclusively grown under AL condition. At L4 stage, larvae were washed off the plates and transferred onto fresh NGM agar (10 animals per plate) using the COPAS Biosort system. NGM plates were prepared with a ring consisting of 2 % palmitic acid (w/v) dissolved in absolute ethanol to prevent animals escaping from the plates [100]. Worms were transferred onto fresh plates daily during the egg-laying period. After the reproductive period, animals were transferred every second day. Animals that did not move after repeated stimulus were considered as dead. Animals that crawled away from the plate or with bursted vulva were excluded from the analysis. The total number of 100 animals was used for each feeding condition and experiment. All lifespan experiments were performed three times. Maximum lifespan was defined as the mean of the 10 % long lived animals.

2.7 Age pigment measurements

Analysis of autofluorescent *age pigment* was performed by fluorescence microscopy and spectrofluorometrically [101]. Wild-type animals grown under AL and two different DR conditions (DR0.7, DR1.5) were harvested at day one of adulthood. For microscopic analysis, animals were incubated in 2 % NaN₃ and washed twice in M9 buffer. A Zeiss Axio Observer D1 inverted microscope (Zeiss, Germany) with the filter set 49 (excitation G 365; beam splitter FT 395; emission BP 445/50) and a 20x/0.50 M27 objective was used to visualize autofluorescent *age pigment* in the intestine. Images were captured with an Axiocam MRm camera. 10-15 animals were imaged for each condition and experiment. Three biological replicates were performed. Spectrofluorometric quantification of *age pigment* in worm homogenates was performed in a 96 well format. The volume of each homogenate was adjusted to 9 µg protein per well. The total volume per well was adjusted to 100 µl with H₂O_{bidest} and

NET-CHAPS. *Age pigment* fluorescence intensity was determined using a Tecan spectrofluorometer (Tecan infinite[®] M200, Crailsheim, Germany) at an excitation of 340 nm and an emission of 380 nm [101]. The homogenates of three independent biological replicates for each condition were measured three times.

2.8 Oil Red O staining

AL fed and dietary restricted (DR0.7, DR1.5) wild-type worms were harvested at day one of adulthood. Animals were washed in PBS buffer and fixed with 4 % paraformaldehyde (PFA) for 15 min. After three freeze and thaw cycles in liquid nitrogen, worms were washed in PBS buffer, followed by a dehydration step in 60 % isopropanol. Animals were stained in filtered Oil Red O staining solution (60 % Oil Red O stock solution (5 mg/ml isopropanol)/40 % H₂O_{bidest}) over night. After washing in PBS, worms were analyzed using an Axio Observer D1 inverted microscope (Zeiss, Germany). Photographs of 10-15 worms per feeding condition were taken by AxioCam MRm camera (Zeiss, Germany) and a 20x/0.50 M27 objective at a fixed exposure time. All experiments were performed three times.

2.9 BODIPY[™] 493/503 staining

Synchronized wild-type worms grown under either AL or DR condition (DR0.7, DR1.5) were harvested at different developmental stages (L2, L4, adulthood). Fixative BODIPY[™] 493/503 (Invitrogen, Darmstadt, Germany) staining was performed as previously described [98]. Briefly, animals were washed in M9 buffer and incubated for 15 min in 4 % PFA. After three times of freeze/thaw in liquid nitrogen, animals were washed in M9 buffer and stained with BODIPY[™] 493/503 (1 µg/ml M9 buffer, stock solution 1 mg/ml in DMSO) for 1 h. After final wash steps, animals were used for microscopic analysis. To image BODIPY[™] 493/503 fluorescence signals in whole animals, a Zeiss Axio Observer D1 inverted microscope and the filter 38HE (excitation, BP 470/40; beam splitter FT 495; emission BP 525/50) was used. Images were taken by an AxioCam MRm camera (Zeiss, Germany) at fixed exposure times. Objects were magnified using a 20x/0.50 M27 objective. Photographs were taken from 25-50 animals per condition. All experiments were performed four to five times.

2.10 Determination of number and size of lipid droplets

To determine the number and size of lipid droplets, BODIPYTM 493/503 positive structures in pharynx and tail region of L2, L4 and adult staged wild-type animals were imaged using confocal laser scanning microscopy (Leica TCS SP). A HCX PL APO CS 63.0x/1.32 oil immersion objective and Leica LAS AF software was used to collect z-stacks with a step size of 0.5 μm (image format: 158x158 μm^2 , 1024x1024 pixels). Z-stacks consisted of 20 to 110 plane images depending on the position and developmental stage of the animal. Images of eight to ten animals per condition and developmental stage were taken using identical settings and exposure times. Z-stacks of pharynx and tail regions were analyzed using ImageJ software (version 1.42q, Object Counter3D plugin [102, 103]). BODIPYTM 493/503 positive droplets were automatically identified via adaptive thresholding. The volume (μm^3) of each droplet was calculated by summing up the voxels. The total droplet number, total droplet volume and mean droplet volume in pharynx and tail region was calculated using Microsoft Office Excel 2003 software. The volume of BODIPYTM 493/503 positive droplets was classified into different categories: 0-10 μm^3 (0-2.66 μm in diameter), 10-25 μm^3 (2.67-3.63 μm in diameter), 25-50 μm^3 (3.64-4.57 μm in diameter) and >50 μm^3 (>4.57 μm in diameter).

2.11 Imaging of lipid droplets by coherent anti-Stokes Raman scattering microscopy

CARS microscopy was performed at the group of Prof Dr. Andreas Zumbusch (Department of Chemistry, University of Konstanz, Germany) using a custom setup based on a TCS SP5 MP confocal and a multiphoton microscope (Leica, Wetzlar, Germany). Pump pulses were generated by a Ti:sapphire laser centred at 720 nm (Coherent Mira, Santa Clara, CA). As excitation source for the Stokes beams (905.5 nm), the output of an optical parametric amplifier/oscillator (APE, Berlin, Germany) was used. Both laser beams were electronically synchronized (Coherent SynchroLock, Santa Clara, CA). Images were generated at a laser frequency difference of 2,845 cm^{-1} corresponding to the aliphatic CH vibrational resonance. The anti-Stokes signal was detected at 597 nm in forward direction by a photomultiplier. Objects were 400-fold magnified using an oil immersion objective. For sample preparation, worms were washed twice in M9 buffer, resuspended in 2 % NaN_3 ,

placed on a glass slide and covered with a second slide. Z-stacks of CARS microscopy images were generated using the Leica ALS AF software (Lite, Version 2.1.1 build 4443). Z-stack consisted of 16-47 plane images covering an area of $246.03 \times 92.13 \mu\text{m}^2$ (1200x600 pixels) in the xy plane and a depth of 22.5-36.0 μm (step size 1.5 μm) along the z axis depending on the covered region and size of the animal. Plane images of the pharynx, central and tail region of each nematode were captured.

2.12 Whole genome gene expression analysis

Synchronized wild-type worms cultivated under AL or DR conditions (DR0.7, DR1.5) were harvested at L4 and adult stage. After washing in M9 buffer, worms were resuspended in 350 μl RTL buffer (RNeasy Mini Kit, QIAGEN, Hilden, Germany), disrupted in the Precellys 24 homogenizer (Peqlab, Erlangen, Germany) and subjected to an additional homogenization step using QIAshredder spin columns (QIAGEN, Hilden, Germany). Total RNA was isolated using the RNeasy Mini Kit. On-column DNAase digestion was performed to eliminate genomic DNA (RNase-Free DNase Set, QIAGEN, Hilden, Germany). The quality and yield of the preparation was assessed using a 2100 Bioanalyzer (Agilent Technologies, Waldbronn, Germany).

Labeled cRNA was generated, hybridized and processed by imaGenes expression profiling service (Berlin, Germany) using customized 8x60K *C. elegans* Agilent microarrays (imaGenes/SourceBioscience, Steffen Hennig). Normalization was done by 'quantile normalization' using the R-package [104]. After normalization, each data set included 26,843 gene expression values of four biological replicates for DR and AL treated control group. Fold-changes of intensities were calculated from the arithmetic mean of gene expression values between DR and AL group (L4 stage: DR1.5 vs AL, DR0.7 vs AL; adult stage: DR1.5 vs AL, DR0.7 vs AL). The significance was calculated using an unpaired t-test with unequal variance (Welch-test). P values $p > 0.05$ were considered as not significant. Genes with a fold-change > 2.0 were considered as differentially regulated.

2.13 Statistical analysis

Statistical analysis was performed with Microsoft Excel (2003) and GraphPad Prism (Version 4.0). Significances were calculated using one-way ANOVA and unpaired t-test (two tailed). Welch-correction was used if variances were different. Logrank t-test was used for lifespan analysis. Differences were considered statistically significant at $p < 0.05$ (*), $p < 0.01$ (**) and $p < 0.001$ (***)

The DR protocol was optimized in order to study the effect of DR during development from hatching until reaching adulthood on body composition and fat distribution of the worms. This method allows a standardized variation of the extent of DR without starvation, dauer formation or developmental arrest of the animals. In brief, adjusted optical densities (250 μ l, OD₆₀₀ = 0.3 to 6.0, represents DR 0.3 to 6.0) of *E. coli* strain OP50 were spread onto antibiotic-free agar plates and were incubated for 16 h at 37 °C. For DR conditions, bactopectone as sole carbon source for bacterial growth was omitted from the NGM. This leads to different optical densities of bacteria per agar plate depending on the OD of seeded OP50 (e. g. DR 1.5: OD₆₀₀ = 0.56 \pm 0.05; DR 0.7: OD₆₀₀ = 0.32 \pm 0.03; mean \pm SD). For AL condition, standard NGM was used resulting in a thick bacteria lawn (OD₆₀₀ = 25.85 \pm 1.19). To standardize food availability per worm, 500 synchronized embryos were sorted onto AL and DR agar plates by flow cytometry and were cultivated at 20 °C until reaching the L2, L4 or adult stage. To exclude starvation, worms were transferred in L4 stage to fresh agar plates.

3.2 Influence of dietary restriction on body size

To evaluate the DR protocol, the body proportion of AL and DR fed adult wild-type worms was determined. Data derived from bright-field microscopy images (Figure 2 A-D, Table 2). We found that decreasing bacteria concentrations on DR plates led to a continuous decrease in body width (Figure 2 B), length (Figure 2 C) and volume (Figure 2 D). Marginal or no effects were observed at mild DR conditions (DR6.0, DR3.0). Under moderate (DR1.5 and DR1.0) and harsh DR conditions (DR0.7 and DR0.3), the body size parameters were drastically reduced. Interestingly, the body width decreased to a greater extent than the length. At the most stringent DR condition (DR0.3), width declined to approximately 68 %, whereas length was reduced to about 74 % when compared with AL fed worms (Table 2). The body volume of DR0.3 fed worms (1.3 nl) decreased by a factor of 3 (34.8 \pm 2.1 % of AL). Flow cytometry based TOF (time of flight) and extinction (ext) values, which serve as approximations for length [98] and volume of the worm, confirmed the microscopic body proportion measurements in a large number of worms (Figure 2 E,F). Together, we obtained an inverse linear relationship between the extent of DR (0.3 to 6.0) and body size reduction demonstrating dose dependency of our DR regimes.

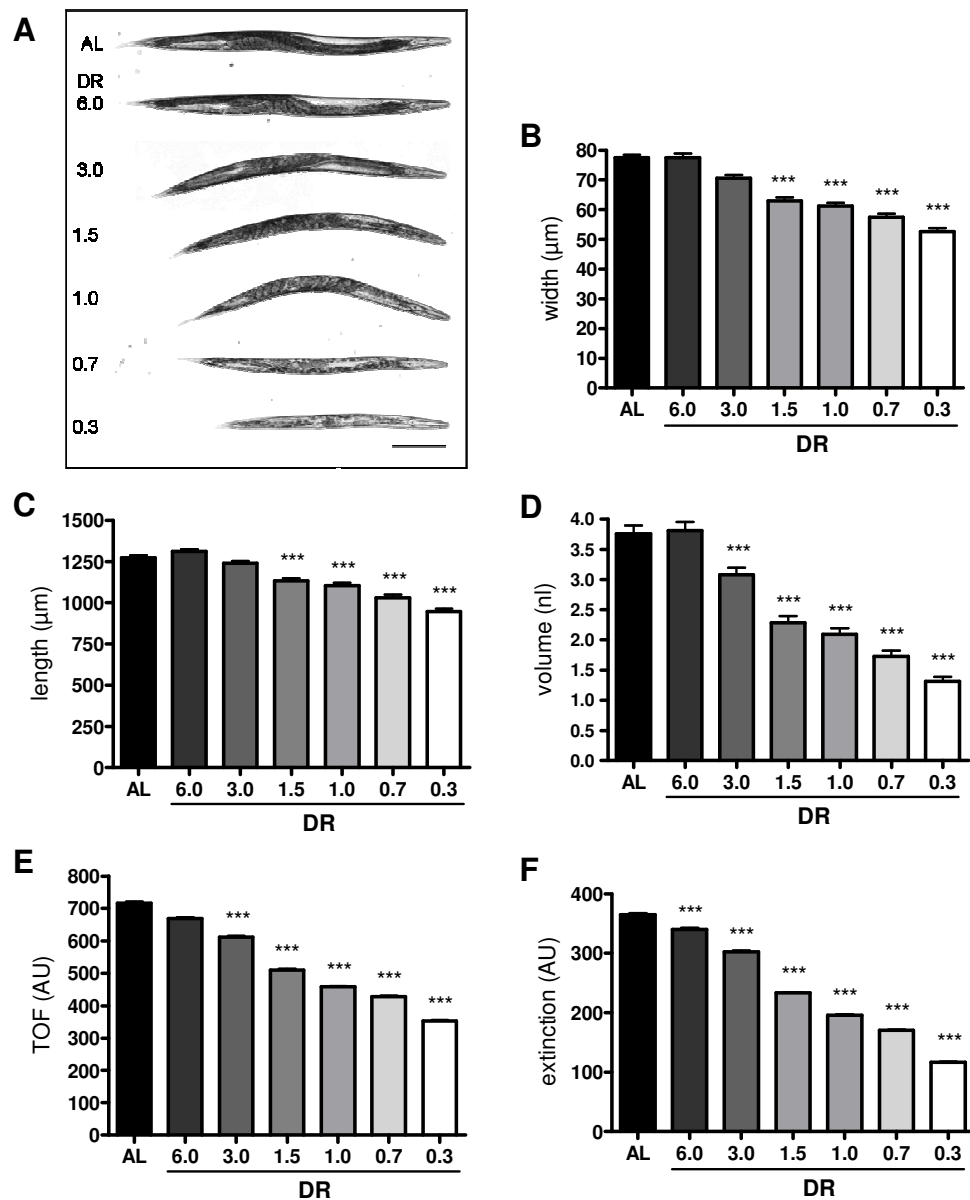


Figure 2. Influence of dietary restriction on body proportion

Wild-type nematodes were cultivated under AL or specified DR condition and analyzed at first day of adulthood. (A) Representative bright-field microscopy photographs of nematodes ($n > 50$ per condition) in dependence on OP50 density. The anterior part is on the right. Magnification 50x; scale bar, 200 μm . (B-D). Data for body width (μm), length (μm) and volume (nl) of single worms ($n > 50$ per condition) derived from bright-field microscopy images. The body volume was calculated using a worm adapted cylinder volume formula, which includes area and perimeter of single animals. Comparative calculations between AL and DR treated animals are provided in Table 2. (E, F) Time of flight (TOF, AU) and extinction (AU) values ($n > 500$ per condition) were collected by COPAS Biosort system. Significant differences were analyzed using ANOVA followed by an unpaired t-test of AL and respective DR condition. Bars represent a mean \pm SEM from two to three independent experiments (** $p < 0.001$). AU = arbitrary unit.

Table 2. Body proportion of *C. elegans* cultivated at different dietary restriction conditions

Extent of DR	Width (% of AL)	Length (% of AL)	Volume (% of AL)
DR 6.0	100.05 ± 1.78	102.94 ± 1.12	101.27 ± 3.94
DR 3.0	91.06 ± 1.34	97.39 ± 1.11	81.88 ± 3.11
DR 1.5	81.22 ± 1.52	89.06 ± 1.19	60.67 ± 2.95
DR 1.0	79.01 ± 1.38	86.72 ± 1.26	55.62 ± 2.68
DR 0.7	74.19 ± 1.55	80.97 ± 1.40	45.86 ± 2.74
DR 0.3	67.82 ± 1.54	74.28 ± 1.40	34.83 ± 2.08

Results for width, length and volume of adult wild-type worms grown at denoted DR conditions are shown as percent of AL treated control group (mean ± SD for AL: width = 77.54 ± 0.94 μm, length = 1274 ± 12.08 μm, volume = 3.76 ± 0.13 nl). Data derived from bright-field microscopy images (see Figure 2). For calculations, the total number of worms per condition was n>50. Results are represented as mean ± SEM of two to three independent experiments.

For further experiments, one moderate (DR1.5) and one more stringent (DR0.7) DR condition was used. In order to examine whether DR has an influence on larval body size, the body volume of L2 and L4 larvae was calculated from microscopic images (Figure 3). Under AL condition, body volume of L2 larvae was in mean 0.075 μm³ (± 0.005, SEM), while L4 animals exhibited a mean body volume of 0.58 μm³ (± 0.011). Body volume of dietary restricted L2 larvae was similar at DR0.7 and even slightly increased at DR1.5 when compared to AL fed animals. In addition, a slight increase in body size was observed in L4 larvae cultivated at moderate and stringent DR condition (Figure 3 A,B). Thus, a DR-dependent reduction in body size was initially found at the adult stage (Figure 3 C).

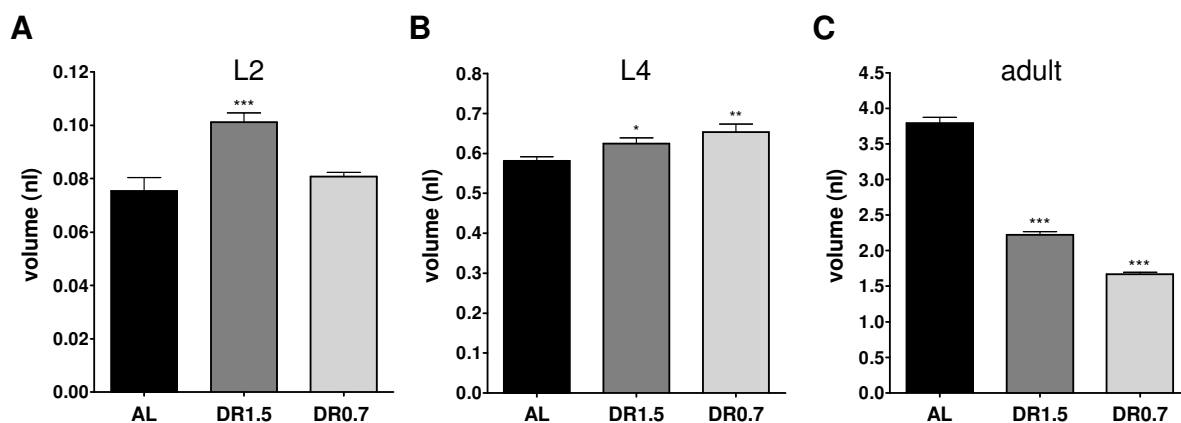


Figure 3. Influence of dietary restriction on body volume of larvae and adult worms

Wild-type nematodes were cultivated under AL and two different DR conditions (DR1.5, DR0.7) and harvested at (A) L2 stage, (B) L4 stage and (C) first day of adulthood. Animals were used for bright-field microscopy. Body volume (nl) was calculated from microscopy images of 15-25 worms per feeding condition and experiment using a worm adapted cylinder volume formula. Data derived from four independent experiments. Data are shown as mean \pm SEM. Significant differences were calculated between AL and respective DR condition using unpaired t-test (* $p < 0.05$, ** $p < 0.01$, *** $p < 0.001$).

3.3 Influence of dietary restriction on locomotion and feeding rates

Motility may confound effects of DR on body composition and fat distribution. Therefore locomotion parameters of adult worms on agar plates were analyzed using a computer tracking system. Moderate (DR1.5) as well as stringent DR (DR0.7) did not change body bend frequency in relation to AL condition (Figure 4 A). Likewise, whole animal motility of AL and dietary restricted worms was similar (Figure 4 B). Moderate DR slightly increased the head motility of worms, whereas no significant modification was observed at DR0.7 (Figure 4 C; AL: $0.070 \pm 0.002 \text{ mm s}^{-1}$, DR1.5: $0.088 \pm 0.002 \text{ mm s}^{-1}$, DR0.7: $0.080 \pm 0.003 \text{ mm s}^{-1}$; mean \pm SEM). The increase in head motility might indicate an alteration in the food seeking behaviour during DR.

Pharyngeal pumping frequency is often used as an indicator for the *C. elegans* feeding rate, and its decrease is a crucial DR parameter [33, 105]. AL fed adult worms exhibited pumping rates ($299.0 \pm 2.4 \text{ pumps/min}$; mean \pm SEM) that were in agreement with literature data [106]. Exposure of worms to DR1.5 induced a slightly decrease in pharyngeal pumping whereas cultivation at DR0.7 led to similar pumping rates relative to AL condition (Figure 4 D, DR1.5: $278.9 \pm 2.97 \text{ pumps/min}$, DR0.7:

287.1 ± 5.25 pumps/min). In summary, results indicate that dietary restricted worms do not compensate the reduced food supply by substantial changes in their locomotion behaviour or by increased feeding rates.

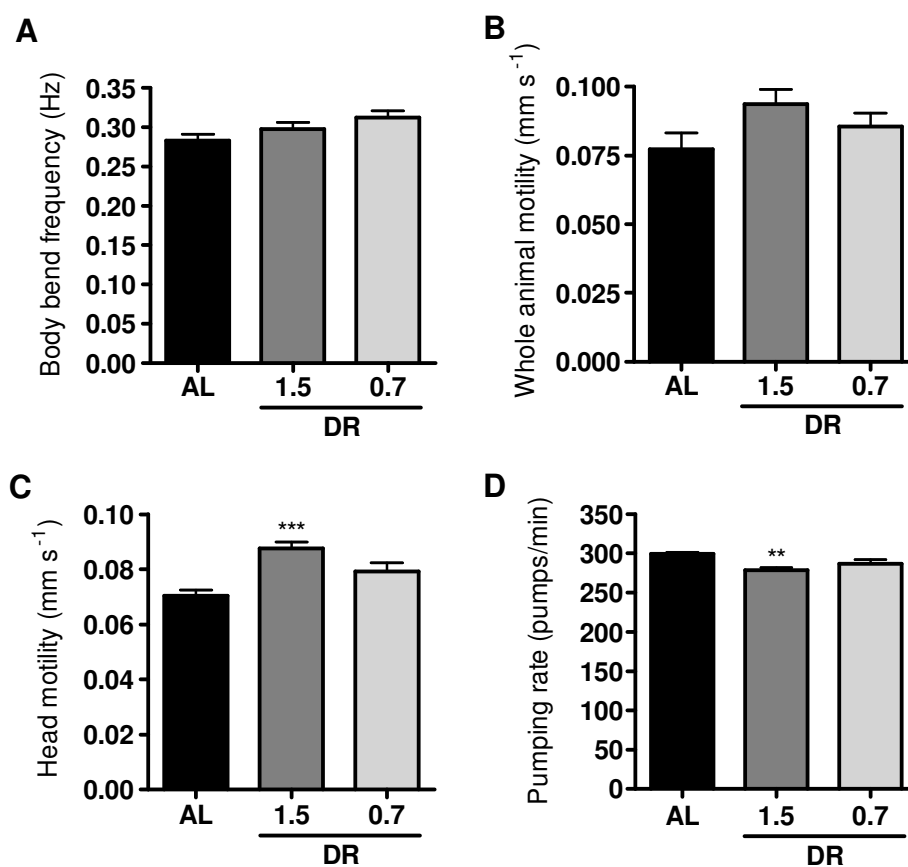


Figure 4. Influence of dietary restriction on motility and pumping rate

Body bend frequency (A), whole animal motility (B) and head motility (C) of dietary restricted (DR1.5 and DR0.7) and AL fed wild-type worms were analyzed using a worm tracking software (see Materials and Methods). Nematodes were analyzed at first day of adulthood. (A) Results for body bend frequency (Hz) are represented as mean ± SEM of three experiments with 20-30 animals each. (B, C) Bars represent mean motilities (mm s⁻¹) ± SEM of three experiments with 20 individuals each (***)p<0.001). (D) Mean pharyngeal pumping rate of adult wild-type worms cultivated at either AL or DR condition (DR1.5, DR0.7) was obtained from three experiments with 15-20 individuals each. Error bars represent a SEM. Significant decrease in pharyngeal pumping of DR1.5 worms is indicated by asterisks (**p<0.01). Significant differences were analyzed using unpaired t-test and are always understood between AL and respective DR condition.

3.4 Influence of dietary restriction on lifespan and *age pigment* accumulation

Lifespan extension is a well established effect of DR. Thus, lifespan analysis was performed in order to validate the DR protocol (Figure 5 A, Table 3). In comparison to AL fed worms (16.7 ± 5.4 d for mean, 29.4 ± 4.0 d for maximum lifespan), the mean

and maximum lifespan of DR1.5 treated worms was significantly increased (22.6 ± 5.7 d, 31.4 ± 1.8 d). At DR0.7, we observed a further increase in mean and maximum lifespan relative to moderate DR condition (24.9 ± 5.7 d, 32.9 ± 1.7 d). As reported [26], a considerable increase in lifespan was also observed for the *daf-2* mutant (29.7 ± 12.7 d for mean, 55.5 ± 1.4 d for maximum lifespan), which served as a control in this study.

Table 3. Mean and maximum lifespan of dietary restricted *C. elegans*

	AL	DR1.5	DR0.7	<i>daf-2</i>
Mean	16.7 ± 5.4	22.6 ± 5.7 ***	24.9 ± 5.7 ***	29.7 ± 12.7 ***
% increase		35.5 ± 10.2	49.2 ± 18.0	78.0 ± 11.9
Maximum	29.4 ± 4.0	31.4 ± 1.8 ***	32.9 ± 1.7 ***	55.5 ± 1.4 ***

Data are represented as mean lifespan and percent of AL from three independent experiments. Maximum lifespan was calculated from the average age at death of the 10th percentile survivors. Errors demonstrate standard deviation (\pm SD). P values were calculated between AL and respective DR using unpaired t-test (*** $p < 0.001$).

Several studies indicate that DR does not only extend lifespan but also retards aging with regard to senescence and age-related diseases [101, 107, 108]. Conserved age-associated biomarkers including autofluorescent lipofuscin and advanced glycation end-products have been identified to accumulate during aging from nematodes to humans [109, 110]. To test whether DR leads to a reduced *age pigment* accumulation, lipofuscin autofluorescence intensity was analyzed via fluorescence microscopy. In accordance to literature [101, 111], autofluorescent *age pigment* was detected in the intestine of the worms accumulating in small granules (Figure 5 B). At first day of adulthood, autofluorescence intensities obtained from dietary restricted worms were significantly lower than in AL fed animals. This decrease in *age pigment* was confirmed by quantitative spectrofluorometric analysis [101] in worm homogenates (Figure 5 C). In comparison to AL condition, DR reduced *age pigment* levels per worm to 70 % (DR1.5) and 40 % (DR0.7). Thus, moderate and stringent DR conditions extend mean and maximal lifespan and reduce *age pigment* accumulation.

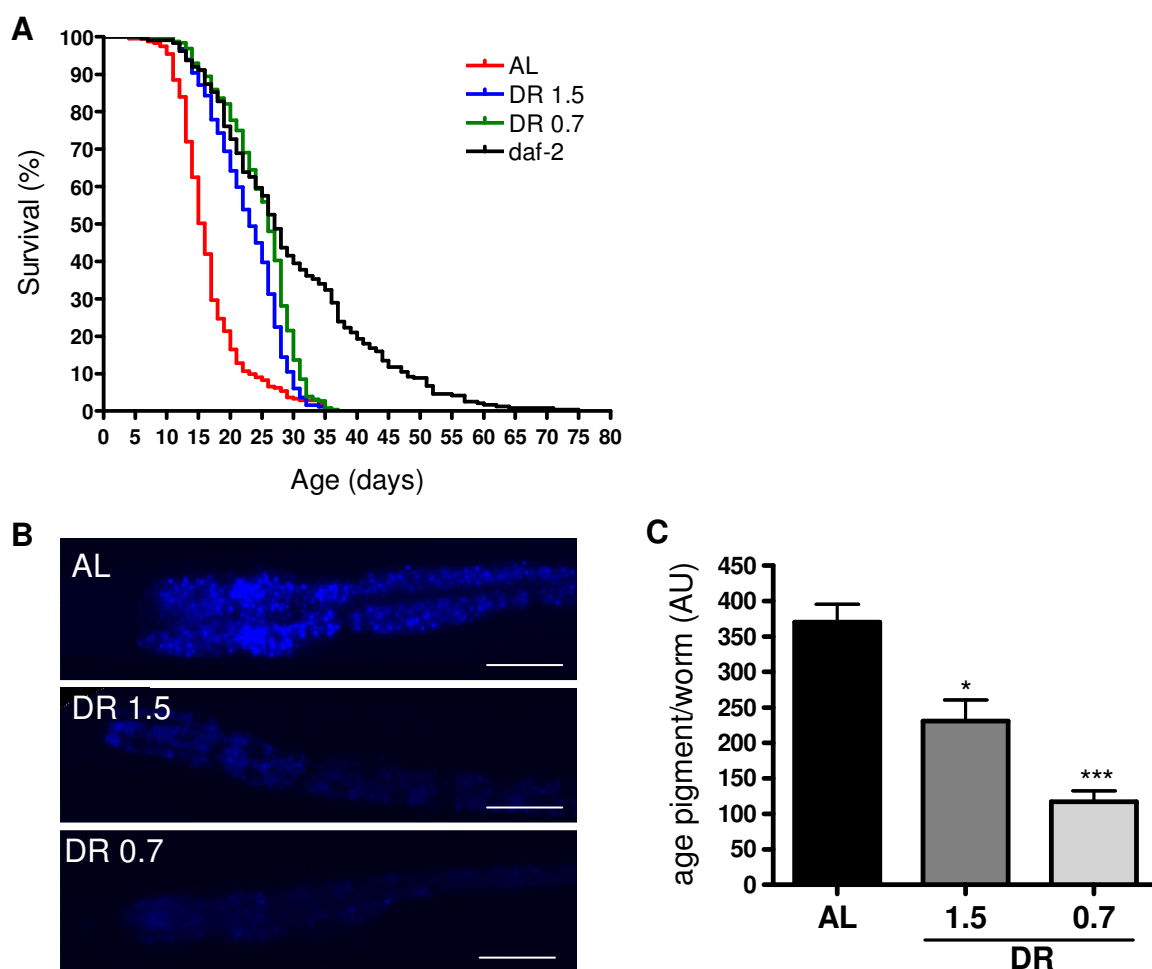


Figure 5. Influence of dietary restriction on lifespan and accumulation of *age pigment*

Survival curves were recorded for wild-type grown under either AL or two different DR (DR1.5, DR0.7) conditions and for AL fed *daf-2* mutant. Survival is represented by Kaplan-Meier curves (%-fraction alive) as mean of three experiments with 100 individuals each. Mean and maximum lifespan, standard deviation and statistical significance are provided in Table 3. (B-C) Autofluorescence measurements of age related biomarkers in dietary restricted wild-type at day one of adulthood. (B) Fluorescence microscopy of AL fed or DR (DR1.5, DR0.7) living nematodes using the DAPI channel (ex 365, em 445/50). Representative images document different amounts of autofluorescent *age pigment* in the intestine. Magnification 200x; scale bar, 50 μ m. (C) Spectrofluometric analysis of autofluorescent *age pigment* in worm homogenates. AL and DR (DR1.5, DR0.7) treated worms were disrupted and homogenates were adjusted to equal protein amounts. Results of *age pigment* per worm (autofluorescence, AU) are represented as mean \pm SEM of three experiments. Significant differences were calculated between AL and respective DR condition using unpaired t-test (* $p < 0.05$, *** $p < 0.001$).

3.5 Influence of dietary restriction on the fat-to-fat-free mass ratio

During analysis of body proportions via bright-field microscopy images we noticed a pale phenotype of dietary restricted adults (Figure 2 A). This could be related to intestinal fat granules and/or lysosomal related organelles [45]. Therefore, analysis of body composition was carried out at L4 and adult stage using triglyceride (TAG, fat mass) and protein (fat-free mass) measurements. The fat-to-fat-free mass as an important physiological parameter to evaluate body composition and adiposity was calculated based on TAG and protein values. In L4 larvae, TAG content per worm was slightly increased under moderate and stringent DR condition, whereas protein content per worm was marginally reduced (Figure 6 A/B). The resulting fat-to-fat-free mass ratio of L4 larvae (0.112 ± 0.010 , mean \pm SEM) was significantly increased when compared with AL fed worms (0.070 ± 0.009) (Figure 6 C). In adulthood, both DR conditions led to a significant and drastic decrease in fat and protein content per worm relative to AL condition (Figure 6 A,B). Notably, under DR the protein content per worm decreased to a greater extent than TAG levels. As a consequence, the fat-to-fat-free mass ratio of dietary restricted adult worms was 47 to 70 % higher relative to AL fed animals (Figure 6 C). The obtained fat-to-fat-free mass ratio of AL fed worms (L4: 0.06; adult: 0.16) was similar to literature (~ 0.07 to 0.11 in young adults and ~ 0.14 to 0.26 in adult worms) [112-115]. Thus, biochemical measurements of L4 larvae and adult worms revealed that DR induced a remarkable shift to a higher fat-to-fat-free mass ratio.

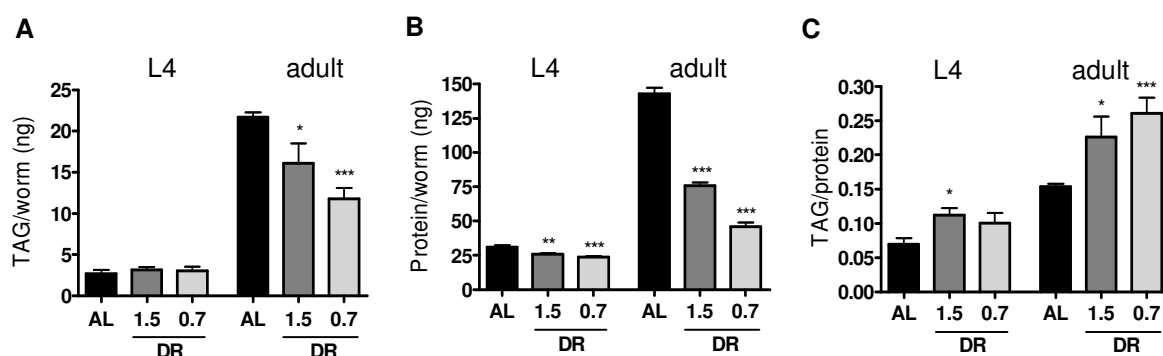


Figure 6. Influence of dietary restriction on body composition

Body composition including (A) TAG content per worm (ng), (B) protein content per worm (ng/w) and (C) TAG/protein ratio of AL and DR (DR1.5, DR0.7) fed wild-type worms were compared. Animals were grown until L4 larval stage or first day of adulthood. Results are represented as mean \pm SEM of three independent experiments. Significant differences were analyzed between AL and respective DR condition using unpaired t-test (* $p < 0.05$, *** $p < 0.001$). (* $p < 0.05$, ** $p < 0.005$, *** $p < 0.001$).

3.6 Influence of dietary restriction on lipid droplet size

We next asked whether the increased fat-to-fat-free mass ratio was associated with changes in LD appearance. For this purpose, we used a BODIPY 493/505 based fixative staining method, which stains exclusively LDs at all fat storage sites of *C. elegans* [98]. Conventional fluorescence microscopy of adult AL fed worms after BODIPY 493/505-staining revealed a high density of small-sized LDs that were fine dispersed and mainly located in the intestine and hypodermis (Figure 7 A). Moderate as well as stringent DR caused a reduction of the intestinal LD number in comparison to AL worms (Figure 7 B, C).

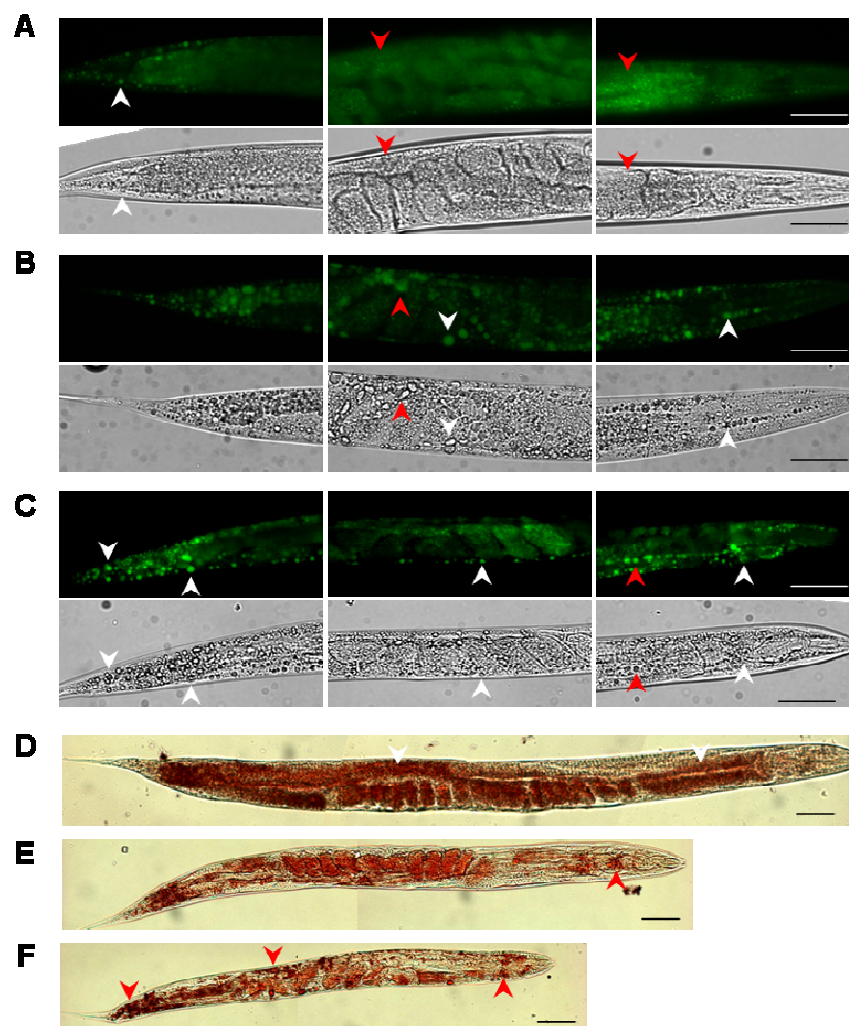


Figure 7. Fat staining of dietary restricted adult *C. elegans*

(A-C) BODIPY 493/503 fluorescence microscopy and corresponding bright-field microscopy images of AL (A), DR1.5 (B) and DR0.7 (C) fed wild-type worms at first day of adulthood. (D-F) Oil red O staining of AL (D), DR1.5 (E) and DR0.7 (F) treated adult wild-type worms. Magnification of all photographs 200x; scale bar, 50 μ m. The anterior part is on the right. Arrow heads indicate lipid droplets (LD) in the intestine (red) or in the hypodermis (white).

Most notably, DR increased the size of LDs in both, intestinal and hypodermal cells. Particularly, most of these enlarged LDs were accumulated in hypodermal cells of pharynx and tail region. The LD expansion phenotype of adult worms grown under DR was even visible in corresponding bright-field microscopy images and was confirmed by Oil red O staining (Figure 7 D-F). Images of Oil red O staining further suggested a more drastic LD enlargement at DR0.7 relative to DR1.5.

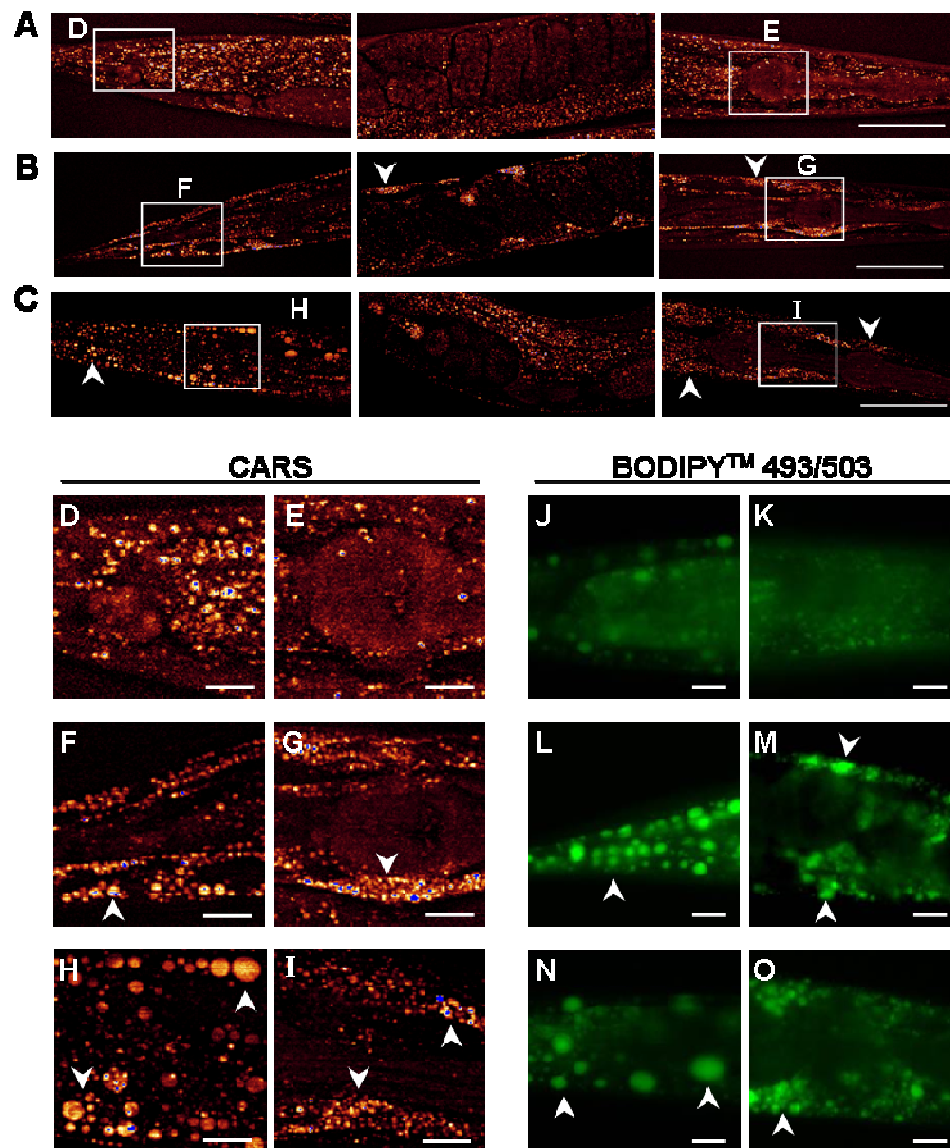


Figure 8. Imaging of lipid droplets in dietary restricted adult *C. elegans* by coherent anti-Stokes Raman scattering microscopy and BODIPY 493/503-based staining

Visualization of LDs via label-free coherent anti-Stokes Raman scattering (CARS) microscopy (A-I) of one-day-old adult wild-type worms grown on AL (A), DR1.5 (B) and DR0.7 (C) agar plates. Photographs of the pharynx region (on the right), the central region and tail region (on the left) are represented as maximum projection of 16-47 plane images from a z-stack at 1.5 μ m interval depending on the respective

body region. Magnification 630x. (D, F, H) Detailed view of lipid droplets in tail region. (E, G, I) Detailed view of LDs in pharynx region. (J-O) Distribution of BODIPY 493/503 stained LDs is in agreement to CARS microscopy images. BODIPY 493/503 fluorescence microscopy images of AL (J, K), DR1.5 (L, M) and DR0.7 (N, O) treated worms. (J, L, N) Detailed view of pharynx region. (K, M, O) Detailed view of tail region. Magnification 400x. Arrow heads indicate an accumulation of hypodermal lipid droplets. Scale bar, 50 μm ; 10 μm in detailed view.

In order to verify the observed expansion of LDs under DR, non-invasive coherent anti-Stokes Raman scattering (CARS) microscopy was performed (Figure 8). This label-free imaging technique allows a selective visualization of lipids in living animals such as *C. elegans* [82]. It is based on the characteristic vibration of abundant carbon-hydrogen bonds in lipids at 2845 cm^{-1} [82]. Importantly, CARS microscopy confirmed the DR induced enlargement of LDs (Figure 8 B-C; F-I) as observed by the two different fat staining methods. The detailed view of pharynx and tail region demonstrated an accumulation of enlarged LDs in worms cultivated at stringent and moderate DR (Figure 8 F-I). In contrast, only small-sized LDs were detected in hypodermal cells of AL fed worms (Figure 8 D-E). Moreover, comparative analysis of CARS (Figure 7 D-I) and BODIPY 493/503 images (Figure 8 J-O) illustrated similar sizes and distribution of LDs in AL and DR animals, respectively.

3.7 Influence of dietary restriction on lipid droplet size and distribution during development

To investigate the LD expansion phenotype in more detail, confocal laser scanning (CLS) microscopy of BODIPY 493/503 stained L2 larvae, L4 larvae and adult worms was performed. The enlargement of intestinal and hypodermal LDs under moderate and stringent DR condition was observed in L2 larvae (Figure 9) and L4 larvae (Figure 10) when compared with AL fed animals. In dietary restricted adult worms, the abundance of expanded LDs in the intestine was reduced relative to larval stages, and large-sized LDs were predominantly observed in hypodermal cells of pharynx and tail regions (Figure 11). In summary, DR increased the LD size in intestinal and hypodermal cells of L2 and L4 larvae. In adulthood, expanded LDs under DR were mainly located in the hypodermis.

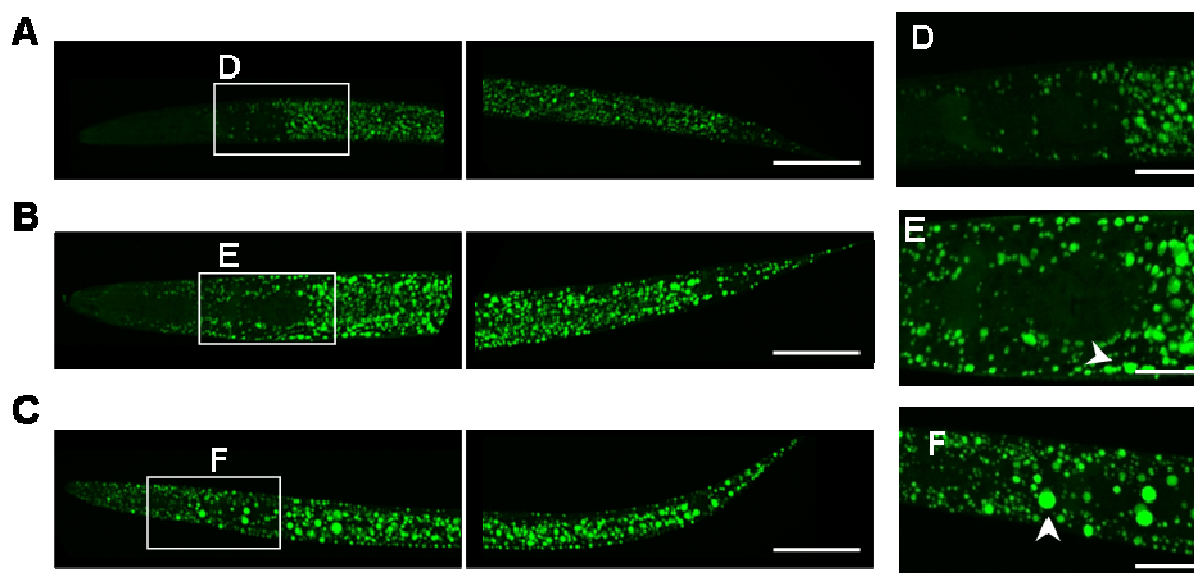


Figure 9. Imaging of lipid droplets in dietary restricted L2 larvae by confocal laser scanning microscopy

Wild-type animals were cultivated on AL (A), DR 1.5 (B) and DR 0.7 (C) agar plates until reaching the L2 stage and harvested for BODIPY 493/503 staining. Images derived from confocal laser scanning (CLS) microscopy are shown as maximum projection of 20-30 images from a z-stack at 0.5 μm interval. The anterior part is on the left. (D-F) Magnification of LDs in pharynx region. Arrow heads indicate enlarged hypodermal LDs. Magnification 630x.

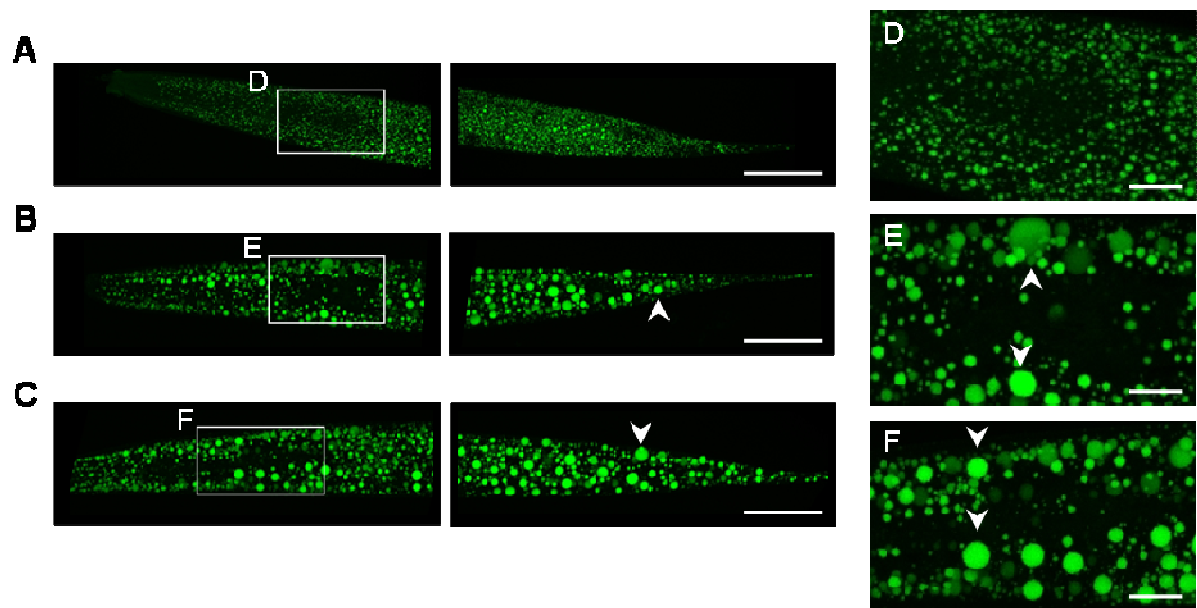


Figure 10. Imaging of lipid droplets in dietary restricted L4 larvae by confocal laser scanning microscopy

Wild-type animals grown on AL (A), DR1.5 (B) and DR0.7 (C) plates were harvested at L4 stage and used for BODIPY 493/503 staining. Images derived from CLS microscopy and are shown as maximum projection of ~40 images from a z-stack at 0.5 μm interval. The anterior part is on the left, the posterior on the right. (D-F) Detailed view of the pharynx region. Arrow heads indicate enlarged hypodermal LDs. Magnification 630x.

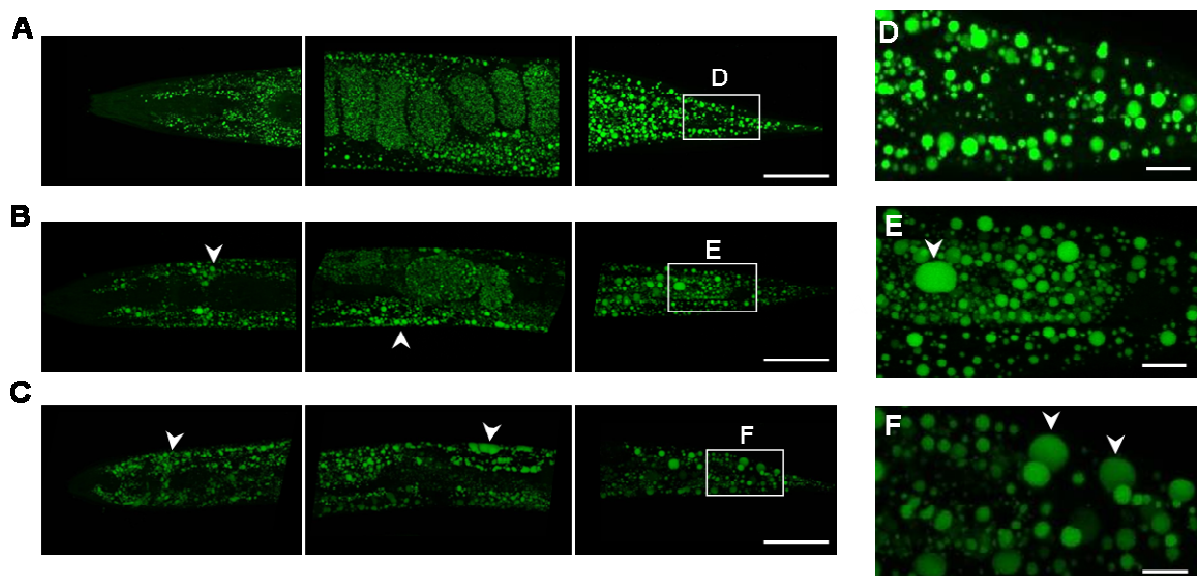


Figure 11. Imaging of lipid droplets in dietary restricted adult worms by confocal laser scanning microscopy

BODIPY 493/503 staining of adult wild-type worms cultivated under AL (A), DR1.5 (B) and DR0.7 (C) condition. CLS microscopy images of pharynx (on the right), central and tail region (on the left) are shown as maximum projection of 70-110 images from a z-stack at 0.5 μm interval. (D-F) Detailed view of tail region. Arrow heads indicate hypodermal LDs. Magnification 630x.

3.7.1 Influence of dietary restriction on the relative number of large-sized lipid droplets in dependence on the developmental stage

To quantify the observed enlargement of LDs in response to DR, the relative distribution of BODIPY-labeled LDs in pharynx and tail region that were 0-10 μm^3 , 10-25 μm^3 , 25-50 μm^3 and >50 μm^3 in volume was calculated from single z-stacks of CLS microscopy images (Figure 12). This classification revealed that small-sized LDs <10 μm^3 in volume represented 88.8 to 97.9 % of detected LDs at all developmental stages and at all feeding conditions. In comparison with AL condition, DR increased the relative number of medium-sized LDs (10-25 μm^3) of L2 and L4 larvae by a factor of 2.1 to 3.3. At both larval stages, the relative abundance of large-sized (25-50 μm^3) and very large-sized (>50 μm^3) LDs increased up to 12-fold in dietary restricted animals compared with AL condition. In tail region of dietary restricted L4 larvae, the relative number of very large LDs was actually up to 15.2-fold higher. In adulthood, the relative number of LDs 10-25 μm^3 in volume was similar between DR and AL conditions. The relative volume of large-sized LDs (25-50 μm^3) was up to 2.5-fold increased in pharynx region of DR worms, whereas in tail region the percentage was similar between DR and AL. In comparison, percentage of very large LDs (>50 μm^3) was up to 7.1-fold higher in dietary restricted adult worms. Taken together, DR increased the number of enlarged LDs in pharynx and tail region. The extent of the DR-induced LD expansion was dependent on the respective body region as well as on the developmental stage.

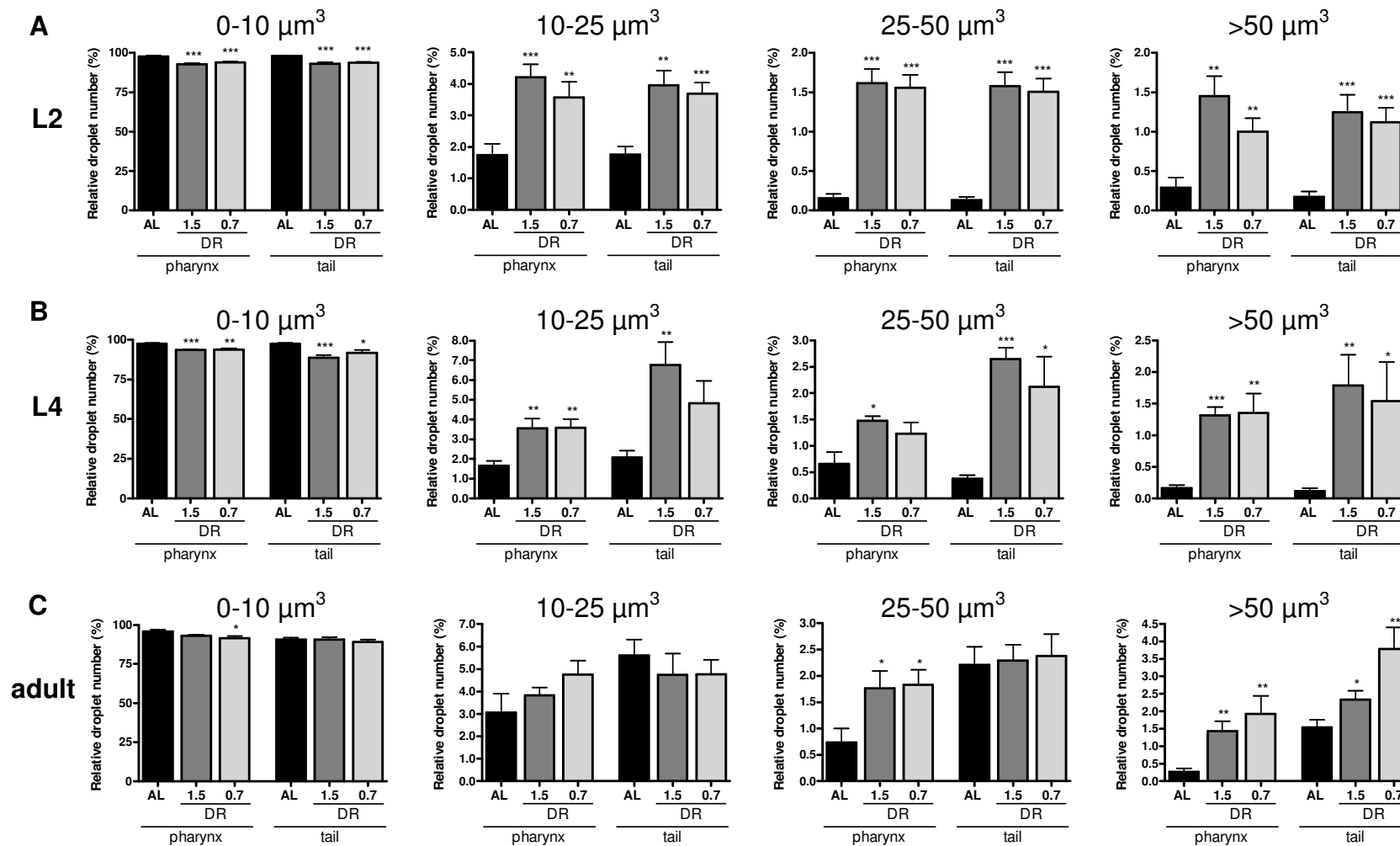


Figure 12. Size classification of BODIPY 493/503-stained lipid droplets in pharynx and tail region of dietary restricted larvae and adult *C. elegans* The volumes of all BODIPY 493/503-positive droplets in pharynx and tail region of AL and DR (DR1.5, DR0.7) treated wild-type animals were obtained from single z-stacks of CLS microscopy images. The relative number of lipid droplets (%) that are 0-10 μm^3 , 10-25 μm^3 , 25-50 μm^3 and >50 μm^3 in volume was calculated for L2 larvae (A), L4 larvae (B) and adult worms (C). Data derive from eight to ten animals per feeding condition and developmental stage, respectively. Results are shown as mean \pm SEM from three independent experiments. Significant differences were analyzed using unpaired t-test of AL and respective DR condition (* $p < 0.05$, ** $p < 0.01$, *** $p < 0.001$).

3.7.2 Influence of dietary restriction on the mean LD volume and on the volume-% of large-sized LDs (>50 μm^3)

The mean LD volume of all BODIPY-labeled LDs in pharynx and tail region was calculated from single z-stacks of CLS microscopy images. Moderate and stringent DR (DR1.5, DR0.7) increased the mean LD volume of L2 larvae, L4 larvae and adult worms in comparison with respective AL condition (Figure 13 A-C). In pharynx region, the mean droplet size of dietary restricted animals was 1.8 to 2.5-fold increased. Mean droplet volume of tail regions was up to 3.3-fold elevated. In addition, we determined the LD surface based on the mean LD volume and found that LD expansion under DR led to a 14-32 % reduction of the surface to volume ratio (Table 4).

For further comparison, the volume of large-sized LDs (>50 μm^3) was expressed as percentage of the total LD volume (Figure 13 D-F). This parameter displays the relative proportion of fat stored in large LDs. In AL fed worms large-sized droplets represented 5.5 to 39.9 % of the total LD volume droplet fraction depending on the developmental stage and body region. In comparison with AL condition, moderate and stringent DR significantly increased the volume-% of LD fraction >50 μm^3 by a factor of 1.5 to 6.3 in L2 larvae and 3.0 to 5.3 in L4 larvae. In adulthood, LD fraction >50 μm^3 represented 42.6 to 43.3 % (AL: 8.37 %) and 60.7 to 64.9 % (AL: 39.9 %) of the total LD volume in pharynx and tail region of DR fed worms, respectively.

Table 4. Surface to volume ratio of lipid droplets under *ad libitum* (AL) and dietary restriction (DR) condition

stage	AL		DR 1.5		DR 0.7	
	pharynx	tail	pharynx	tail	pharynx	tail
L2	4.0	4.0	3.0	2.7	3.2	2.9
L4	4.0	4.1	3.2	2.8	3.0	3.1
adult	3.6	2.8	2.9	2.4	2.6	2.4

Dietary restriction (DR1.5, DR0.7) reduces the surface to volume ratio of LDs in comparison to AL condition. The LD surface (μm^2) was calculated from the mean LD volume (μm^3) of all BODIPY 493/503-labeled droplets in pharynx and tail region of L2 larvae, L4 larvae and adult wild-type animals. The mean LD volumes (\pm SEM) are illustrated in Figure 12.

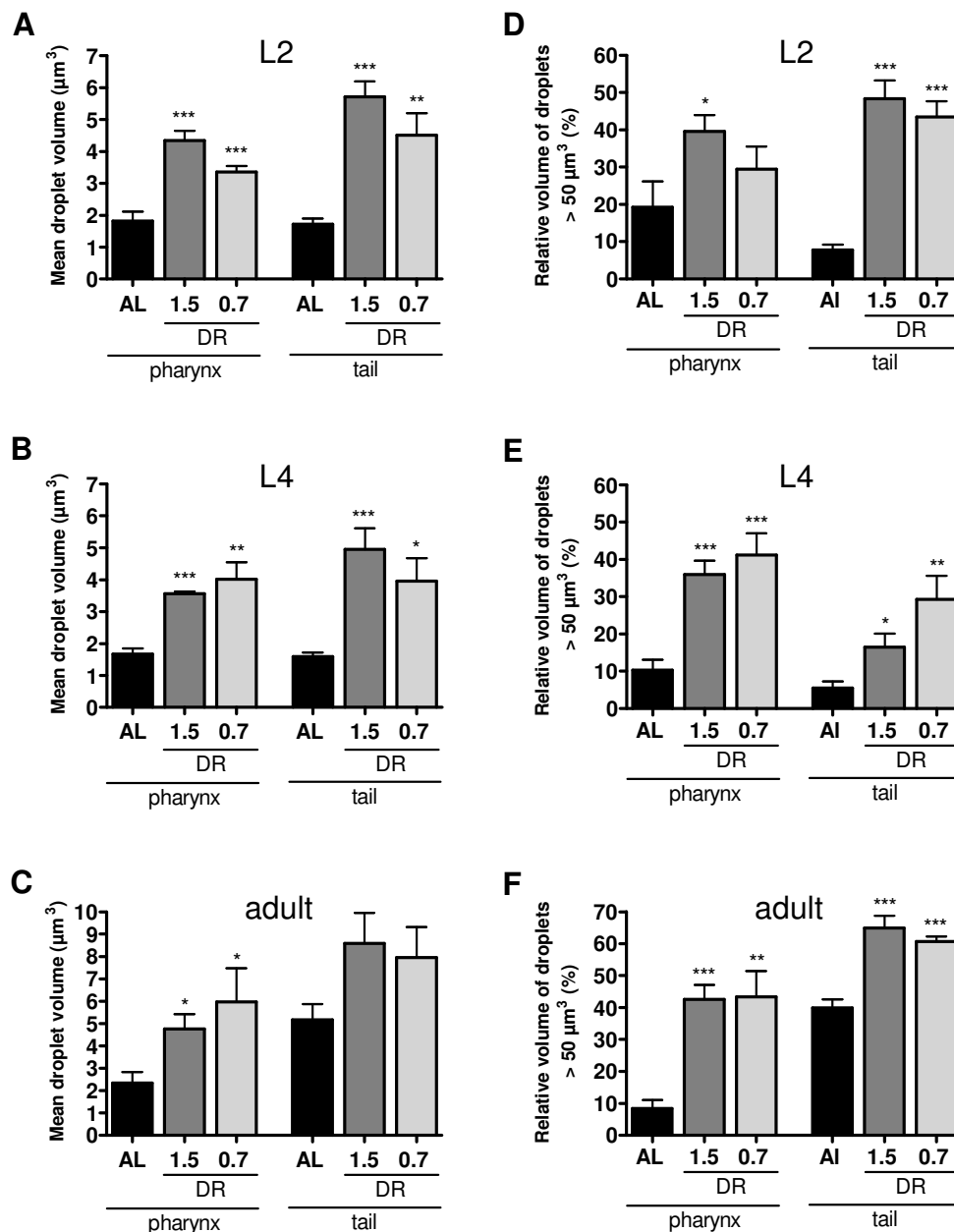


Figure 13. Mean lipid droplet volume and volume-% of large-sized lipid droplets (>50 μm³) of dietary restricted larval and adult animals

Mean LD volume (μm³) (A-C) and percentage volume of large-sized LDs (>50 μm³) on the total volume of all detected droplets (%) (D-F) within pharynx and tail region was quantified in L2 and L4 larvae and adult wild-type worms. Animals were fed on AL or two different DR conditions (DR1.5, DR0.7). LDs were visualized by BODIPY 493/503 staining. LD volumes were calculated from z-stacks of CLS microscopy images. Eight to ten animals were analyzed per condition and experiment. Results are shown as mean ± SEM from three independent experiments. Significant differences were analyzed using unpaired t-test of AL and respective DR condition (*p<0.05, **p<0.01, ***p<0.001).

In summary, under DR up to 65 % of the total LD volume was represented by large-sized LDs (>50 μm³). We also screened for the maximum-sized LDs located in

pharynx and tail regions of larvae and adult worms (Table 5). In average, maximum-sized LDs were enlarged by a factor of about 2 to 5 in dietary restricted animals when compared with AL. The largest LDs were detected in the tail region of dietary restricted adult worms (DR1.5: 609 ± 93 DR0.7: 408 ± 68 ; mean \pm SEM of the five largest LDs).

Table 5. Volume of the maximum-sized lipid droplets under *ad libitum* (AL) and dietary restriction (DR) condition

stage	AL		DR 1.5		DR 0.7	
	pharynx	tail	pharynx	tail	pharynx	tail
L2	69 ± 12	56 ± 6	168 ± 25	141 ± 17	123 ± 15	115 ± 12
L4	66 ± 8	54 ± 7	128 ± 15	113 ± 13	214 ± 23	149 ± 28
adult	58 ± 9	213 ± 21	235 ± 29	609 ± 93	285 ± 48	406 ± 68

Data derive from CLS microscopy images of BODIPY staining wild-type nematodes. The maximum LD volume (μm^3) indicates the average size of the five largest LDs detected in respective pharynx and tail region of single animals cultivated at AL and two different DR (DR1.5, DR0.7) conditions. Data are shown as mean \pm SEM of eight to ten animals.

3.8 Analysis of gene expression profiles in dietary restricted *C. elegans*

To identify candidate genes that might be responsible for the DR induced increase in the fat-to-fat-free ratio and enlargement of LDs gene expression profiling was performed by using microarrays. At L4 stage and adulthood, we compared genome wide mRNA steady-state levels of AL fed *C. elegans* to that of dietary restricted animals cultivated under stringent (DR0.7) or moderate (DR1.5) DR. For comparison, all genes were considered that were significantly regulated (fold-change >2.0 ; $p < 0.05$, t-test) under both DR conditions relative to AL treated control group. We found 263 genes that were significantly up-regulated or down-regulated in L4 larvae cultivated under DR1.5 and DR0.7 (Set I, Figure 14 A). At the adult stage 2736 genes were significantly regulated under both, DR1.5 and DR0.7 (set II). The combination of these two gene sets identified 124 shared genes that were significantly regulated at both developmental stages and both DR conditions (Figure 14B, supplementary Table S1). These genes were considered as DR response genes. Examination of the predicted molecular functions using the gene ontology (GO) annotation for *C. elegans* revealed assignments for 72 of the 124 DR response

genes (Table 6). Related annotations were combined into broader categories including fatty acid (FA)

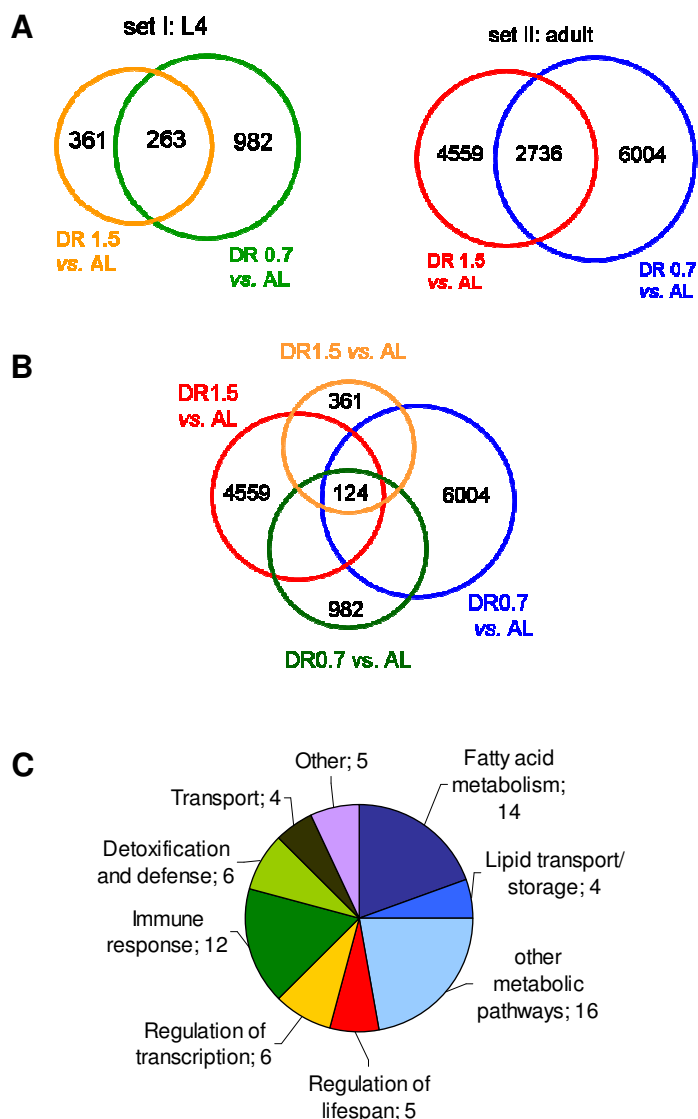


Figure 14. Illustration of shared genes regulated under stringent and moderate DR in wild-type L4 larvae and adults

(A) Comparison of significantly up- and down-regulated genes in L4 larvae (set I) and adult worms (set II) grown under DR1.5 and DR0.7 relative to AL treated control group. Numbers of regulated genes within each subset are listed. Intersections represent shared regulated genes. Selected criteria for inclusion in the gene subsets were a fold change in expression to exceed 2-fold and a confidence level of 95 % ($p < 0.05$, t-test). (B) Combination of the 2 sets revealed shared regulated genes ('DR response genes') used for subsequent analysis. (C) The pie chart represents the functional categories of shared DR response genes based on their related molecular function using gene ontology (GO) annotation for *C. elegans* (WormBase, release WS 198). Genes with unknown function are excluded in this analysis.

metabolism and other metabolic processes, lipid transport and storage, regulation of lifespan, regulation of transcription, immune response, detoxification and defense, transport and other functions (Figure 13 C). As a second approach to analyze and interpret gene expression data, candidate genes known to be involved in lipid

metabolism and in modulating LD size were selected. The fold changes of these genes between AL and DR conditions are summarized in supplementary Table S2.

Table 6. Summary of dietary restriction (DR) response genes in *C. elegans*

Gene	Description ^a	Fold change of regulation ^b			
		DR1.5	L4 DR0.7	adult DR1.5	DR0.7
<u>Fatty acid metabolism</u>					
lipogenesis					
<i>fat-5</i>	Δ-9 fatty acid desaturase	3.7	3.6	2.3	2.5
Y48A6B.9	Putative mitochondrial trans-2-enol-CoA reductase (FA elongation) ^c	2.7	3.9	2.7	2.7
Y53G8B.2	Diacylglycerol acyltransferase (DGAT)	3.5	5.1	2.6	2.6
β-oxidation					
<i>acs-2</i>	Fatty acid acyl-CoA synthetase	2.4	3.2	8.3	12.0
<i>acs-7</i>	Fatty acid acyl-CoA synthetase	-4.5	-2.3	-5.3	-7.6
T20B3.1	Carnitine acyltransferase	2.4	3.7	10.1	9.2
K09H11.1.1	Acyl-CoA dehydrogenase, mitochondrial	2.2	2.6	2.0	2.2
F58F9.7.1	Acyl-CoA oxidase, peroxisomal	2.1	2.7	2.4	2.3
F58F9.7.3	Acyl-CoA oxidase, peroxisomal	2.0	2.7	2.6	2.4
lipolysis					
<i>lips-6</i>	Triacylglycerol lipase (class 2)	11.1	12.8	2.7	4.0
C40H1.8.1	Predicted lipase (class3)	-3.7	-4.2	-4.0	-3.0
<i>lips-11</i>	Triacylglycerol lipase	-4.3	-5.6	-3.1	-4.3
<i>lips-12</i>	Triacylglycerol lipase (class2)	-2.2	-2.3	-3.3	-3.9
<i>lipl-5</i>	Triglyceride lipase- cholesterol esterase	-3.7	-4.2	-2.4	-2.2
<u>Lipid transport/ storage</u>					
<i>far-3</i>	Fatty acid/retinol binding protein	10.7	13.4	3.7	3.1
F22E5.1	Lipid storage	-2.1	-4.3	-20.7	-17.9
<i>swt-1</i>	Sweet sugar transporter family member; lipid storage	2.1	2.3	4.0	4.0
<i>vit-1</i>	Lipoprotein, lipid transporter activity	-2.5	-6.2	-15.9	-49.5
<u>Other metabolic pathways</u>					
<i>ugt-63</i>	UDP-glucuronosyl and UDP-glucosyl transferase	-6.6	-9.5	-29.1	-30.5
<i>ugt-15</i>	UDP-glucuronosyl and UDP-glucosyl transferase	42.7	31.5	6.3	6.8

Continued Table 6.

Gene	Description ^a	Fold change of regulation ^b			
		L4		adult	
		DR1.5	DR0.7	DR1.5	DR0.7
<i>ugt-8</i>	UDP-glucuronosyl and UDP-glucosyl transferase	-2.6	-2.6	-7.2	-5.8
<i>ugt-53</i>	UDP-glucuronosyl and UDP-glucosyl transferase	-3.0	-4.0	-3.0	-3.7
<i>ugt-18</i>	UDP-glucuronosyl and UDP-glucosyl transferase	12.2	13.9	34.0	41.7
Y4C6B.6	Beta-glucocerebrosidase; lysosome organization, carbohydrate and sphingolipid metabolic process	6.2	7.0	31.8	34.1
<i>dhs-18</i>	Dehydrogenase, short chain	2.2	3.5	3.8	3.7
<i>dhs-9</i> (Y32H12A.3.1)	Short-chain dehydrogenase/ reductase	2.2	3.2	2.3	2.6
<i>dhs-9</i> (Y32H12A.3.2)	Short-chain dehydrogenase/ reductase	2.3	3.2	2.2	2.5
<i>cth-1</i> (F22B8.6.1)	Putative cystathionine gamma-lyase, amino acid metabolic process	3.3	2.6	2.1	2.1
<i>cth-1</i> (F22B8.6.2)	Putative cystathionine gamma-lyase, amino acid metabolic process	3.3	2.6	2.1	2.2
<i>asns-2</i>	Asparagine synthase (glutamine-hydrolyzing)	2.2	3.6	7.8	7.6
C01B10.7	Transferase activity	-2.3	-4.5	-5.3	-7.6
C42D4.2	Carboxylesterase and related proteins	-2.0	-4.1	-8.2	-10.9
F10C2.3	Catalytic activity	2.6	2.9	3.0	2.5
F54F3.4	Reductase with broad range of substrate specificities	2.9	4.1	5.0	5.7
<u>Regulation of lifespan</u>					
<i>dct-8</i>	DAF-16/FOFO controlled, germline Tumor affecting	8.1	26.4	8.3	9.8
<i>dod-23</i>	Downstream of DAF-16 (regulated by DAF-16) family member	-2.4	-2.9	-2.2	-2.6
<i>hsp-12.3</i>	Small heat-shock protein, response to heat	4.9	6.3	3.0	3.0
<i>mtl-2</i>	Metallothionein, functions in metall detoxification and homeostasis and stress adaptation; plays a role in regulating growth and fertility, determination of adult lifespan	3.2	3.9	2.8	3.1
T16G1.7	Orthologous to human gene ALIAS DLC1 CANDIDATE TUMOR SUPPRESSOR GENE (DLEC1)	8.4	10.5	10.2	13.6
<u>Regulation of transcription</u>					
<i>djr-1.2</i>	DJ-1 (mammalian transcriptional regulator) related	3.2	4.7	2.2	3.0

Continued Table 6.

Gene	Description ^a	Fold change of regulation ^b			
		L4		adult	
		DR1.5	DR0.7	DR1.5	DR0.7
<i>nhr-74</i>	Nuclear hormone receptor	2.8	2.7	-16.5	-18.4
<i>nhr-117</i> (F16B4.12a)	Nuclear hormone receptor	2.3	2.8	4.1	4.8
<i>nhr-117</i> (F16B4.12b)	Nuclear hormone receptor	2.3	2.8	4.1	4.8
<i>nhr-244</i>	Nuclear hormone receptor	2.4	2.6	-10.2	-9.4
<i>oac-20</i>	O-Acyltransferase homolog	-2.1	-2.5	-2.6	-4.8
<u>Immune response</u>					
<i>clec-169</i>	C-type lectin	-2.7	-3.8	-6.5	-4.9
<i>clec-68</i>	C-type lectin	6.8	5.4	2.3	4.1
<i>clec-150</i>	C-type lectin	-2.2	-2.7	-3.6	-4.5
<i>clec-50</i>	C-type lectin	-2.5	-2.5	-3.0	-3.6
<i>clec-237</i>	C-type lectin	-3.6	-4.0	-2.9	-3.5
<i>clec-4</i>	C-type lectin	2.2	2.6	-2.2	-2.4
<i>clec-97</i>	C-type lectin	-2.7	-3.1	-3.3	-2.8
F35E12.5	CUB-like domain bearing protein	-3.0	-3.8	-24.7	-30.3
F55G11.4	CUB-like domain bearing protein	-3.7	-3.9	-11.5	-11.8
F55G11.7.2	CUB-like domain bearing protein	-2.0	-2.2	-5.8	-6.7
<i>ilys-5</i>	Lysozyme activity	-2.4	-2.3	-18.6	-25.8
<i>spp-17</i>	Saposin-like protein family member	-2.0	-3.3	-7.2	-14.6
<u>Detoxification and defense</u>					
<i>cyp-34A1</i>	Cytochrome P450 CYP2 subfamily member	9.2	16.4	3.8	4.0
<i>cyp-35C1</i>	Cytochrome P450 CYP2 subfamily member	-2.9	-3.5	-16.6	-20.5
<i>cyp-35D1</i>	Cytochrome P450 CYP2 subfamily member	-5.5	-8.1	-15.7	-33.0
<i>cyp-35A5</i>	Cytochrome P450 CYP2 subfamily member, lipid storage	-4.3	-6.5	-22.0	-27.7
<i>cyp-35A3</i>	Cytochrome P450 CYP2 subfamily member, lipid storage	-2.8	-3.3	-12.5	-13.0
<i>scl-6</i>	Defense-related protein containing SCP domain	-3.7	-2.9	-53.2	-46.7
<u>Transport</u>					
<i>amt-4</i>	Ammonia permease	-2.1	-2.8	-7.6	-7.3

Continued Table 6.

Gene	Description ^a	Fold change of regulation ^b			
		L4		adult	
		DR1.5	DR0.7	DR1.5	DR0.7
C18D1.2	Permease of the major facilitator superfamily	4.5	6.4	3.9	5.5
F56A4.10	Permease of the major facilitator superfamily	-2.3	-2.4	-6.2	-8.7
Y19D10A.8	Transmembrane transport, predicted	-2.1	-2.2	-3.1	-9.5
<u>Other functions</u>					
C15C8.3	Aspartyl protease	-2.1	-3.7	-24.3	-14.8
<i>ins-12</i>	Hormone activity	2.5	2.5	-3.4	-4.3
<i>scav-5</i>	Plasma membrane glycoprotein CD36 and related membrane receptors; cell adhesion	-2.1	-2.6	-6.2	-6.2
<i>str-9</i>	Seven TM Receptor; 7-transmembrane olfactory family member	2.5	3.1	2.3	2.9
<i>wrt-8</i>	Sonic hedgehog and related proteins; cell-cell signaling	2.3	2.7	6.4	8.0

The table shows the predicted molecular functions and fold changes in gene expression of DR response genes including splice variants that were commonly regulated under moderate and stringent DR (DR1.5 and DR0.7) in L4 and adult wild-type worms. Genes with unknown function are excluded in this table. Criteria for inclusion in this data set were a fold-change >2.0 and significance threshold of p-value <0.05 (unpaired t-test). The entire list which includes all 124 DR response genes is provided as supplementary table (Table S1).

^aDescription of genes is based on the gene ontology (GO) annotation for *C. elegans* (WormBase, www.wormbase.org, release WS 198) unless otherwise noted.

^bFold changes are always understood between DR and AL group. A positive number indicates a higher gene expression in DR animals. In case of down-regulated genes, the fold-change was calculated as 1/ratio and a minus was added to the quotient. A negative number consequently indicates a lower gene expression in DR animals.

^cDescription is based on Kyoto Encyclopedia of Genes and Genomes (KEGG, www.genome.jp/kegg/, release 61.0).

3.8.1 Influence of dietary restriction on the expression of genes involved in fatty acid metabolism and other metabolic pathways

14 of the 72 annotated genes regulated in response to DR are predicted to encode enzymes involved in fatty acid metabolism (Table 6). We identified several genes of mitochondrial and peroxisomal β -oxidation up-regulated under DR in L4 larvae and adults. These include the mitochondrial acyl-CoA synthetase encoding gene *acs-2*, one carnitine acyltransferase, an acyl-CoA dehydrogenase and two splice variants of a putative acyl-CoA oxidase. Four genes encoding triacylglycerol lipases were down-regulated in response to DR. One lipase encoding gene (*lips-6*) was up-regulated and showed increased fold changes at L4 compared to the adult stage.

The diacylglycerol acyltransferase (DGAT) gene (Y53G8B.2) was significantly up-regulated in dietary restricted L4 larvae and adults. DGAT is a key enzyme of *de novo* synthesis of triacylglycerols (TAG). Expression levels of *fat-5* encoding a $\Delta 9$ desaturase were significantly up-regulated under DR relative to AL condition. Further, expression of Y48A6B.9 gene was stimulated in response to DR. Y48A6B.9 is predicted to encode a putative trans-2-enol-CoA reductase participating in FA elongation. Fatty acid/retinol binding protein encoding *far-3* was up-regulated and exhibited increased fold changes at L4 in comparison to the adult stage. Two other DR response genes, F22E5.1 and K02D7.5, are predicted to function in lipid storage. A strong down-regulation (up to 49.5 fold in DR0.7 fed adults) was observed for *vit-1*, which encodes a lipoprotein functioning in lipid transport. We also found that DR altered the expression of genes involved in other metabolic pathways. For example, of five UDP-glucuronosyl/UDP-glucosyl transferase encoding genes expected to function in carbohydrate metabolism and lipid glycosylation, three genes were repressed, whereas two genes were up-regulated. Further, the expression of two genes predicted to function in amino acid metabolism, one putative cystathionine gamma-lyase (*cth-1*) and one asparagine synthase (*asns-2*), was up-regulated under stringent and moderate DR in L4 larvae and adult animals.

3.8.2 Influence of dietary restriction on life span extension, immune response, detoxification and transcriptional regulation

As expected, DR altered the expression of genes predicted to function in the determination of lifespan (Table 6): two DAF-16 controlled genes (*dct-8* and *dod-23*), the metallothionein encoding *mtl-2* and the T16G1.7 gene, which encodes an orthologue of the human tumor suppressor gene DLEC1. Only one of these genes, *dod-23*, was down-regulated, whereas expression of the other genes was up-regulated in response to DR. Furthermore, we identified several DR response genes involved in immune response (Table 6): seven C-type lectin encoding genes, three genes encoding a CUB-like bearing protein, saposin B encoding *spp-17* and *ilys-5*, which encodes an invertebrate lysozyme family member. Interestingly, expression of these genes was consistently down-regulated under DR with exception of C-type lectin encoding gene *cllec-68*, which was repressed during the L4 and adult stage. DR also influenced the expression of six genes related to detoxification and defense, including cytochrome P450 family members and *scl-6*, which encodes a defense-related protein. Of these genes, five were down-regulated, whereas only *cyp-34A1* was up-regulated under DR. Another group of DR-response genes is involved in the transcriptional regulation. We found that three nuclear hormone receptor (NHR) encoding genes (*nhr-74*, *nhr-117*, *nhr-244*) were consistently up-regulated in dietary restricted L4 larvae (Table 3). In contrast, DR led to the repression of *nhr-74* and *nhr-244* at the adult stage. Further, expression of *djr-1.2* encoding a DJ-1 (mammalian transcriptional regulator) related protein was stimulated in response to DR, whereas O-acyltransferase homolog *oac-20* was down-regulated.

3.8.3 Comparison between dietary restriction and fasting responses

To investigate whether DR and fasting can be differentiated regarding the regulation of genes involved in lipid metabolism, we compared our gene expression data to that of fasting response genes [116]. Van Gist *et al.* (2005) analyzed the expression of 97 genes belonging to glucose and lipid metabolism in response to a 12 h food deprivation period in wild-type animals by using quantitative RT-PCR (Figure 15). At L4 stage, eight of the fasting responsive genes were similarly regulated under moderate and/or stringent DR (Figure 15 A). In contrast, twelve lipid metabolism genes, which were regulated under fasting, were not regulated under DR.

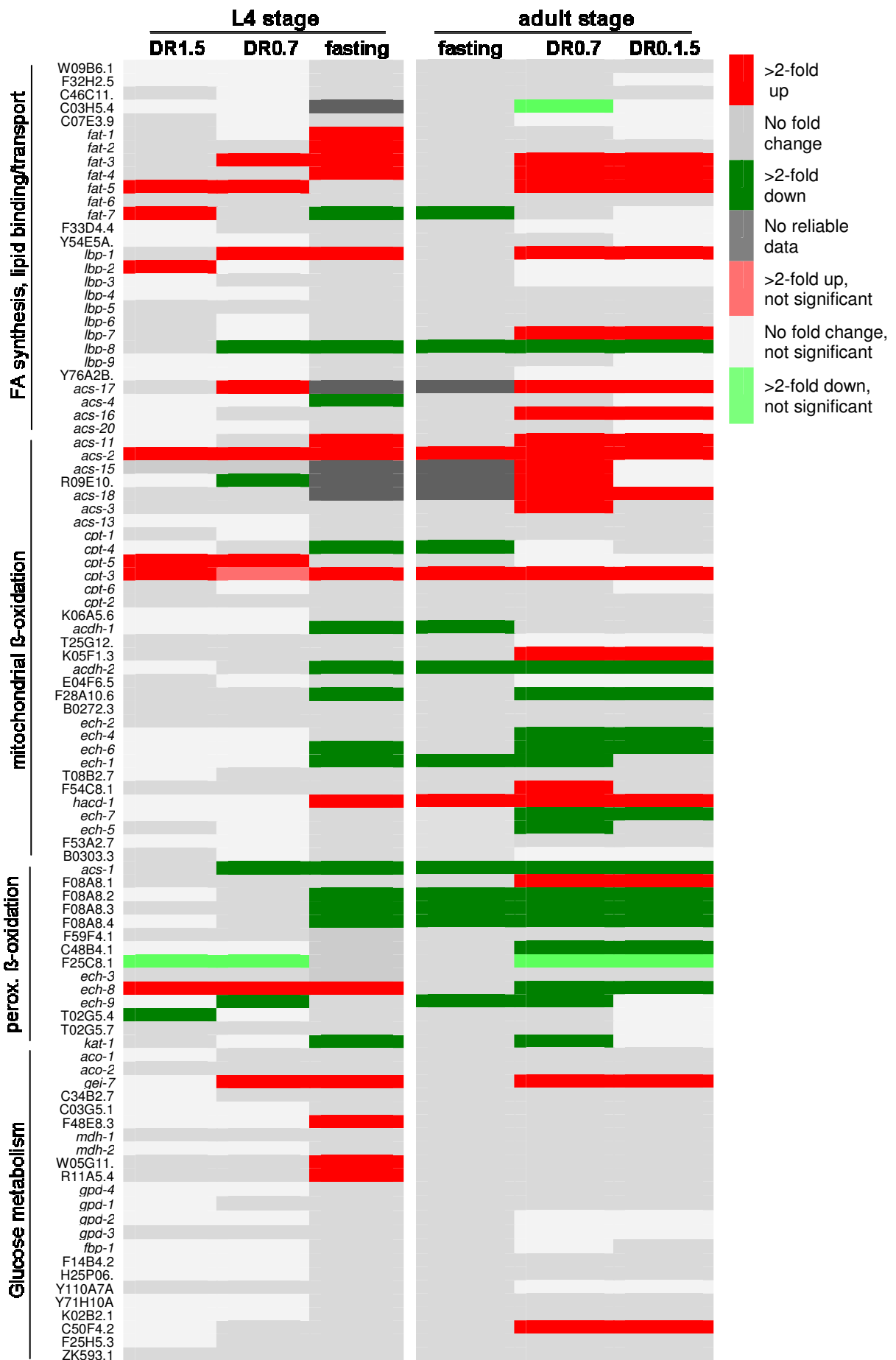


Figure 15. Regulation of genes involved in glucose and lipid metabolism under fasting and two different dietary restriction conditions.

Changes in expression of glucose and lipid metabolism genes are compared between fasted and dietary restricted (DR1.5, DR0.7) L4 larvae and adult worms. Gene expression data from fasted animals were obtained from Van Gilst *et al.* [116]. Genes significantly up-regulated under fasting and DR (minimum fold change of >2, p-value <0.05) in comparison to AL condition are shown in red. Light red indicates genes that were not significantly up-regulated (p-value >0.05). Significantly down-regulated genes (minimum fold-change of >2.0, p-value <0.05) in comparison to AL condition are represented in green. Light green indicates not significantly up-regulated genes. Genes expressed at similar levels (p-value <0.05) in fasted or DR animals and respective AL group are shown in grey. Light grey indicates not significant values.

Five of the DR responsive genes were not influenced by fasting. In adulthood, eleven candidate genes were similarly regulated in fasted and dietary restricted adult worms (Figure 15 B). Three genes were exclusively regulated under fasting. In turn, 21 of the DR response genes were not regulated upon fasting. In summary, four candidate genes (*lbp-8*, *acs-2*, *cpt-3*, *acs-1*) were similarly regulated in response to fasting and DR at L4 and adult stage, respectively. Five genes (*fat-5*, *fat-7*, *acs-11*, *cpt-4*, F28A10.6) were differentially regulated between fasted and dietary restricted animals at both stages. Thus, besides similarities, DR and fasting can be differentiated regarding their regulation of several genes involved in glucose and lipid metabolism.

4 Discussion

DR is the only environmental intervention shown to extend lifespan in a variety of organisms. Thus, many studies performing DR in *C. elegans* have focussed on the effects of DR on longevity in order to unravel the underlying mechanisms. In contrast, studies focussing on the influence of DR on lipid metabolism and fat storage in wild-type nematodes are rare. In this study, we have described an effective regime to examine the effects of DR from hatching until reaching adulthood on *C. elegans* fat storage and mobilization. It was shown that long-term DR leads to a prolonged lifespan and a reduced body size of wild-type animals which are well characterized parameters of DR. The influence of moderate and harsh DR conditions on body proportion, body composition, LD enlargement and distribution in larvae and adult worms will be discussed. Further, DR-induced changes in gene expression will be carefully related to the observed DR phenotypes.

4.1 Development of a solid medium based dietary restriction protocol

The optimized DR method described in this study is based on solid medium, the reduction of the bacterial food source by omitting bactopectone and the standardization of food availability per worm. In order to evaluate our DR method lifespan analysis as a crucial parameter for a DR effect was performed. As reviewed by Mair *et al.* [33], the mean lifespan expansion induced by DR varies in wild-type worms between 16.4 % [117] and 140 % [28] dependent on the applied method. We observed a mean lifespan expansion of about 50 % under stringent DR (DR0.7) indicating the usefulness of our DR method. Moreover, body bend frequency, whole animal motility and pharyngeal pumping rate were not substantially influenced by DR. Thus, food restriction induced by our method is not compensated by a reduced locomotion and/or an elevated feeding rate.

In comparison to other DR regimes on solid medium [11, 22, 41] the protocol described in this study offers several advantages. First, it minimizes possible side-effects of antibiotic or heat treatment due to the fact that exclusion of peptone and serial dilution of living *E. coli* is the sole intervention. Second, we were able to control the food availability per worm using flow-cytometry based sorting of a defined

number of embryos per plate. Serial dilution of the bacterial food source resulted in a dose-dependent reduction of body size in adulthood indicating standardized DR conditions. Third, it enables the application of DR during development from hatching throughout development. Several other regimes, including diluting bacteria in liquid medium, axenic media, dietary deprivation or DR on agar plates, initiate DR in *C. elegans* at L4 stage or during adulthood to avoid detrimental effects on development or surviving [22, 28, 33, 35, 37, 39-41, 46]. Using our method, the onset of DR from hatching throughout larval development did not induced larval arrest or dauer stage. However, developmental time from L4 to the adult stage was slightly delayed under moderate and stringent DR (74 h and 76 h after hatch at 20°C) in comparison to AL condition (72 h after hatch at 20°C). Since reproduction is an energy consuming process [10, 33, 37, 38], this developmental delay may result from the need to mobilize fat stores under food limiting conditions to provide energy required for oocyte maturation and fertility.

4.2 Regulation of energy metabolism genes under fasting and dietary restriction conditions

To examine whether our DR regime differs from fasting, gene expression data of dietary restricted animals was compared to gene expression data of fasted wild-type animals [116]. We found that DR induced changes in the expression of several lipid metabolism genes considerably distinct from changes depending on fasting. For example, the fasting-repressed $\Delta 9$ desaturase encoding gene *fat-7* was up-regulated in dietary restricted L4 larvae while moderate DR (DR1.5) had no influence on its expression at the adult stage. *fat-7* is a target gene of the nuclear hormone receptor NHR-49, which is homologues to human PPAR α and likely involved in mediating fasting responses in *C. elegans* [116]. However, two other NHR-49 targets, *acs-2* and *lbp-8*, were similarly regulated under fasting and DR condition. Thus, DR and fasting responses might trigger in part similar pathways. Most notably, both regimes differ in their regulation of a remarkable number of genes involved in fat metabolism. In summary, considering the regulation on gene expression levels, these findings provide first evidence that our DR regime differs from fasting.

4.3 Dietary restriction and the influence on body size of wild-type nematodes

A reduction in body size under nutrient-limiting conditions has been observed in several species including *Drosophila* and mice [7, 118]. In line with this, we found an inverse linear relationship between body size and the extent of DR in adult *C. elegans*. At the harshest DR condition (DR0.3), body volume was reduced by approximately 65% of AL fed animals. The observed body sizes of AL and DR treated worms were similar to those reported in other studies performing DR in *C. elegans* [42, 119]. For example, Tain *et al.* [42] found a likewise decrease of 63% in body size of dietary restricted adult wild type worms. Consistent with literature, reduction of body size under DR was initially observed at the adult stage, whereas at larval stages body volume was similar between AL fed and dietary restricted animals [42, 120]. We further observed that body width decreased to a greater extent than body length under DR. This may reflect an effective adaptation to reduced basal energy expenditure because the surface (S) of the cylindrical worm ($S = (p \cdot l) + 2 \cdot (\pi \cdot r^2)$; p, perimeter) is more influenced by the width ($2 \times r$) than the length (l).

The DR induced reduction in body size was accompanied by a reduced protein content of adult worms. A close correlation between body size and protein content in *C. elegans* was also observed in an other experimental set-up [120]. The authors proposed that body size is controlled by the insulin/IGF-1 signaling pathway, which responds to the nutritional state and promotes cell growth by increasing the protein synthesis. DR-dependent reduction of body size in *C. elegans* has been also correlated with reduced levels of hypodermal endoreduplication, which effects growth in adulthood [42]. In this context, the sensory EGL-4/SMA/MAB pathway has been proposed to regulate ploidy in response to DR.

Reduction in body size during DR might also arise from a decreased synthesis of phospholipids. In *C. elegans*, the glycerophospholipids phosphoethanolamine and phosphatidylcholine (PC) account for 55% and 32% of the total phospholipids, respectively [121]. Both, *de novo* synthesis of phospholipids and triacylglycerides (TAGs) require diacylglycerol (DAG) as substrate. Conversion of DAG into TAG is catalyzed by diacylglycerol transferase (DGAT) [122]. Gene expression analysis revealed that moderate as well as stringent DR led to an up-regulation of DGAT encoding gene Y53G8B.2. Assuming an increased *de novo* TAG synthesis by DGAT,

this might cause substrate deficiency for the synthesis of phospholipids which are the major component of cell membranes. Thus, DR-dependent reduction in body size might be mediated by a reduced polyploidy, protein synthesis and/ or *de novo* synthesis of phospholipids.

4.4 Dietary restriction-dependent expansion of lipid droplets and the regulation of genes involved in lipid metabolism

In the present study, we used different fat staining methods and non-invasive CARS microscopy to visualize fat stores in dietary restricted wild-type worms and compared them with AL fed animals. In *C. elegans*, fat is mainly stored in the intestine and hypodermis [64, 71]. Recently, Zhang *et al.* [64] provided evidence for LDs as ubiquitous fat storage organelles in the nematode that are morphologically and functionally distinct from lysosomes and lysosome-related organelles. Surprisingly, moderate as well as stringent DR during development led to a remarkable LD expansion in intestinal and hypodermal cells. The LD expansion was found throughout development. Of note, the observed LD phenotype under DR is considerable distinct from the phenotype of fasted animals. Upon fasting, *C. elegans* mobilizes TAGs from intestinal fat stores, which causes a drastic decrease in the number and size of LDs [44-46, 91, 123].

Gene expression analysis identified several lipogenesis genes that were up-regulated under moderate and stringent DR in both, L4 and adult stage. These genes are involved in lipid synthesis (i.e. Y53G8B.2/DGAT), lipid binding (i.e. *far-3*), fatty acid desaturation (i.e. *fat-5*/ $\Delta 9$ fatty acid desaturase) and elongation (Y48A6B.9/trans-2-enol-CoA reductase). Assuming that gene expression is translated into enzymatic activity, up-regulation of these genes might increase *de novo* synthesis of TAGs. This hypothesis is supported by our unexpected finding that DR led to an increased fat-to-fat-free mass ratio in L4 larvae and adult worms. In line with this, mild calorie restriction in mice led to fat accumulation [124]. We suppose that during DR increased synthesis of TAGs via up-regulation of lipogenesis genes may be accompanied by an expansion of LD size.

Several studies indicate that storage efficiency of TAGs within LDs is likely dependent on the generation of monounsaturated fatty acids (MUFAs) [125, 126].

For example, it has been demonstrated in chinese hamster ovary cells and in *Drosophila* that supplementation with oleic acid (C18:1) leads to TAG accumulation [78]. Further, supplementation with vaccenic acid (C18:1n7) increased TAG levels and LD size in *C. elegans* peroxisomal β -oxidation mutants [64]. In this study, we found an up-regulation of $\Delta 9$ desaturase *fat-5*. FAT-5 catalyzes the desaturation of palmitic acid (16:0) into palmitoleic acid (C16:1), which serves as substrate for elongation to vaccenic acid [127, 128]. Thus, increased *fat-5* expression likely enhances palmitoleic acid levels, which might promote LD enlargement under DR. Additionally, DGAT encoding gene Y53G8B.2, up-regulated under DR, links TAG synthesis to LD size. It was shown that mammalian DGAT translocates to the LD surface when fatty acid enter the cells in order to promote lipid production and storage [68]. Recently, Y53G8B.2 has been identified as one of the LD-associated proteins in *C. elegans* [129] suggesting a function in TAG assembly into LDs. Taken together, DR-induced up-regulation of lipogenesis genes such as *fat-5* and DGAT might contribute to the LD expansion phenotype.

Interestingly, DR did not only increase the expression of genes involved in lipid synthesis but also induced genes functioning in lipid breakdown (Table 6). We found that genes encoding for enzymes that catalyze the first three steps of mitochondrial β -oxidation (*acs-2*/acyl-CoA synthetase, T20B3.1/carnitine acyltransferase, K09H11.1/acyl-CoA dehydrogenase) were up-regulated in dietary restricted L4 and adult animals. DR also increased the expression of F58F9.7/acyl-CoA oxidase which belongs to peroxisomal β -oxidation (Table 6). Moreover, triacylglycerol lipase *lips-6* was up-regulated in response to DR suggesting an increased TAG hydrolysis. Based on gene expression data, DR seems to stimulate both, TAG synthesis and lipolysis. Recently, it has been demonstrated in adult *C. elegans* males that both, lipid degradation and protein biosynthesis are enhanced during the early period of starvation [44]. The increase in protein synthesis was accompanied by a simultaneous degradation of *de novo* synthesized protein suggesting a high protein turnover. Increased metabolic activity in the initial phase of starvation was characterized by a rapid depletion of intestinal lipid stores, likely to facilitate energy consuming reactions such as ribosome biogenesis. Starvation-induced ribosome biogenesis was regulated by the DAF-2 insulin/IGF-1-receptor signaling and reticular activating system (RAS) pathway in order to maintain normal physiological functions

during transient food deprivation. Based on the study in *C. elegans* males, we hypothesize that an up-regulation of both, TAG *de novo* synthesis and lipolysis may indicate an elevated lipid turnover. This enhanced lipid turnover might be an adaptation during long-term DR to preserve vital functions essential for survival and reproduction. Besides, a simultaneous up-regulation of opposite pathways of FA metabolism might also reflect a tissue-specific regulation.

The ratio of surface phospholipids to core neutral lipids may be an important determinant of LD size. Depletion of PC, which represents the most abundant phospholipid in the LD monolayer, leads to enlargement of LDs [72, 77, 92, 130]. PC can be synthesized either from choline by the Kennedy pathway or by S-adenosylmethionine (SAM) dependent methylation of phosphatidylethanolamine in mammals or of phosphoethanolamine in nematodes and plants [131-133]. Knockdown of the key enzyme of the Kennedy pathway, CTP:phosphocholine cytidyltransferase (CCT), leads to decreased PC levels and to a drastically increased LD size in *Drosophila* S2 cells [77, 130]. Likewise, repression of genes mediating methylation-dependent PC synthesis in *C. elegans* (*sams-1*, *pmt-1*) leads to large intestinal LDs [92, 93]. Recently, SREBP-1 has been identified as a transcriptional activator of genes involved in the one-carbon cycle and LD accumulation [93]. SREBP-1 target genes include *sams-1*, *pmt-2*, folic acid transporter *fol-2* and several other genes. Because key genes of PC synthesis are not consistently regulated under DR in larvae and adult worms (supplementary Table S2), DR induced enlargement of LDs seems not to be mediated by a perturbed SAM-dependent PC synthesis. Of course, we cannot exclude a post-transcriptional effect of DR on these genes.

The expansion of LDs in *sams-1* and *pmt-1* depleted *C. elegans* was associated with reduced PC and increased TAG levels indicating a reciprocal regulation of PC and TAG synthesis [92]. In this context, we speculate that up-regulation of DGAT under DR may indirectly reduce *de novo* synthesis of phospholipids leading to LD enlargement under DR. One model explaining expansion of LDs under conditions of reciprocal regulation of TAG and phospholipids involves the fusion of LDs [77, 130, 134]. It has been reported that during incorporation of lipids into LDs, PC homeostasis at the expanding monolayer is essential to stabilize the organelles and to prevent their coalescence [77, 130]. In turn, PC deficiency during LD growth leads

to fusion of LDs because of instability. We therefore speculate that LD expansion by fusion could be a DR-induced mechanism to reduce the surface to volume ratio of LDs and to facilitate the maintenance of phospholipid homeostasis.

In *C. elegans*, a small number of genes implicated in modulation of LD size have been described (see Table 1). These include genes involved in peroxisomal (*maoc-1*, *dhs-28*, *daf-22*) and mitochondrial (*acs-3*) β -oxidation, lipid binding (*lbp-5*, *acbp-1*) and phospholipid synthesis (*sams-1*, *pmt-1*). LD expansion has been also observed for *C. elegans* deficient for the KLF-3/Krüppel-like transcription factor [89]. Mutations in these genes caused enlargement of LDs in intestinal cells and was accompanied by increased TAG levels, with exception of *acbp-1* mutant animals exhibiting reduced TAG amounts. For example, functional loss of ACS-3/acyl-CoA resulted in the formation of large LDs due to an elevated fatty acid uptake and increased *de novo* lipid synthesis [71]. Since all of these known *C. elegans* genes modulating LD size are not consistently regulated by DR in larvae and adult worms we suggested that they do not play a substantial role for the observed enlargement of LDs under DR. Again, a post-transcriptional effect of DR on these genes cannot be excluded.

4.5 Dietary restriction and development-dependent changes in the distribution of enlarged lipid droplets in intestine and hypodermis

LD expansion in *C. elegans* mutants was observed in the intestine but not in other fat storage sites [64, 71, 88-94]. In the present study, we found that DR causes an expansion of LDs in the intestine as well as in the hypodermis of larvae (L2, L4) and adults. Notably, in adult dietary restricted worms, large-size LDs were mainly located in hypodermal cells accompanied by a reduction of the number of intestinal LDs. Thus, in adulthood, intestinal fat storage seems to be reduced under DR whereas hypodermal fat seems to be more lipolysis resistant.

To provide evidence for this hypothesis, we searched for differences in the regulation of DR response genes between L4 and adult animals. First of all, of FA metabolism genes that were commonly regulated in L4 and adult stage, lipogenesis genes (*fat-5*, Y48A6B.9; Y53G8B.2) were stronger up-regulated in L4, whereas genes involved in mitochondrial β -oxidation (*acs-2*; T20B3.1) were stronger induced in the adult stage (Table 6). Second, we searched for DR-influenced genes implicated in lipid metabolism that were oppositely regulated between L4 and adult animals

(supplementary Table S2). We identified four genes of mitochondrial β -oxidation, including three ACS paralogues (*acs-3*, *acs-15* and *acs-18*) and acyl-CoA dehydrogenase *acdH-8* which were up-regulated in adult worms but not in L4 larvae. Interestingly, the fasting induced lipase gene *fil-1* was significantly up-regulated under DR in adulthood but not in L4 stage. FIL-1 is related to mammalian ATGL and is involved in mobilization of lipids from intestinal LDs upon starvation [135, 136]. Moreover, two cytochrome P450 (CYP) encoding genes (*cyp-35A3* and *cyp-35A5*) were drastically down-regulated in adulthood relative to L4 stage (Table 6) in response to DR. These genes have been also implicated in intestinal fat storage function [48, 123]. Thus, the observed reduction in abundance and size of intestinal LDs in adult worms might be mediated by an up-regulation of intestinal specific genes of lipolysis and mitochondrial β -oxidation. Because hypodermal abundance of LD was not reduced under DR in adulthood, we suppose a different maintenance capacity of intestinal and hypodermal fat stores.

4.6 Lipid droplet expansion and down-regulation of lipase encoding genes

Formation of enlarged LDs has been functionally associated with an increased resistance of stored lipids to lipolysis. Studies indicate that due to the reduction of the LD surface relative to its volume, lipids are less accessible to membrane associated lipases [64, 77]. In *Drosophila*, large LDs were slower metabolized than smaller ones and provided a survival advantage during starvation [77]. In *C. elegans*, peroxisomal β -oxidation mutant *dhs-28* contains enlarged LDs in the intestine that were resistant to fasting and lipase induced lipolysis [64]. Over-expression of adipose triglyceride lipase *atgl-1* (C05D11.7) caused a drastic reduction of TAG levels in wild-type and to a minor/ lesser extent in *dhs-28* animals. ATGL lipase is also important for the hydrolysis of TAGs from LDs in *Drosophila* and mammals [70, 135]. In the present study, mRNA levels of *atgl-1* were not significantly altered under DR (supplementary Table S2). However, of commonly regulated genes four out of five lipase genes were down-regulated (*lipl-5*, *lips-6*, *lips-12* and C40H1.8), which may indicate decreased lipolysis rates (Table 6). Thus, we assume that the reduction of the surface to volume ratio by LD expansion in the one case and the reduced activity of lipases in the other case might be protective mechanisms to prevent excessive breakdown of stored lipids and to release energy stores more slowly during DR.

4.7 Dietary restriction-dependent regulation of genes involved in determination of lifespan, detoxification and innate immunity

Moderate and stringent DR influenced the expression of several genes involved in lifespan extension including two DAF-16/FOXO regulated genes, heat shock protein *hsp-12.3* and metallothionein *mtl-2* (Table 6). DAF-16, a forkhead transcription factor (FOXO), controls lifespan in response to insulin/insulin-like growth factor 1 signaling [137-139]. Downstream targets of DAF-16 include genes involved in oxidative stress response, DNA repair, cell-cycle arrest and apoptosis [140, 141]. *dct-8* acts to suppress tumor growth in *C. elegans* [142], thus DR-dependent up-regulation might promote tumor resistance and longevity.

Heat shock proteins are molecular chaperones involved in stress responses. Among other heat shock proteins *hsp-12.3* is up-regulated in long-lived *daf-2(m41)* mutant linking protection against cellular stress to longevity [58]. Accordingly, DR increased *hsp-12.3* expression suggesting an enhanced stress response. Metallothioneins have anti-apoptotic properties by scavenging free radicals and protecting cells from oxidative stress [143]. *C. elegans* expresses two metallothioneins encoded by *mtl-1* and *mtl-2*. *mtl-2* expression is strongly induced upon heavy metal exposure [144, 145]. A lifespan prolonging effect of MTL has been demonstrated in mice and *C. elegans* [38, 146]. In addition, caloric restriction increased MTL expression in mice, *Drosophila* and *C. elegans* suggesting a role of MTL in nutrition [38, 147, 148]. For example, induction of DR by using chemically defined liquid medium prolonged lifespan in the nematode and was accompanied by an enhanced *mtl-2* expression. In agreement, we found that moderate and stringent DR increased *mtl-2* expression suggesting a role in DR mediated lifespan extension. In summary, up-regulation of genes involved in protection against cellular stress might contribute to lifespan extension in dietary restricted worms.

DR led to a drastic down-regulation of several genes assumed to function in detoxification. These include cytochrome P450 family members, UDP-glucuronosyltransferases (UGT) and defense-related gene *scl-6* (Table 6). In vertebrates, cytochrome P450 (CYP) and UGTs are involved in phase I and II detoxification [149]. Whereas the role of CYPs and UGTs is well characterized in vertebrates, their function in *C. elegans* is largely unknown. However, several CYP (*cyp-35A3*, *cyp-35A5*, *cyp-35C1*) and UGT (*ugt-8*, *ugt-53*) encoding genes as well as *scl-6*, all of them down-regulated under DR, are inducible by xenobiotics [149-151].

Notably, *scl-6* was the strongest regulated gene among shared DR response genes (up to 53.2 fold) (Table 6). These results strongly suggest a reduced detoxification capacity under DR. It is further known that CYPs are not only involved in detoxification but also in synthetic processes such as steroid and FA synthesis [152]. For example, *C. elegans* CYP member DAF-9 generates steroid ligands that bind to the nuclear hormone receptor DAF-12, thus regulating dauer formation and lifespan [153, 154]. Moreover, two of the DR responsive CYP genes (*cyp-35A3*, *cyp-35A5*) are involved in the maintenance of FA diversity necessary for synthetic and signaling processes [123]. Decrease in *cyp* expression under DR is in agreement to studies in which caloric restriction led to a decreased enzymatic activity of several CYPs in rat liver [155, 156]. Because phase I and II detoxification require a lot of energy [152], down-regulation of genes involved in these processes might be an adaptive strategy to save energy under DR.

A considerable number of annotated DR response genes regulated in L4 and adult animals have a putative function in *C. elegans* innate immunity such as C-type lectins, and invertebrate-type lysozyme (*ilys-5*) (Table 6). C-type lectin domain (CTLN) containing proteins function in cell adhesion, glycoprotein clearance and recognition of specific pathogen molecules [157, 158]. Pathogen-induced up-regulation has been demonstrated for four out of seven DR responsive *cllec* genes, including *cllec-4*, *cllec-50*, *cllec-68*, *cllec-150* [157-160]. DR led to the repression of *cllec-50*, *cllec-150* and *cllec-4*, with exception of *cllec-4* which was up-regulated in L4 larvae. In contrast, DR increased expression of *cllec-68* indicating a DR-specific regulation of immune response.

Antimicrobial activity has been reported for a variety of invertebrate-type (i-type) lysozymes (summarized in [161]). I-type lysozymes can have muramidase, isopeptidase and non-enzymatic antibacterial activity [161-163]. DR drastically repressed *ilys-5* (up to 25.8 fold). Though antimicrobial activity has not been described for *ilys-5* so far, down-regulation of *ilys-5* might indicate that antimicrobial activity is reduced in response to DR. Overall the majority of DR-responsive genes expected being involved in immunity were down-regulated. Pathogen defense might be decreased due to the fact that exposure of worms to bacteria is drastically reduced under DR conditions. Alternatively, repression of these genes might reflect a weak immune system resulting from food restriction [164, 165].

4.8 Conclusion and perspectives

DR during development resulted in several profound morphological and physiological changes in *C. elegans* wild-type (Figure 16). Besides well-known DR effects such as lifespan extension and reduction of the adult body size, we found that long-term DR from hatching until reaching the adult stage increased the fat-to-fat-free mass and caused a remarkable expansion of LDs in the intestine and hypodermis. In line with this, gene expression data revealed an up-regulation of genes involved in lipogenesis.

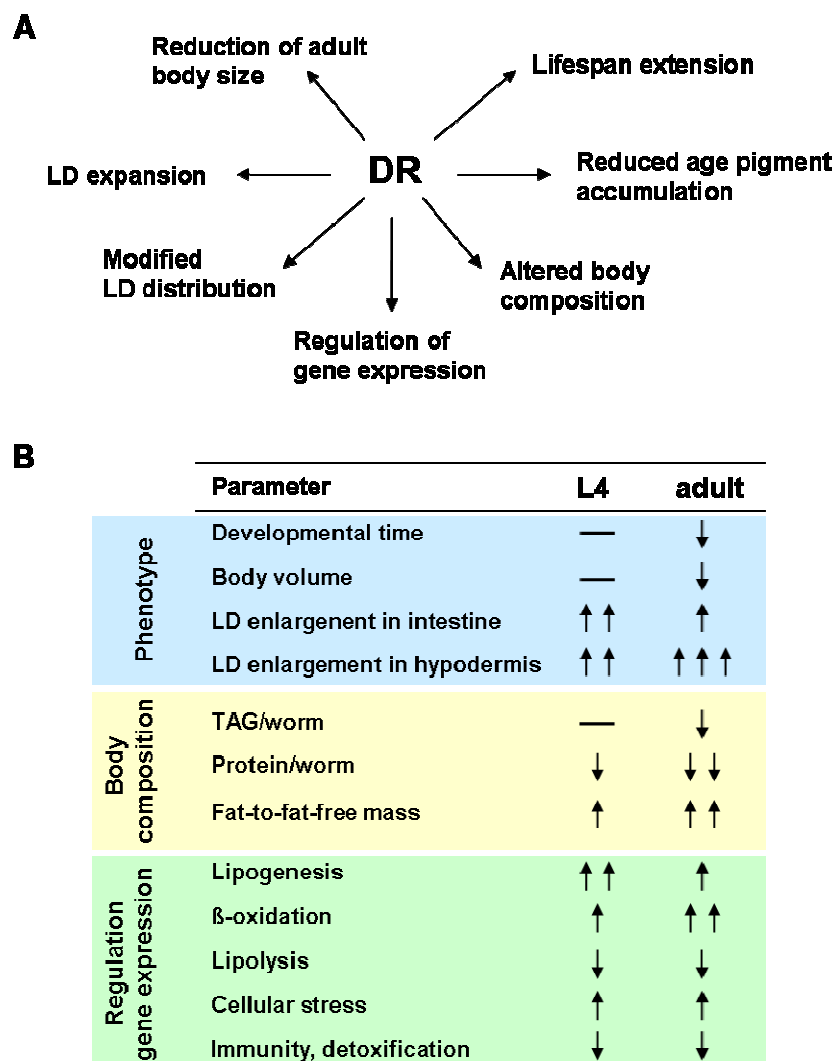


Figure 16. Summary of DR-induced effects on *C. elegans* phenotypes

A. DR-mediated changes of different phenotypes observed in larval and adult wild-type nematodes cultivated under moderate and stringent DR described in this study. B. Effects of DR on apparent phenotypes, body composition and gene expression were different in dependence on the developmental stage. Arrows indicate the degree of modification compared to AL animals. (↑) indicates an increase/up-regulation, (↓) indicates a decrease/down-regulation, (—) means no difference to AL group.

Thin layer chromatography and gas chromatography would be the methods of choice in order to examine whether DR has an influence on the relative abundance of TAGs, phospholipids and cholesterol esters as well as on FA composition.

The mechanism leading to LD expansion is not fully uncovered. One of the proposed models describes a fusion mechanism, in which TAG assimilation into LDs causes relative PC deficiency at the expanding monolayer and subsequently to instability and coalescence of LDs [67, 166, 167]. We hypothesize that under DR up-regulation of DAGT driven TAG synthesis may lead to a deficient *de novo* synthesis of phospholipids. Thus, LD fusion might be a possible mechanism to maintain phospholipid homeostasis at the LD surface. Quantification of phospholipids is certainly required to verify this assumption. In addition, analysis of the LD phenotype after knock-down of DGAT (Y53G8B.2) via RNA interference (RNAi) would be one strategy to provide evidence for the postulated role of DGAT in LD enlargement under DR. LD expansion in *C. elegans* mutants with an impaired SAM-dependent PC synthesis was rescued by choline supplementation [92, 93]. In this context, choline rescue experiments would be essential to test whether there is a relationship between LD expansion and choline deficiency under DR.

The DR-induced LD expansion phenotype observed in this study is considerable distinct from the fat phenotype upon starvation. Food deprivation causes a drastic degradation of intestinal lipids resulting in a pale, lipid depleted phenotype [44-46]. Enlargement of LDs in response to DR might be an adaptive strategy of wild-type worms to protect stored lipids against excessive degradation. Retardation of lipolysis may provide a survival advantage under permanent nutrient limiting conditions.

Long-term DR led to a differential distribution of enlarged LDs between larvae and adult worms. In contrast to larvae, enlarged LDs of adult worms were mainly located in hypodermal cells, whereas the number and size of LDs in the intestine seemed to be reduced. This decrease is reminiscent of the starvation-induced lipid depletion phenotype caused by an enhanced TAG hydrolysis [44, 79]. Thus, decreased abundance of enlarged LDs in the intestine of adult worms might be also due to an increased TAG hydrolysis. In agreement with that, expression of genes involved in FA breakdown and lipolysis were up-regulated in dietary restricted adults compared to larval stages.

It is not known whether intestinal and hypodermal LDs have a similar lipid composition [60]. With the identification of protein marker of LDs in *C. elegans* [129],

it will be of interest to examine whether large-sized LDs of intestine and hypodermis differ in their protein composition decorating the LD surface. In addition, the use of LD marker would confirm results obtained by fat staining and CARS microscopy.

In conclusion this study gives a first insight into the regulation of *C. elegans* fat stores during DR. Gene expression data might provide the basis for future RNAi approaches in order to identify candidate genes responsible for the DR-mediated LD expansion. The balance between energy acquisition and expenditure is critical for survival and reproductive success of animals. Thus, an increase in the fat-to-fat-free mass and storage of *de novo* synthesized TAGs into enlarged, lipolysis-resistant LDs might be an adaptive strategy in dietary restricted *C. elegans* to conserve fat stores.

References

1. Masoro, E.J. (2005). Overview of caloric restriction and ageing. *Mech Ageing Dev* 126, 913-922.
2. Weindruch, R., Naylor, P.H., Goldstein, A.L., and Walford, R.L. (1988). Influences of aging and dietary restriction on serum thymosin alpha 1 levels in mice. *J Gerontol* 43, B40-42.
3. Adams, M.M., Shi, L., Linville, M.C., Forbes, M.E., Long, A.B., Bennett, C., Newton, I.G., Carter, C.S., Sonntag, W.E., Riddle, D.R., and Brunso-Bechtold, J.K. (2008). Caloric restriction and age affect synaptic proteins in hippocampal CA3 and spatial learning ability. *Exp Neurol* 211, 141-149.
4. Martin, B., Mattson, M.P., and Maudsley, S. (2006). Caloric restriction and intermittent fasting: two potential diets for successful brain aging. *Ageing Res Rev* 5, 332-353.
5. Michels, K.B., and Ekblom, A. (2004). Caloric restriction and incidence of breast cancer. *Jama* 291, 1226-1230.
6. Hursting, S.D., Perkins, S.N., Phang, J.M., and Barrett, J.C. (2001). Diet and cancer prevention studies in p53-deficient mice. *J Nutr* 131, 3092S-3094S.
7. Weindruch, R., Walford, R.L., Fligiel, S., and Guthrie, D. (1986). The retardation of aging in mice by dietary restriction: longevity, cancer, immunity and lifetime energy intake. *J Nutr* 116, 641-654.
8. Lane, M.A., Ingram, D.K., and Roth, G.S. (1999). Calorie restriction in nonhuman primates: effects on diabetes and cardiovascular disease risk. *Toxicol Sci* 52, 41-48.
9. Lakowski, B., and Hekimi, S. (1998). The genetics of caloric restriction in *Caenorhabditis elegans*. *Proc Natl Acad Sci U S A* 95, 13091-13096.
10. Houthoofd, K., Braeckman, B.P., Lenaerts, I., Brys, K., De Vreese, A., Van Eygen, S., and Vanfleteren, J.R. (2002). Axenic growth up-regulates mass-specific metabolic rate, stress resistance, and extends life span in *Caenorhabditis elegans*. *Exp Gerontol* 37, 1371-1378.
11. Hosono, R., Nishimoto, S., and Kuno, S. (1989). Alterations of life span in the nematode *Caenorhabditis elegans* under monoxenic culture conditions. *Exp Gerontol* 24, 251-264.
12. Jiang, J.C., Jaruga, E., Repnevskaya, M.V., and Jazwinski, S.M. (2000). An intervention resembling caloric restriction prolongs life span and retards aging in yeast. *Faseb J* 14, 2135-2137.
13. Austad, S.N. (1989). Life extension by dietary restriction in the bowl and doily spider, *Frontinella pyramitela*. *Exp Gerontol* 24, 83-92.

14. Stuchlikova, E., Juricova-Horakova, M., and Deyl, Z. (1975). New aspects of the dietary effect of life prolongation in rodents. What is the role of obesity in aging? *Exp Gerontol* *10*, 141-144.
15. Kealy, R.D., Lawler, D.F., Ballam, J.M., Mantz, S.L., Biery, D.N., Greeley, E.H., Lust, G., Segre, M., Smith, G.K., and Stowe, H.D. (2002). Effects of diet restriction on life span and age-related changes in dogs. *J Am Vet Med Assoc* *220*, 1315-1320.
16. Mair, W., and Dillin, A. (2008). Aging and survival: the genetics of life span extension by dietary restriction. *Annu Rev Biochem* *77*, 727-754.
17. Guarente, L. (2005). NO link between calorie restriction and mitochondria. *Nat Chem Biol* *1*, 355-356.
18. Sinclair, D.A. (2005). Toward a unified theory of caloric restriction and longevity regulation. *Mech Ageing Dev* *126*, 987-1002.
19. Vellai, T., Takacs-Vellai, K., Zhang, Y., Kovacs, A.L., Orosz, L., and Muller, F. (2003). Genetics: influence of TOR kinase on lifespan in *C. elegans*. *Nature* *426*, 620.
20. Kapahi, P., Zid, B.M., Harper, T., Koslover, D., Sapin, V., and Benzer, S. (2004). Regulation of lifespan in *Drosophila* by modulation of genes in the TOR signaling pathway. *Curr Biol* *14*, 885-890.
21. Kaeberlein, M., Powers, R.W., 3rd, Steffen, K.K., Westman, E.A., Hu, D., Dang, N., Kerr, E.O., Kirkland, K.T., Fields, S., and Kennedy, B.K. (2005). Regulation of yeast replicative life span by TOR and Sch9 in response to nutrients. *Science* *310*, 1193-1196.
22. Greer, E.L., Dowlatshahi, D., Banko, M.R., Villen, J., Hoang, K., Blanchard, D., Gygi, S.P., and Brunet, A. (2007). An AMPK-FOXO pathway mediates longevity induced by a novel method of dietary restriction in *C. elegans*. *Curr Biol* *17*, 1646-1656.
23. Kenyon, C. (2005). The plasticity of aging: insights from long-lived mutants. *Cell* *120*, 449-460.
24. Russell, S.J., and Kahn, C.R. (2007). Endocrine regulation of ageing. *Nat Rev Mol Cell Biol* *8*, 681-691.
25. Clancy, D.J., Gems, D., Hafen, E., Leivers, S.J., and Partridge, L. (2002). Dietary restriction in long-lived dwarf flies. *Science* *296*, 319.
26. Kenyon, C., Chang, J., Gensch, E., Rudner, A., and Tabtiang, R. (1993). A *C. elegans* mutant that lives twice as long as wild type. *Nature* *366*, 461-464.
27. Dorman, J.B., Albinder, B., Shroyer, T., and Kenyon, C. (1995). The *age-1* and *daf-2* genes function in a common pathway to control the lifespan of *Caenorhabditis elegans*. *Genetics* *141*, 1399-1406.

28. Houthoofd, K., Braeckman, B.P., Johnson, T.E., and Vanfleteren, J.R. (2003). Life extension via dietary restriction is independent of the Ins/IGF-1 signalling pathway in *Caenorhabditis elegans*. *Exp Gerontol* *38*, 947-954.
29. Greer, E.L., Banko, M.R., and Brunet, A. (2009). AMP-activated protein kinase and FoxO transcription factors in dietary restriction-induced longevity. *Ann N Y Acad Sci* *1170*, 688-692.
30. Panowski, S.H., Wolff, S., Aguilaniu, H., Durieux, J., and Dillin, A. (2007). PHA-4/Foxa mediates diet-restriction-induced longevity of *C. elegans*. *Nature* *447*, 550-555.
31. An, J.H., and Blackwell, T.K. (2003). SKN-1 links *C. elegans* mesendodermal specification to a conserved oxidative stress response. *Genes Dev* *17*, 1882-1893.
32. Singh, V., and Aballay, A. (2006). Heat-shock transcription factor (HSF)-1 pathway required for *Caenorhabditis elegans* immunity. *Proc Natl Acad Sci U S A* *103*, 13092-13097.
33. Mair, W., Panowski, S.H., Shaw, R.J., and Dillin, A. (2009). Optimizing dietary restriction for genetic epistasis analysis and gene discovery in *C. elegans*. *PLoS One* *4*, e4535.
34. Greer, E.L., and Brunet, A. (2009). Different dietary restriction regimens extend lifespan by both independent and overlapping genetic pathways in *C. elegans*. *Aging Cell* *8*, 113-127.
35. Park, S.K., Link, C.D., and Johnson, T.E. (2010). Life-span extension by dietary restriction is mediated by NLP-7 signaling and coelomocyte endocytosis in *C. elegans*. *Faseb J* *24*, 383-392.
36. Castelein, N., Hoogewijs, D., De Vreese, A., Braeckman, B.P., and Vanfleteren, J.R. (2008). Dietary restriction by growth in axenic medium induces discrete changes in the transcriptional output of genes involved in energy metabolism in *Caenorhabditis elegans*. *Biotechnol J* *3*, 803-812.
37. Klass, M.R. (1977). Aging in the nematode *Caenorhabditis elegans*: major biological and environmental factors influencing life span. *Mech Ageing Dev* *6*, 413-429.
38. Szewczyk, N.J., Udranszky, I.A., Kozak, E., Sunga, J., Kim, S.K., Jacobson, L.A., and Conley, C.A. (2006). Delayed development and lifespan extension as features of metabolic lifestyle alteration in *C. elegans* under dietary restriction. *J Exp Biol* *209*, 4129-4139.
39. Kaeberlein, T.L., Smith, E.D., Tsuchiya, M., Welton, K.L., Thomas, J.H., Fields, S., Kennedy, B.K., and Kaeberlein, M. (2006). Lifespan extension in *Caenorhabditis elegans* by complete removal of food. *Aging Cell* *5*, 487-494.

40. Lee, G.D., Wilson, M.A., Zhu, M., Wolkow, C.A., de Cabo, R., Ingram, D.K., and Zou, S. (2006). Dietary deprivation extends lifespan in *Caenorhabditis elegans*. *Aging Cell* 5, 515-524.
41. Chen, D., Thomas, E.L., and Kapahi, P. (2009). HIF-1 modulates dietary restriction-mediated lifespan extension via IRE-1 in *Caenorhabditis elegans*. *PLoS Genet* 5, e1000486.
42. Tain, L.S., Lozano, E., Saez, A.G., and Leroi, A.M. (2008). Dietary regulation of hypodermal polyploidization in *C. elegans*. *BMC Dev Biol* 8, 28.
43. Avery, L., and Horvitz, H.R. (1990). Effects of starvation and neuroactive drugs on feeding in *Caenorhabditis elegans*. *J Exp Zool* 253, 263-270.
44. Tan, K.T., Luo, S.C., Ho, W.Z., and Lee, Y.H. (2011). Insulin/IGF-1 receptor signaling enhances biosynthetic activity and fat mobilization in the initial phase of starvation in adult male *C. elegans*. *Cell Metab* 14, 390-402.
45. McKay, R.M., McKay, J.P., Avery, L., and Graff, J.M. (2003). *C. elegans*: a model for exploring the genetics of fat storage. *Dev Cell* 4, 131-142.
46. Bishop, N.A., and Guarente, L. (2007). Two neurons mediate diet-restriction-induced longevity in *C. elegans*. *Nature* 447, 545-549.
47. Steinkraus, K.A., Smith, E.D., Davis, C., Carr, D., Pendergrass, W.R., Sutphin, G.L., Kennedy, B.K., and Kaeberlein, M. (2008). Dietary restriction suppresses proteotoxicity and enhances longevity by an hsf-1-dependent mechanism in *Caenorhabditis elegans*. *Aging Cell* 7, 394-404.
48. Ashrafi, K., Chang, F.Y., Watts, J.L., Fraser, A.G., Kamath, R.S., Ahringer, J., and Ruvkun, G. (2003). Genome-wide RNAi analysis of *Caenorhabditis elegans* fat regulatory genes. *Nature* 421, 268-272.
49. Kimura, K.D., Tissenbaum, H.A., Liu, Y., and Ruvkun, G. (1997). *daf-2*, an insulin receptor-like gene that regulates longevity and diapause in *Caenorhabditis elegans*. *Science* 277, 942-946.
50. Sze, J.Y., Victor, M., Loer, C., Shi, Y., and Ruvkun, G. (2000). Food and metabolic signalling defects in a *Caenorhabditis elegans* serotonin-synthesis mutant. *Nature* 403, 560-564.
51. Greer, E.R., Perez, C.L., Van Gilst, M.R., Lee, B.H., and Ashrafi, K. (2008). Neural and molecular dissection of a *C. elegans* sensory circuit that regulates fat and feeding. *Cell Metab* 8, 118-131.
52. Soukas, A.A., Kane, E.A., Carr, C.E., Melo, J.A., and Ruvkun, G. (2009). Rictor/TORC2 regulates fat metabolism, feeding, growth, and life span in *Caenorhabditis elegans*. *Genes Dev* 23, 496-511.
53. Yang, F., Vought, B.W., Satterlee, J.S., Walker, A.K., Jim Sun, Z.Y., Watts, J.L., DeBeaumont, R., Saito, R.M., Hyberts, S.G., Yang, S., Macol, C., Iyer, L.,

- Tjian, R., van den Heuvel, S., Hart, A.C., Wagner, G., and Naar, A.M. (2006). An ARC/Mediator subunit required for SREBP control of cholesterol and lipid homeostasis. *Nature* *442*, 700-704.
54. Atherton, H.J., Jones, O.A., Malik, S., Miska, E.A., and Griffin, J.L. (2008). A comparative metabolomic study of NHR-49 in *Caenorhabditis elegans* and PPAR-alpha in the mouse. *FEBS Lett* *582*, 1661-1666.
55. Walker, A.K., Yang, F., Jiang, K., Ji, J.Y., Watts, J.L., Purushotham, A., Boss, O., Hirsch, M.L., Ribich, S., Smith, J.J., Israelian, K., Westphal, C.H., Rodgers, J.T., Shioda, T., Elson, S.L., Mulligan, P., Najafi-Shoushtari, H., Black, J.C., Thakur, J.K., Kadyk, L.C., Whetstine, J.R., Mostoslavsky, R., Puigserver, P., Li, X., Dyson, N.J., Hart, A.C., and Naar, A.M. (2010). Conserved role of SIRT1 orthologs in fasting-dependent inhibition of the lipid/cholesterol regulator SREBP. *Genes Dev* *24*, 1403-1417.
56. McElwee, J., Bubb, K., and Thomas, J.H. (2003). Transcriptional outputs of the *Caenorhabditis elegans* forkhead protein DAF-16. *Aging Cell* *2*, 111-121.
57. Murphy, C.T., McCarroll, S.A., Bargmann, C.I., Fraser, A., Kamath, R.S., Ahringer, J., Li, H., and Kenyon, C. (2003). Genes that act downstream of DAF-16 to influence the lifespan of *Caenorhabditis elegans*. *Nature* *424*, 277-283.
58. Halaschek-Wiener, J., Khattra, J.S., McKay, S., Pouzyrev, A., Stott, J.M., Yang, G.S., Holt, R.A., Jones, S.J., Marra, M.A., Brooks-Wilson, A.R., and Riddle, D.L. (2005). Analysis of long-lived *C. elegans* *daf-2* mutants using serial analysis of gene expression. *Genome Res* *15*, 603-615.
59. Perez, C.L., and Van Gilst, M.R. (2008). A ¹³C isotope labeling strategy reveals the influence of insulin signaling on lipogenesis in *C. elegans*. *Cell Metab* *8*, 266-274.
60. Mullaney, B.C., and Ashrafi, K. (2009). *C. elegans* fat storage and metabolic regulation. *Biochim Biophys Acta* *1791*, 474-478.
61. Watts, J.L. (2009). Fat synthesis and adiposity regulation in *Caenorhabditis elegans*. *Trends Endocrinol Metab* *20*, 58-65.
62. Furuhashi, M., and Hotamisligil, G.S. (2008). Fatty acid-binding proteins: role in metabolic diseases and potential as drug targets. *Nat Rev Drug Discov* *7*, 489-503.
63. Tikou, P.E., Gracey, A.Y., Macartney, A.I., Beynon, R.J., and Cossins, A.R. (1996). Cold-induced expression of delta 9-desaturase in carp by transcriptional and posttranslational mechanisms. *Science* *271*, 815-818.
64. Zhang, S.O., Box, A.C., Xu, N., Le Men, J., Yu, J., Guo, F., Trimble, R., and Mak, H.Y. (2010). Genetic and dietary regulation of lipid droplet expansion in *Caenorhabditis elegans*. *Proc Natl Acad Sci U S A* *107*, 4640-4645.

65. Goodman, J.M. (2008). The gregarious lipid droplet. *J Biol Chem* *283*, 28005-28009.
66. Puri, V., and Czech, M.P. (2008). Lipid droplets: FSP27 knockout enhances their sizzle. *J Clin Invest* *118*, 2693-2696.
67. Martin, S., and Parton, R.G. (2006). Lipid droplets: a unified view of a dynamic organelle. *Nat Rev Mol Cell Biol* *7*, 373-378.
68. Kuerschner, L., Moessinger, C., and Thiele, C. (2008). Imaging of lipid biosynthesis: how a neutral lipid enters lipid droplets. *Traffic* *9*, 338-352.
69. Zhang, P., Na, H., Liu, Z., Zhang, S., Xue, P., Chen, Y., Pu, J., Peng, G., Huang, X., Yang, F., Xie, Z., Xu, T., Xu, P., Ou, G., Zhang, S.O., and Liu, P. Proteomic study and marker protein identification of *caenorhabditis elegans* lipid droplets. *Mol Cell Proteomics*.
70. Gronke, S., Mildner, A., Fellert, S., Tennagels, N., Petry, S., Muller, G., Jackle, H., and Kuhnlein, R.P. (2005). Brummer lipase is an evolutionary conserved fat storage regulator in *Drosophila*. *Cell Metab* *1*, 323-330.
71. Mullaney, B.C., Blind, R.D., Lemieux, G.A., Perez, C.L., Elle, I.C., Faergeman, N.J., Van Gilst, M.R., Ingraham, H.A., and Ashrafi, K. (2010). Regulation of *C. elegans* fat uptake and storage by acyl-CoA synthase-3 is dependent on NR5A family nuclear hormone receptor *nhr-25*. *Cell Metab* *12*, 398-410.
72. Bartz, R., Li, W.H., Venables, B., Zehmer, J.K., Roth, M.R., Welti, R., Anderson, R.G., Liu, P., and Chapman, K.D. (2007). Lipidomics reveals that adiposomes store ether lipids and mediate phospholipid traffic. *J Lipid Res* *48*, 837-847.
73. Greenberg, A.S., Egan, J.J., Wek, S.A., Garty, N.B., Blanchette-Mackie, E.J., and Londos, C. (1991). Perilipin, a major hormonally regulated adipocyte-specific phosphoprotein associated with the periphery of lipid storage droplets. *J Biol Chem* *266*, 11341-11346.
74. Wang, C., Liu, Z., and Huang, X. (2012). Rab32 is important for autophagy and lipid storage in *Drosophila*. *PLoS One* *7*, e32086.
75. Zehmer, J.K., Huang, Y., Peng, G., Pu, J., Anderson, R.G., and Liu, P. (2009). A role for lipid droplets in inter-membrane lipid traffic. *Proteomics* *9*, 914-921.
76. Liu, P., Bartz, R., Zehmer, J.K., Ying, Y.S., Zhu, M., Serrero, G., and Anderson, R.G. (2007). Rab-regulated interaction of early endosomes with lipid droplets. *Biochim Biophys Acta* *1773*, 784-793.
77. Krahmer, N., Guo, Y., Wilfling, F., Hilger, M., Lingrell, S., Heger, K., Newman, H.W., Schmidt-Supprian, M., Vance, D.E., Mann, M., Farese, R.V., Jr., and Walther, T.C. (2011). Phosphatidylcholine synthesis for lipid droplet expansion is mediated by localized activation of CTP:phosphocholine cytidyltransferase. *Cell Metab* *14*, 504-515.

78. Listenberger, L.L., Han, X., Lewis, S.E., Cases, S., Farese, R.V., Jr., Ory, D.S., and Schaffer, J.E. (2003). Triglyceride accumulation protects against fatty acid-induced lipotoxicity. *Proc Natl Acad Sci U S A* *100*, 3077-3082.
79. Marcinkiewicz, A., Gauthier, D., Garcia, A., and Brasaemle, D.L. (2006). The phosphorylation of serine 492 of perilipin a directs lipid droplet fragmentation and dispersion. *J Biol Chem* *281*, 11901-11909.
80. Narbonne, P., and Roy, R. (2009). *Caenorhabditis elegans* dauers need LKB1/AMPK to ration lipid reserves and ensure long-term survival. *Nature* *457*, 210-214.
81. Wang, M.C., O'Rourke, E.J., and Ruvkun, G. (2008). Fat metabolism links germline stem cells and longevity in *C. elegans*. *Science* *322*, 957-960.
82. Hellerer, T., Axang, C., Brackmann, C., Hillertz, P., Pilon, M., and Enejder, A. (2007). Monitoring of lipid storage in *Caenorhabditis elegans* using coherent anti-Stokes Raman scattering (CARS) microscopy. *Proc Natl Acad Sci U S A* *104*, 14658-14663.
83. Cassada, R.C., and Russell, R.L. (1975). The dauerlarva, a post-embryonic developmental variant of the nematode *Caenorhabditis elegans*. *Dev Biol* *46*, 326-342.
84. Wang, J., and Kim, S.K. (2003). Global analysis of dauer gene expression in *Caenorhabditis elegans*. *Development* *130*, 1621-1634.
85. Wadsworth, W.G., and Riddle, D.L. (1989). Developmental regulation of energy metabolism in *Caenorhabditis elegans*. *Dev Biol* *132*, 167-173.
86. Klass, M., and Hirsh, D. (1976). Non-ageing developmental variant of *Caenorhabditis elegans*. *Nature* *260*, 523-525.
87. Hu, P.J. (2007). Dauer. *WormBook*, 1-19.
88. Joo, H.J., Yim, Y.H., Jeong, P.Y., Jin, Y.X., Lee, J.E., Kim, H., Jeong, S.K., Chitwood, D.J., and Paik, Y.K. (2009). *Caenorhabditis elegans* utilizes dauer pheromone biosynthesis to dispose of toxic peroxisomal fatty acids for cellular homeostasis. *Biochem J* *422*, 61-71.
89. Zhang, J., Bakheet, R., Parhar, R.S., Huang, C.H., Hussain, M.M., Pan, X., Siddiqui, S.S., and Hashmi, S. (2011). Regulation of fat storage and reproduction by Kruppel-like transcription factor KLF3 and fat-associated genes in *Caenorhabditis elegans*. *J Mol Biol* *411*, 537-553.
90. Xu, M., Joo, H.J., and Paik, Y.K. (2011). Novel functions of lipid-binding protein 5 in *Caenorhabditis elegans* fat metabolism. *J Biol Chem* *286*, 28111-28118.
91. Elle, I.C., Simonsen, K.T., Olsen, L.C., Birck, P.K., Ehmsen, S., Tuck, S., Le, T.T., and Faergeman, N.J. (2011). Tissue- and paralogue-specific functions of

- acyl-CoA-binding proteins in lipid metabolism in *Caenorhabditis elegans*. *Biochem J* 437, 231-241.
92. Li, Y., Na, K., Lee, H.J., Lee, E.Y., and Paik, Y.K. (2011). Contribution of *sams-1* and *pmt-1* to lipid homeostasis in adult *Caenorhabditis elegans*. *J Biochem* 149, 529-538.
 93. Walker, A.K., Jacobs, R.L., Watts, J.L., Rottiers, V., Jiang, K., Finnegan, D.M., Shioda, T., Hansen, M., Yang, F., Niebergall, L.J., Vance, D.E., Tzoneva, M., Hart, A.C., and Naar, A.M. (2011). A conserved SREBP-1/phosphatidylcholine feedback circuit regulates lipogenesis in metazoans. *Cell* 147, 840-852.
 94. Spanier, B., Lasch, K., Marsch, S., Benner, J., Liao, W., Hu, H., Kienberger, H., Eisenreich, W., and Daniel, H. (2009). How the intestinal peptide transporter PEPT-1 contributes to an obesity phenotype in *Caenorhabditis elegans*. *PLoS One* 4, e6279.
 95. Brenner, S. (1974). The genetics of *Caenorhabditis elegans*. *Genetics* 77, 71-94.
 96. Knight, C.G., Patel, M.N., Azevedo, R.B., and Leroi, A.M. (2002). A novel mode of ecdysozoan growth in *Caenorhabditis elegans*. *Evol Dev* 4, 16-27.
 97. Salomon, M.P., Ostrow, D., Phillips, N., Blanton, D., Bour, W., Keller, T.E., Levy, L., Sylvestre, T., Upadhyay, A., and Baer, C.F. (2009). Comparing mutational and standing genetic variability for fitness and size in *Caenorhabditis briggsae* and *C. elegans*. *Genetics* 183, 685-692, 681SI-619SI.
 98. Klapper, M., Ehmke, M., Palgunow, D., Bohme, M., Matthaus, C., Bergner, G., Dietzek, B., Popp, J., and Doring, F. (2011). Fluorescence-based fixative and vital staining of lipid droplets in *Caenorhabditis elegans* reveal fat stores using microscopy and flow cytometry approaches. *J Lipid Res* 52, 1281-1293.
 99. Schlotterer, A., Hamann, A., Kukudov, G., Ibrahim, Y., Heckmann, B., Bozorgmehr, F., Pfeiffer, M., Hutter, H., Stern, D., Du, X., Brownlee, M., Bierhaus, A., Nawroth, P., and Morcos, M. (2010). Apurinic/aprimidinic endonuclease 1, p53, and thioredoxin are linked in control of aging in *C. elegans*. *Aging Cell* 9, 420-432.
 100. Miller, D.L., and Roth, M.B. (2009). *C. elegans* are protected from lethal hypoxia by an embryonic diapause. *Curr Biol* 19, 1233-1237.
 101. Gerstbrein, B., Stamatias, G., Kollias, N., and Driscoll, M. (2005). In vivo spectrofluorimetry reveals endogenous biomarkers that report healthspan and dietary restriction in *Caenorhabditis elegans*. *Aging Cell* 4, 127-137.
 102. Rasband, W.S. (1997-2011). ImageJ (U. S. National Institutes of Health, Bethesda, Maryland, USA, <http://imagej.nih/ij/>).

103. Abramoff, M.D., Magalhaes, P.J., Ram, S.J. (2004). Image Processing with ImageJ. *Biophotonics International* 11, 36-42.
104. Bolstad, B.M., Irizarry, R.A., Astrand, M., and Speed, T.P. (2003). A comparison of normalization methods for high density oligonucleotide array data based on variance and bias. *Bioinformatics* 19, 185-193.
105. Gems, D., Sutton, A.J., Sundermeyer, M.L., Albert, P.S., King, K.V., Edgley, M.L., Larsen, P.L., and Riddle, D.L. (1998). Two pleiotropic classes of *daf-2* mutation affect larval arrest, adult behavior, reproduction and longevity in *Caenorhabditis elegans*. *Genetics* 150, 129-155.
106. Raizen, D.M., Lee, R.Y., and Avery, L. (1995). Interacting genes required for pharyngeal excitation by motor neuron MC in *Caenorhabditis elegans*. *Genetics* 141, 1365-1382.
107. Liepa, G.U., Masoro, E.J., Bertrand, H.A., and Yu, B.P. (1980). Food restriction as a modulator of age-related changes in serum lipids. *Am J Physiol* 238, E253-257.
108. Ward, W.F. (1988). Food restriction enhances the proteolytic capacity of the aging rat liver. *J Gerontol* 43, B121-124.
109. Yin, D. (1996). Biochemical basis of lipofuscin, ceroid, and age pigment-like fluorophores. *Free Radic Biol Med* 21, 871-888.
110. Ulrich, P., and Cerami, A. (2001). Protein glycation, diabetes, and aging. *Recent Prog Horm Res* 56, 1-21.
111. Clokey, G.V., and Jacobson, L.A. (1986). The autofluorescent "lipofuscin granules" in the intestinal cells of *Caenorhabditis elegans* are secondary lysosomes. *Mech Ageing Dev* 35, 79-94.
112. Brooks, K.K., Liang, B., and Watts, J.L. (2009). The influence of bacterial diet on fat storage in *C. elegans*. *PLoS One* 4, e7545.
113. Takahashi, K., Yoshina, S., Masashi, M., Ito, W., Inoue, T., Shiwaku, H., Arai, H., Mitani, S., and Okazawa, H. (2009). Nematode homologue of PQBP1, a mental retardation causative gene, is involved in lipid metabolism. *PLoS One* 4, e4104.
114. Hench, J., Bratic Hench, I., Pujol, C., Ipsen, S., Brodesser, S., Mourier, A., Tolnay, M., Frank, S., and Trifunovic, A. (2011). A tissue-specific approach to the analysis of metabolic changes in *Caenorhabditis elegans*. *PLoS One* 6, e28417.
115. Zarse, K., and Ristow, M. (2008). Antidepressants of the serotonin-antagonist type increase body fat and decrease lifespan of adult *Caenorhabditis elegans*. *PLoS One* 3, e4062.

116. Van Gilst, M.R., Hadjivassiliou, H., and Yamamoto, K.R. (2005). A *Caenorhabditis elegans* nutrient response system partially dependent on nuclear receptor NHR-49. *Proc Natl Acad Sci U S A* *102*, 13496-13501.
117. Schulz, T.J., Zarse, K., Voigt, A., Urban, N., Birringer, M., and Ristow, M. (2007). Glucose restriction extends *Caenorhabditis elegans* life span by inducing mitochondrial respiration and increasing oxidative stress. *Cell Metab* *6*, 280-293.
118. Robertson, F.W. (1959). *Studies in Quantitative Inheritance*. Xii. Cell Size and Number in Relation to Genetic and Environmental Variation of Body Size in *Drosophila*. *Genetics* *44*, 869-896.
119. Houthoofd, K., Braeckman, B.P., Lenaerts, I., Brys, K., De Vreese, A., Van Eygen, S., and Vanfleteren, J.R. (2002). No reduction of metabolic rate in food restricted *Caenorhabditis elegans*. *Exp Gerontol* *37*, 1359-1369.
120. So, S., Miyahara, K., and Ohshima, Y. (2011). Control of body size in *C. elegans* dependent on food and insulin/IGF-1 signal. *Genes Cells* *16*, 639-651.
121. Satouchi, K., Hirano, K., Sakaguchi, M., Takehara, H., and Matsuura, F. (1993). Phospholipids from the free-living nematode *Caenorhabditis elegans*. *Lipids* *28*, 837-840.
122. Yen, C.L., Stone, S.J., Koliwad, S., Harris, C., and Farese, R.V., Jr. (2008). Thematic review series: glycerolipids. DGAT enzymes and triacylglycerol biosynthesis. *J Lipid Res* *49*, 2283-2301.
123. Aarnio, V., Lehtonen, M., Storvik, M., Callaway, J.C., Lakso, M., and Wong, G. (2011). *Caenorhabditis Elegans* Mutants Predict Regulation of Fatty Acids and Endocannabinoids by the CYP-35A Gene Family. *Front Pharmacol* *2*, 12.
124. Li, X., Cope, M.B., Johnson, M.S., Smith, D.L., Jr., and Nagy, T.R. (2010). Mild calorie restriction induces fat accumulation in female C57BL/6J mice. *Obesity (Silver Spring)* *18*, 456-462.
125. Listenberger, L.L., Ory, D.S., and Schaffer, J.E. (2001). Palmitate-induced apoptosis can occur through a ceramide-independent pathway. *J Biol Chem* *276*, 14890-14895.
126. Castro, C., Sar, F., Shaw, W.R., Mishima, M., Miska, E.A., and Griffin, J.L. (2012). A metabolomic strategy defines the regulation of lipid content and global metabolism by Delta9 desaturases in *Caenorhabditis elegans*. *BMC Genomics* *13*, 36.
127. Watts, J.L., and Browse, J. (2000). A palmitoyl-CoA-specific delta9 fatty acid desaturase from *Caenorhabditis elegans*. *Biochem Biophys Res Commun* *272*, 263-269.
128. Watts, J.L., and Browse, J. (2002). Genetic dissection of polyunsaturated fatty acid synthesis in *Caenorhabditis elegans*. *Proc Natl Acad Sci U S A* *99*, 5854-5859.

129. Zhang, P., Na, H., Liu, Z., Zhang, S., Xue, P., Chen, Y., Pu, J., Peng, G., Huang, X., Yang, F., Xie, Z., Xu, T., Xu, P., Ou, G., Zhang, S.O., and Liu, P. (2012). Proteomic study and marker protein identification of *Caenorhabditis elegans* lipid droplets. *Mol Cell Proteomics*.
130. Guo, Y., Walther, T.C., Rao, M., Stuurman, N., Goshima, G., Terayama, K., Wong, J.S., Vale, R.D., Walter, P., and Farese, R.V. (2008). Functional genomic screen reveals genes involved in lipid-droplet formation and utilization. *Nature* *453*, 657-661.
131. Brendza, K.M., Haakenson, W., Cahoon, R.E., Hicks, L.M., Palavalli, L.H., Chiapelli, B.J., McLaird, M., McCarter, J.P., Williams, D.J., Hresko, M.C., and Jez, J.M. (2007). Phosphoethanolamine N-methyltransferase (PMT-1) catalyses the first reaction of a new pathway for phosphocholine biosynthesis in *Caenorhabditis elegans*. *Biochem J* *404*, 439-448.
132. Palavalli, L.H., Brendza, K.M., Haakenson, W., Cahoon, R.E., McLaird, M., Hicks, L.M., McCarter, J.P., Williams, D.J., Hresko, M.C., and Jez, J.M. (2006). Defining the role of phosphomethylethanolamine N-methyltransferase from *Caenorhabditis elegans* in phosphocholine biosynthesis by biochemical and kinetic analysis. *Biochemistry* *45*, 6056-6065.
133. Vance, J.E., and Vance, D.E. (2004). Phospholipid biosynthesis in mammalian cells. *Biochem Cell Biol* *82*, 113-128.
134. Nagayama, M., Uchida, T., and Gohara, K. (2007). Temporal and spatial variations of lipid droplets during adipocyte division and differentiation. *J Lipid Res* *48*, 9-18.
135. Zimmermann, R., Strauss, J.G., Haemmerle, G., Schoiswohl, G., Birner-Gruenberger, R., Riederer, M., Lass, A., Neuberger, G., Eisenhaber, F., Hermetter, A., and Zechner, R. (2004). Fat mobilization in adipose tissue is promoted by adipose triglyceride lipase. *Science* *306*, 1383-1386.
136. Jo, H., Shim, J., Lee, J.H., Lee, J., and Kim, J.B. (2009). IRE-1 and HSP-4 contribute to energy homeostasis via fasting-induced lipases in *C. elegans*. *Cell Metab* *9*, 440-448.
137. Ogg, S., Paradis, S., Gottlieb, S., Patterson, G.I., Lee, L., Tissenbaum, H.A., and Ruvkun, G. (1997). The Fork head transcription factor DAF-16 transduces insulin-like metabolic and longevity signals in *C. elegans*. *Nature* *389*, 994-999.
138. Lin, K., Dorman, J.B., Rodan, A., and Kenyon, C. (1997). *daf-16*: An HNF-3/forkhead family member that can function to double the life-span of *Caenorhabditis elegans*. *Science* *278*, 1319-1322.
139. Furuyama, T., Nakazawa, T., Nakano, I., and Mori, N. (2000). Identification of the differential distribution patterns of mRNAs and consensus binding sequences for mouse DAF-16 homologues. *Biochem J* *349*, 629-634.

140. Mukhopadhyay, A., Oh, S.W., and Tissenbaum, H.A. (2006). Worming pathways to and from DAF-16/FOXO. *Exp Gerontol* *41*, 928-934.
141. Birkenkamp, K.U., and Coffey, P.J. (2003). Regulation of cell survival and proliferation by the FOXO (Forkhead box, class O) subfamily of Forkhead transcription factors. *Biochem Soc Trans* *31*, 292-297.
142. Pinkston-Gosse, J., and Kenyon, C. (2007). DAF-16/FOXO targets genes that regulate tumor growth in *Caenorhabditis elegans*. *Nat Genet* *39*, 1403-1409.
143. Swindell, W.R. (2011). Metallothionein and the biology of aging. *Ageing Res Rev* *10*, 132-145.
144. Hockner, M., Dallinger, R., and Sturzenbaum, S.R. (2011). Nematode and snail metallothioneins. *J Biol Inorg Chem* *16*, 1057-1065.
145. Ye, B., Rui, Q., Wu, Q., and Wang, D. (2010). Metallothioneins are required for formation of cross-adaptation response to neurobehavioral toxicity from lead and mercury exposure in nematodes. *PLoS One* *5*, e14052.
146. Yang, X., Doser, T.A., Fang, C.X., Nunn, J.M., Janardhanan, R., Zhu, M., Sreejayan, N., Quinn, M.T., and Ren, J. (2006). Metallothionein prolongs survival and antagonizes senescence-associated cardiomyocyte diastolic dysfunction: role of oxidative stress. *Faseb J* *20*, 1024-1026.
147. Swindell, W.R. (2008). Comparative analysis of microarray data identifies common responses to caloric restriction among mouse tissues. *Mech Ageing Dev* *129*, 138-153.
148. Zid, B.M., Rogers, A.N., Katewa, S.D., Vargas, M.A., Kolipinski, M.C., Lu, T.A., Benzer, S., and Kapahi, P. (2009). 4E-BP extends lifespan upon dietary restriction by enhancing mitochondrial activity in *Drosophila*. *Cell* *139*, 149-160.
149. Reichert, K., and Menzel, R. (2005). Expression profiling of five different xenobiotics using a *Caenorhabditis elegans* whole genome microarray. *Chemosphere* *61*, 229-237.
150. Menzel, R., Bogaert, T., and Achazi, R. (2001). A systematic gene expression screen of *Caenorhabditis elegans* cytochrome P450 genes reveals CYP35 as strongly xenobiotic inducible. *Arch Biochem Biophys* *395*, 158-168.
151. Lewis, J.A., Szilagyi, M., Gehman, E., Dennis, W.E., and Jackson, D.A. (2009). Distinct patterns of gene and protein expression elicited by organophosphorus pesticides in *Caenorhabditis elegans*. *BMC Genomics* *10*, 202.
152. Gems, D., and McElwee, J.J. (2005). Broad spectrum detoxification: the major longevity assurance process regulated by insulin/IGF-1 signaling? *Mech Ageing Dev* *126*, 381-387.

153. Jia, K., Albert, P.S., and Riddle, D.L. (2002). DAF-9, a cytochrome P450 regulating *C. elegans* larval development and adult longevity. *Development* *129*, 221-231.
154. Gerisch, B., Weitzel, C., Kober-Eisermann, C., Rottiers, V., and Antebi, A. (2001). A hormonal signaling pathway influencing *C. elegans* metabolism, reproductive development, and life span. *Dev Cell* *1*, 841-851.
155. Cancino-Badias, L., Reyes, R.E., Nosti, R., Perez, I., Dorado, V., Caballero, S., Soria, A., Camacho-Carranza, R., Escobar, D., and Espinosa-Aguirre, J.J. (2003). Modulation of rat liver cytochrome P450 by protein restriction assessed by biochemical and bacterial mutagenicity methods [corrected]. *Mutagenesis* *18*, 95-100.
156. Mao, Z.L., Tam, Y.K., and Coutts, R.T. (2006). Effect of protein and calorie malnutrition on drug metabolism in rat - in vitro. *J Pharm Pharm Sci* *9*, 60-70.
157. O'Rourke, D., Baban, D., Demidova, M., Mott, R., and Hodgkin, J. (2006). Genomic clusters, putative pathogen recognition molecules, and antimicrobial genes are induced by infection of *C. elegans* with *M. nematophilum*. *Genome Res* *16*, 1005-1016.
158. Schulenburg, H., Hoepfner, M.P., Weiner, J., 3rd, and Bornberg-Bauer, E. (2008). Specificity of the innate immune system and diversity of C-type lectin domain (CTLN) proteins in the nematode *Caenorhabditis elegans*. *Immunobiology* *213*, 237-250.
159. Mallo, G.V., Kurz, C.L., Couillault, C., Pujol, N., Granjeaud, S., Kohara, Y., and Ewbank, J.J. (2002). Inducible antibacterial defense system in *C. elegans*. *Curr Biol* *12*, 1209-1214.
160. Wong, D., Bazopoulou, D., Pujol, N., Tavernarakis, N., and Ewbank, J.J. (2007). Genome-wide investigation reveals pathogen-specific and shared signatures in the response of *Caenorhabditis elegans* to infection. *Genome Biol* *8*, R194.
161. Zhang, H.W., Sun, C., Sun, S.S., Zhao, X.F., and Wang, J.X. (2010). Functional analysis of two invertebrate-type lysozymes from red swamp crayfish, *Procambarus clarkii*. *Fish Shellfish Immunol* *29*, 1066-1072.
162. Baskova, I.P., and Zavalova, L.L. (2008). [Polyfunctionality of destabilase, a lysozyme from a medicinal leech]. *Bioorg Khim* *34*, 337-343.
163. Xue, Q.G., Itoh, N., Schey, K.L., Li, Y.L., Cooper, R.K., and La Peyre, J.F. (2007). A new lysozyme from the eastern oyster (*Crassostrea virginica*) indicates adaptive evolution of i-type lysozymes. *Cell Mol Life Sci* *64*, 82-95.
164. Watson, R.R., and McMurray, D.N. (1979). The effects of malnutrition on secretory and cellular immune processes. *CRC Crit Rev Food Sci Nutr* *12*, 113-159.

165. Hughes, S., and Kelly, P. (2006). Interactions of malnutrition and immune impairment, with specific reference to immunity against parasites. *Parasite Immunol* *28*, 577-588.
166. Farese, R.V., Jr., and Walther, T.C. (2009). Lipid droplets finally get a little R-E-S-P-E-C-T. *Cell* *139*, 855-860.
167. Guo, Y., Cordes, K.R., Farese, R.V., Jr., and Walther, T.C. (2009). Lipid droplets at a glance. *J Cell Sci* *122*, 749-752.

Supplementary

Table S1. Complete list of dietary restriction (DR) response genes

Sequence	Gene	L4 DR1.5 vs AL		L4 DR0.7 vs AL		adult DR1.5 vs AL		adult DR0.7 vs AL	
		ratio ^a	p value ^b	ratio ^a	p value ^b	ratio ^a	p value ^b	ratio ^a	p value ^b
C01B10.7		0,43202	0,00167	0,22461	0,00009	0,18806	0,00468	0,13103	0,00392
C01G6.7	<i>acs-7</i>	2,81801	0,00089	4,39180	0,02097	3,10454	0,00262	3,06882	0,00021
C04F5.7	<i>ugt-63</i>	0,15225	0,00189	0,10475	0,00231	0,03433	0,00131	0,03278	0,00133
C05E11.5	<i>amt-4</i>	0,46985	0,00029	0,36099	0,00024	0,13099	0,00132	0,13720	0,00112
C06B3.3	<i>cyp-35C1</i>	0,34233	0,00016	0,28382	0,00017	0,06011	0,00026	0,04881	0,00033
C09B8.4		0,41778	0,00008	0,28827	0,00005	0,09695	0,00000	0,06355	0,00001
C11E4.7		0,43458	0,00239	0,32179	0,00123	0,16858	0,00045	0,18509	0,00034
C14A6.10		0,37573	0,00029	0,37688	0,00341	0,31578	0,00025	0,26765	0,00069
C15C8.3		0,48464	0,00227	0,26785	0,00015	0,04116	0,00076	0,06749	0,00051
C17C3.19	<i>ins-12</i>	2,49181	0,00300	2,51383	0,00433	0,29009	0,00827	0,23513	0,00875
C17F4.7		0,34658	0,00277	0,24940	0,00024	0,09596	0,00000	0,07384	0,00000
C18D1.2		4,47005	0,00620	6,42614	0,00877	3,85236	0,00217	5,51845	0,00156
C27C7.3	<i>nhr-74</i>	2,75005	0,00006	2,71313	0,01317	0,06074	0,00039	0,05424	0,00019
C29F3.2	<i>wrt-8</i>	2,28336	0,00063	2,69276	0,00091	6,35194	0,03234	7,98767	0,00548
C29F7.t2		0,43705	0,00565	0,29551	0,00217	0,06275	0,00000	0,05040	0,00003
C37A5.t1		0,42794	0,00594	0,31950	0,00304	0,07429	0,00000	0,05457	0,00004
C39E9.4	<i>scl-6</i>	0,26721	0,00002	0,34633	0,00001	0,01878	0,00154	0,02141	0,00146
C40H1.8.1		0,27083	0,00039	0,23674	0,00006	0,24891	0,00489	0,33690	0,00428
C42D4.2		0,48971	0,00065	0,24257	0,00001	0,12219	0,00000	0,09215	0,00000
C44H9.1	<i>ugt-15</i>	42,69997	0,00954	31,49785	0,01954	6,34249	0,00039	6,80534	0,00019
C45B11.3.1	<i>dhs-18</i>	2,20931	0,00888	3,49644	0,02699	3,79201	0,00142	3,70574	0,00008
C49G7.11	<i>djr-1.2</i>	3,21510	0,03625	4,72862	0,00919	2,22144	0,04783	3,01817	0,01087
C54G6.5	<i>spp-17</i>	0,48859	0,00004	0,29872	0,00004	0,13946	0,00024	0,06833	0,00045
D2021.4a		2,03972	0,00031	2,41333	0,00102	2,30302	0,00006	2,41938	0,00020
F09C6.11		2,28423	0,04471	3,19088	0,00425	2,58392	0,02164	3,73194	0,00060
F10C2.3		2,62212	0,03684	2,85934	0,00018	3,00013	0,00071	2,46379	0,00159
F13E9.14		2,34661	0,03684	5,14521	0,01574	3,92767	0,00578	6,55070	0,02491
F13E9.15		3,35069	0,00903	4,89788	0,01338	4,80625	0,00909	7,49380	0,00057
F14H3.10	<i>cyp-35D1</i>	0,18180	0,00030	0,12273	0,00021	0,06377	0,00029	0,03034	0,00079
F15B9.1	<i>far-3</i>	10,70440	0,00039	13,35756	0,00084	3,74708	0,04640	3,10135	0,00321
F15E6.10		2,24578	0,00493	4,05887	0,01561	3,11103	0,00754	2,89078	0,00560
F16B4.12a	<i>nhr-117</i>	2,28234	0,02423	2,79843	0,01066	4,08175	0,00003	4,77548	0,00000
F16B4.12b	<i>nhr-117</i>	2,27381	0,01966	2,78684	0,00625	4,09909	0,00013	4,75487	0,00000
F19G12.t1		0,47438	0,00183	0,24006	0,00012	0,06410	0,00456	0,04890	0,00428
F22A3.6b	<i>ilys-5</i>	0,41308	0,00909	0,42653	0,00813	0,05384	0,00115	0,03872	0,00105
F22B8.6.1	<i>cth-1</i>	3,32440	0,01907	2,59659	0,03915	2,11073	0,02631	2,14030	0,01014
F22B8.6.2	<i>cth-1</i>	3,27922	0,02124	2,64639	0,03592	2,17907	0,02211	2,23465	0,00541
F22E5.1		0,47776	0,01050	0,23353	0,00088	0,04838	0,00048	0,05573	0,00045
F22H10.6		0,43071	0,00732	0,27961	0,00241	0,04992	0,00022	0,04487	0,00020
F27D4.t1		0,46760	0,00906	0,37047	0,00289	0,16026	0,00880	0,14674	0,00797
F28F8.2	<i>acs-2</i>	2,36851	0,01024	3,17112	0,00550	8,33917	0,01079	11,99567	0,00036
F35E12.5		0,33451	0,00029	0,26583	0,00111	0,04048	0,04299	0,03304	0,04036
F35E8.10		3,38910	0,01441	4,85933	0,00620	3,87366	0,00642	4,18085	0,00945
F35E8.13		8,01227	0,01596	11,25021	0,00729	9,97278	0,00680	10,69217	0,01147
F36G9.12	<i>oac-20</i>	0,46838	0,00047	0,39639	0,00010	0,37831	0,00491	0,20786	0,00158
F38A1.14	<i>clec-169</i>	0,36544	0,00089	0,26543	0,00108	0,15375	0,00000	0,20549	0,00000
F38E11.1	<i>hsp-12.3</i>	4,88342	0,01490	6,29820	0,00051	3,03983	0,00004	3,01971	0,00015
F39E9.1		0,37552	0,00022	0,21006	0,00001	0,14387	0,00006	0,10839	0,00021
F49E12.2	<i>dod-23</i>	0,41789	0,01023	0,34017	0,00761	0,44942	0,00002	0,38451	0,00001
F54F3.4		2,91024	0,00013	4,07580	0,01112	5,00771	0,00001	5,65554	0,00002

Continued Table S1

Sequence	Gene	L4 DR1.5 vs AL		L4 DR0.7 vs AL		adult DR1.5 vs AL		adult DR0.7 vs AL	
		ratio ^a	p value ^b	ratio ^a	p value ^b	ratio ^a	p value ^b	ratio ^a	p value ^b
F55B12.10		3,70879	0,01546	7,14236	0,04225	5,91684	0,00109	8,45358	0,01954
F55G11.4		0,26689	0,00013	0,25851	0,00010	0,08690	0,00285	0,08488	0,00326
F55G11.7.2		0,49662	0,00001	0,45952	0,00003	0,17184	0,00200	0,14873	0,00242
F55H12.2		2,20235	0,04933	3,00290	0,00891	2,55917	0,00078	2,88922	0,00143
F56A4.10		0,43001	0,00034	0,41866	0,00011	0,16134	0,00304	0,11441	0,00424
F56D6.1	<i>clec-68</i>	6,81674	0,00234	5,44280	0,01320	2,31151	0,00428	4,10324	0,00043
F56D6.10	<i>dct-8</i>	8,07731	0,00852	26,43315	0,03921	8,28323	0,01742	9,78091	0,00170
F57A10.1	<i>str-9</i>	2,49853	0,04317	3,06848	0,00756	2,33711	0,00276	2,88087	0,00604
F58E6.7		0,35955	0,00025	0,15682	0,00001	0,16364	0,00008	0,08945	0,00066
F58F9.7.1		2,06863	0,00008	2,71289	0,01301	2,42184	0,00597	2,34502	0,00169
F58F9.7.3		2,00597	0,00197	2,73555	0,01214	2,59706	0,00608	2,43779	0,00168
F59E11.7b		2,34331	0,04748	3,74728	0,02161	2,43420	0,01113	3,01860	0,00330
H01M10.3	<i>ttr-42</i>	0,40577	0,04563	0,27947	0,02395	0,48137	0,00036	0,30984	0,00001
H23N18.3	<i>ugt-8</i>	0,38623	0,00005	0,39090	0,00001	0,13803	0,00679	0,17094	0,00669
K01A6.7		3,01011	0,00810	6,85917	0,02018	14,97323	0,00311	26,23800	0,01506
K02D7.5.2	<i>swt-1</i>	2,07473	0,02218	2,30871	0,00808	3,95324	0,00004	3,98225	0,00024
K07C6.5	<i>cyp-35A5</i>	0,23418	0,00000	0,15413	0,00000	0,04541	0,00010	0,03606	0,00007
K09D9.2	<i>cyp-35A3</i>	0,36110	0,01213	0,29907	0,00961	0,08026	0,00687	0,07666	0,00641
K09F5.2	<i>vit-1</i>	0,40203	0,02120	0,16243	0,01158	0,06275	0,00000	0,02022	0,00001
K09H11.1.1		2,15510	0,00056	2,57719	0,02227	2,01886	0,00000	2,19542	0,00000
K10C2.7		0,48451	0,00359	0,34061	0,00136	0,26423	0,00166	0,17729	0,00160
K10C9.9		0,23088	0,00016	0,17664	0,00000	0,20322	0,00140	0,22410	0,00046
M02D8.4c	<i>asns-2</i>	2,19712	0,04540	3,57865	0,01588	7,80824	0,00006	7,56952	0,00011
R06B10.3	<i>clec-150</i>	0,45722	0,00003	0,36522	0,00000	0,27400	0,00001	0,22055	0,00009
R07B1.3	<i>scav-5</i>	0,48519	0,00341	0,38691	0,00006	0,16016	0,00048	0,16098	0,00045
T03D3.1	<i>ugt-53</i>	0,33104	0,00049	0,24699	0,00055	0,32901	0,00001	0,27285	0,00000
T04H1.3	<i>ttr-22</i>	2,14148	0,01157	3,01742	0,01467	4,63800	0,00004	7,01283	0,00000
T08G5.1		3,44494	0,00796	4,81519	0,03267	3,41135	0,00794	3,54624	0,00724
T08G5.10	<i>mtl-2</i>	3,24315	0,00177	3,94271	0,00051	2,79849	0,00110	3,06954	0,00002
T10H4.10	<i>cyp-34A1</i>	9,20141	0,03007	16,35552	0,00225	3,77265	0,00236	4,00455	0,00036
T11F1.3		0,33628	0,01685	0,42764	0,01467	0,07981	0,00300	0,04402	0,00428
T13B5.5	<i>lips-11</i>	0,23434	0,00045	0,17758	0,00089	0,32625	0,01102	0,23196	0,01067
T13B5.6	<i>lips-12</i>	0,45229	0,04873	0,43283	0,03506	0,30232	0,00078	0,25933	0,00118
T16G1.4		2,84200	0,04020	6,62597	0,03336	29,01125	0,00575	33,59784	0,00743
T16G1.7		8,43868	0,00005	10,53486	0,01317	10,24759	0,00321	13,61410	0,00235
T20B3.1		2,37801	0,00133	3,67663	0,02949	10,13373	0,00097	9,23372	0,00004
T23F4.1		2,79027	0,00828	4,84971	0,04083	8,64862	0,00140	11,11017	0,00001
T23F4.3		2,40542	0,00567	4,70279	0,03004	9,02124	0,00001	9,68458	0,00008
W01C9.2		0,23203	0,00189	0,16763	0,00072	2,64538	0,00312	2,42811	0,00016
W02D7.8		2,11495	0,02013	3,21211	0,03335	5,55099	0,00077	6,24744	0,00000
W03D2.1a	<i>pqn-75</i>	2,20124	0,00731	3,13813	0,00391	3,19678	0,00218	4,11284	0,00000
W03D2.1c	<i>pqn-75</i>	2,26541	0,00461	3,03890	0,00679	3,26472	0,00199	4,18705	0,00001
W04E12.8	<i>clec-50</i>	0,40380	0,00006	0,39968	0,00349	0,33203	0,00003	0,28143	0,00006
W06A7.4		0,44776	0,00541	0,43938	0,00382	0,29078	0,00012	0,25277	0,00000
W06D12.3	<i>fat-5</i>	3,69130	0,00517	3,62023	0,04990	2,29319	0,00009	2,51875	0,00687
W06D4.t1		0,49009	0,01357	0,40101	0,00431	0,17899	0,01270	0,16311	0,01160
Y102A5C.7	<i>clec-237</i>	0,27901	0,00004	0,24817	0,00001	0,34219	0,03995	0,28677	0,03083
Y110A2AL.2		5,32998	0,00827	9,69225	0,00542	5,92687	0,00199	9,64086	0,00437
Y19D10A.8		0,48196	0,00004	0,44488	0,00061	0,32295	0,00733	0,10499	0,00104
Y32H12A.3.1	<i>dhs-9</i>	2,21839	0,00429	3,17129	0,00500	2,32625	0,00018	2,57381	0,00109
Y32H12A.3.2		2,31494	0,00462	3,22228	0,00501	2,24544	0,00087	2,48337	0,00252
Y37F4.8		2,23358	0,02932	3,02597	0,01115	7,64479	0,00648	10,28706	0,00328
Y38E10A.5	<i>clec-4</i>	2,22242	0,00337	2,61481	0,01527	0,45624	0,01999	0,42001	0,01354
Y39H10A.1		14,71840	0,01566	35,89409	0,00501	11,33999	0,00339	17,30888	0,00500
Y40C7B.4		0,33791	0,00962	0,34456	0,00617	0,30630	0,00084	0,21336	0,00053
Y45F10D.6		2,18001	0,00649	3,07556	0,01375	3,53176	0,00097	3,85864	0,00029
Y46D2A.2		0,38357	0,00042	0,21436	0,00001	0,16180	0,00004	0,09326	0,00018

Continued Table S1

Sequence	Gene	L4 DR1.5 vs AL		L4 DR0.7 vs AL		adult DR1.5 vs AL		adult DR0.7 vs AL	
		ratio ^a	p value ^b	ratio ^a	p value ^b	ratio ^a	p value ^b	ratio ^a	p value ^b
Y46E12BR.1		2,67509	0,02347	3,86028	0,00610	4,11234	0,00267	4,65756	0,00001
Y48A6B.9		2,68166	0,00479	3,94069	0,01366	2,70410	0,00025	2,70508	0,00000
Y48E1B.8		0,47618	0,02612	0,22660	0,00271	0,00327	0,00020	0,00338	0,00020
Y4C6B.6		0,16228	0,00000	0,14340	0,00000	0,03146	0,00019	0,02932	0,00015
Y53G8B.2		3,53334	0,01908	5,08052	0,02580	2,56510	0,00080	2,57162	0,00017
Y69H2.10a		2,04502	0,02196	3,94445	0,02456	8,32378	0,00022	10,38159	0,00033
Y75B8A.44		0,34594	0,00006	0,32768	0,00000	0,37239	0,00006	0,45646	0,00009
Y8A9A.2		2,78749	0,01703	4,12137	0,00997	10,86006	0,00653	14,13183	0,00113
ZC443.5	<i>ugt-18</i>	12,22660	0,00746	13,88118	0,02776	34,02960	0,00015	41,71220	0,00212
ZK1010.t1		0,43980	0,01290	0,29907	0,00664	0,06245	0,00020	0,04801	0,00016
ZK1025.6	<i>nhr-244</i>	2,39041	0,00002	2,62002	0,00748	0,09787	0,00000	0,10664	0,00000
ZK1290.15		0,29136	0,00001	0,26400	0,00003	0,30683	0,00041	0,28513	0,00012
ZK154.t1		0,45740	0,02638	0,36879	0,01044	0,17125	0,01391	0,15243	0,01267
ZK39.6	<i>clcc-97</i>	0,36425	0,02395	0,32255	0,02381	0,30464	0,00335	0,35934	0,00417
ZK6.7b	<i>lipl-5</i>	0,27163	0,00101	0,23770	0,00219	0,42293	0,00262	0,46416	0,00025
ZK617.2	<i>lips-6</i>	11,14290	0,00391	12,75312	0,00272	2,67551	0,01117	3,98651	0,00084
ZK896.3		0,48522	0,00244	0,41580	0,00155	0,24939	0,00053	0,24980	0,00092

This table contains all 124 DR response genes inclusively splice variants that were significantly regulated in L4 and adult stage cultivated at two different DR conditions (DR1.5, DR0.7). Criteria for inclusion in this data table were a fold-change >2.0 and significance threshold of p-value <0.05.

^aThe ratio was calculated between DR and *ad libitum* (AL) condition and indicates the fold change of gene expression.

^bP values were calculated using unpaired t-test.

Table S2. Dietary restriction (DR) induced alteration of expression of genes implicated in lipid metabolism and storage in *C. elegans*

Description ^a	Fold change of regulation ^b			
	L4		adult	
	DR1.5	DR0.7	DR1.5	DR0.7
Lipases				
<i>hosl-1</i>	1.2	ns	1.0/ -1.1	-1.2/ -1.3
<i>atgl-1</i>	1.7/ 1.4	1.4/ 1.6	ns	-1.3
<i>fil-1</i>	ns	ns	8.4	5.7
<i>fil-2</i>	ns	ns	ns	ns
Mitochondrial β-oxidation				
Mitochondrial acyl-CoA synthetase				
<i>acs-3</i>	1.1	1.1	1.8	2.0
<i>acs-11</i>	ns	1.6	2.5	2.8
<i>acs-13</i>	ns	ns	-1.3	-1.1
<i>acs-15</i>	-1.4	-1.7	1.7	3.5
<i>acs-18</i>	-1.4	-1.7	3.1	6.3
R09E10.4	ns	-2.0	1.2	2.6
Carnitine palmitoyl transferase I				
<i>cpt-1</i>	1.5	ns	1.6	1.4
<i>cpt-3</i>	7.3	ns	25.7	13.6
<i>cpt-4</i>	ns	-1.7	-1.7	ns
<i>cpt-5</i>	2.9	2.3	ns	ns
<i>cpt-6</i>	1.5	ns	ns	-1.4
F41E7.6	-1.7	ns	-5.0	-2.5
F09F3.9	2.9	2.4	ns	ns
Carnitine palmitoyl transferase II				
<i>cpt-2</i>	1.3	1.4	1.1	1.1
Acyl-CoA dehydrogenase				
<i>acdh-1</i>	ns	ns	-1.7	-1.7
<i>acdh-2</i>	ns	-1.7	-11.0	-17.5
E04F6.5	1.2	ns	ns	ns
F28A10.6	-1.4	-1.4	-2.5	-3.3
<i>acdh-8</i>	-1.4	-1.4	3.0	5.7
K06A5.6	ns	ns	-1.3	-1.3
T25G12.5	1.4	1.4	ns	ns
Enoyl-CoA hydratase				
<i>ech-1</i>	ns	ns	-1.7	-2.0
<i>ech-2</i>	1.3	1.4	1.1	1.1
<i>ech-4</i>	ns	ns	-2.0	-2.0
<i>ech-5</i>	-1.3	ns	-1.7	-2.0
<i>ech-6</i>	ns	ns	-2.5	-2.5
<i>ech-7</i>	ns	ns	-2.0	-2.0
Hydroxy-acyl-CoA dehydrogenase				
<i>hacd-1</i>	ns	ns	2.6	3.8
B0272.3	1.4	1.3	1.3	1.3
T08B2.7	ns	1.1	1.1	1.0
F54C8.1	-1.4	-1.7	1.4	2.9
Thiolase				
F53A2.7	ns	ns	-1.4	-1.4
B0303.3	1.1	ns	ns	ns
Peroxisomal β-oxidation				
Acyl-CoA synthetase				
<i>acs-1</i>	-1.3	-2.0	-2.5	-3.3

Continued Table S2

Acyl-CoA oxidase				
F08A8.1	1.6	1.6	2.1	2.2
F08A8.2	ns	-1.4	-2.5	-2.5
F08A8.3	-1.3	-1.3	-5.0	-10.0
F08A8.4	ns	-1.4	-5.0	-3.3
F59F4.1	1.3	1.4	1.2	1.3
C48B4.1	ns	ns	-3.3	-5.0
F25C8.1	ns	ns	ns	ns
Enoyl-CoA hydratase				
<i>ech-3</i>	1.2	1.4	1.3	1.2
<i>ech-8</i>	2.2	3.0	2.2	2.0
<i>ech-9</i>	ns	-2.0	ns	-10.0
Hydratase				
<i>maoc-1</i>	2.0	2.3	1.5	ns
Dehydrogenase				
<i>dhs-28</i>	1.5	1.7	1.5	1.5
Thiolase				
<i>daf-22</i>	1.8	2.1	1.4	1.4
T02G5.4	-3.3	ns	ns	-1.1
T02G5.7	-1.3	-1.4	ns	-1.1
<i>kat-1</i>	-1.1	ns	ns	-2.0
Lipid synthesis				
Fatty acid synthase				
W09B6.1	ns	ns	1.6	1.7
Acetyl-CoA carboxylase				
F32H2.5	ns	ns	ns	1.2
Fatty acid desaturase				
<i>fat-1</i>	1.3	ns	1.4	1.6
<i>fat-2</i>	1.3	ns	2.9	3.5
<i>fat-3</i>	1.9	2.5	6.8	8.2
<i>fat-4</i>	1.1	ns	2.2	2.4
<i>fat-6</i>	1.2	1.2	1.6	1.8
<i>fat-7</i>	2.8	1.9	ns	-1.9
Fatty acid elongase				
<i>elo-1</i>	1.2	ns	1.3	1.2
<i>elo-2</i>	ns	ns	ns	ns
<i>elo-3</i>	-1.7	-1.7	-1.7	-2.0
<i>elo-4</i>	-1.3	-1.3	ns	ns
<i>elo-5</i>	ns	-1.7	-3.3	-2.5
<i>elo-6</i>	ns	ns	-2.0	-1.7
<i>elo-7</i>	-1.3	-1.7	3.3	7.7
<i>elo-8</i>	-1.5	-1.6	3.2	6.2
<i>elo-9</i>	ns	ns	ns	ns
Diacylglycerol-acyltransferase				
F59A1.10	ns	ns	-3.3	-2.5
K07B1.4	ns	ns	ns	-1.1
<i>dgtr-1</i>	ns	-1.1	-1.4	-1.7
Phosphatidylcholine synthesis				
<i>sams-1</i>	ns	ns	-1.3/ 2.0/ -1.7	-1.4/ 2.2/ -1.9
<i>pmt-1</i>	1.4/ 1.3	ns	4.2/ 4.0	4.7/ 4.4
<i>pmt-2</i>	1.5	ns	-1.9	-2.1
<i>pcyt-1</i>	ns	ns	-2.3	-2.6
Lipid transport and storage				
Fatty acid binding protein				

Continued Table S2

<i>lbp-1</i>	1.5	2.0	2.0	2.0
<i>lbp-2</i>	2.1	n.s	n.s	ns
<i>lbp-3</i>	ns	-1.4	n.s	ns
<i>lbp-4</i>	ns	ns	-1.4	-1.4
<i>lbp-5</i>	1.2	1.3	1.3	1.3
<i>lbp-6</i>	1.2	ns	-1.7	-1.7
<i>lbp-7</i>	1.2	ns	2.2	2.6
<i>lbp-8</i>	-1.9	-2.9	-33.3	-40.0
<i>lbp-9</i>	ns	ns	ns	-1.1
Acyl-CoA binding protein				
<i>acbp-1</i>	-1.2	ns	-1.6	-1.7
<i>acbp-3</i>	ns	ns	-2.0	-2.0
<i>acbp-4</i>	-1.4	-1.7	1.6	2.6
<i>acbp-5</i>	ns	ns	ns	1.0
<i>acbp-6</i>	-1.7	-1.9	-2.6	-2.9
lipoprotein				
<i>vit-2</i>	-1.6	-2.0	ns	ns
<i>vit-3</i>	ns	-3.6	-1.5	-2.2
<i>vit-4</i>	ns	-4.3	-1.8	-3.7
<i>vit-5</i>	ns	-2.6	ns	-1.6
<i>vit-6</i>	ns	-1.7/ -2.0	ns	ns
<i>daf-2</i> (insulin/IGF receptor ortholog)	ns	1.6/1.3	1.2/-1.9	1.2/-2.3
<i>daf-7</i> (transforming growth factor)	1.3	1.5	ns	ns
Putative lipid droplet associated				
<i>cav-2</i> (caveolin-related)	1.3	1.4	ns	ns
<i>lpin-1</i>	1.2	1.3	1.2	1.1
Transcription factor				
<i>klf-3</i>	ns	ns	ns	ns
<i>sbp-1</i>	ns	ns	-1.7	-1.8
<i>nhr-49</i>	1.7/1.5	1.6/1.6	1.3/1.2	1.2/1.2
<i>nhr-80</i>	ns	ns	1.8/1.6	1.9/1.7

This table shows the fold changes of mRNA levels of candidate genes expected being involved in lipid metabolism and lipid storage function in response to DR (DR1.5, DR0.7). ^aDescription of genes is based on the gene ontology (GO) annotation for *C. elegans* (WormBase, www.wormbase.org, release WS 198).

^bFold changes are understood between DR and AL group. A positive number indicates a higher gene expression in DR animals. In case of down-regulated genes, the fold change was calculated as 1/ratio, and a minus was added to the quotient. A negative number indicates a lower gene expression under DR. In case of splice variants, fold changes are separated by a slash. Significance threshold was a p value <0.05 (unpaired t-test). ns, not significant.

Danksagung

Ich danke Prof. Frank Döring für die Aufnahme in seine Arbeitsgruppe und die Betreuung meiner Arbeit.

Prof. Thomas Roeder danke ich für die Übernahme der Betreuung an der Mathematisch-Naturwissenschaftlichen Fakultät.

Ich danke Prof. Ralf Schnabel von der TU Braunschweig und seiner gesamten Arbeitsgruppe für den *C elegans* Crash-Kurs, für die Diskussionsbereitschaft und die nützlichen Tipps.

Ich bedanke mich bei Prof. Zumbusch und Martin Winterhalder von der Universität Konstanz, die es mir ermöglicht haben, die CARS-Mikroskopie Versuche dort durchzuführen. Ich möchte mich außerdem ganz herzlich bei der gesamten Arbeitsgruppe Chemie für die nette Aufnahme und die Unterstützung bedanken.

Ich bedanke mich bei der gesamten Arbeitsgruppe der Molekularen Prävention für die gute Zusammenarbeit und die Hilfsbereitschaft. Maja Klapper danke ich für die Einarbeitung und Betreuung. Bei Madeleine Ehmke und Ulla Faust möchte ich mich für die schöne „WG-Zeit“ bedanken. Andreas Ludewig danke ich für die Aufmunterungen und die Hilfe beim Finden der richtigen Worte. Auch möchte ich mich bei allen ehemaligen Arbeitsgruppen-Mitgliedern, insbesondere bei Constance Schmelzer, Kathi Stiebeling und bei meinen Master-Studenten Simone Kohls und Ulf Geisen für die tolle Zusammenarbeit und die schöne Zeit bedanken.

Ich danke Justus, Peter und Bob.

Ich bedanke mich bei meinen Eltern von ganzen Herzen für die Unterstützung, die Aufmunterungen und dafür, dass sie immer für mich da sind.

Ein besonderer Dank geht an Sven Hellmann.

Lebenslauf

Daniela Palgunow

Calvinstr. 9

24114 Kiel

Geboren am 18.04.1979 in Hannover

Staatsangehörigkeit: deutsch

Seit 10/2007 Institut für molekulare Ernährung, CAU Kiel

10/2007 Beginn des Promotionsvorhabens

10/2004 – 09/2006 Masterstudium (M.Sc) Biologie der Zellen, Universität Osnabrück

Masterarbeit im Fach Pflanzenphysiologie,

Betreuerin Prof. DR. R. Scheibe

Thema der Masterarbeit: „Redoxmodifikation der cytosolischen
NAD-Malatehydrogenase-Isoformen als regulatorischer
Mechanismus in *Arabidopsis thaliana*“

10/2001 – 09/2004 Bachelorstudium (B.Sc) Biologie der Zellen, Universität

Osnabrück

Bachelorarbeit im Fach Genetik, Betreuer Prof. Dr. J. Heinisch

Thema der Bachelorarbeit: „ATP-insensitive

Phosphofruktokinase-Mutanten und ihr Einfluss auf den
Glykolysefluss.“

08/1999 – 07/2001 Berufsausbildung zur Biologisch-technischen Assistentin

Staatlich anerkannten Berufsfachschule *Sabine Blindow*

Schulen, Hannover

1999 Abitur

08/1992 – 06/1999 Gymnasium Isernhagen

Erklärung

Hiermit erkläre ich, dass ich die vorliegende Arbeit, abgesehen von der wissenschaftlichen Beratung meines Betreuers, selbständig und ausschließlich unter Verwendung der hierin angegebenen Quellen und Hilfsmittel angefertigt habe. Diese Arbeit wurde bisher weder in Teilen noch vollständig an anderer Stelle im Rahmen eines Prüfungsverfahrens vorgelegt. Die Arbeit ist unter Einhaltung der Regeln guter wissenschaftlicher Praxis der Deutschen Forschungsgemeinschaft entstanden.

Kiel, den

.....

(Daniela Palgunow)

Teile dieser Arbeit wurden zur Veröffentlichung eingereicht:

Palgunow, D.; Klapper, M.; Döring, F.

Dietary restriction enlarges intestinal and hypodermal lipid droplets in *Caenorhabditis elegans*

eingereicht am 24.04.2012 bei Plosone (under review)